

Integrating field and remote sensing approaches to  
evaluate ecosystem services from agriculture in  
smallholder landscapes

by

Sean Patrick Kearney

B.A., Western Washington University, 2008  
M.Sc., The University of California, Davis, 2011

A DISSERTATION SUBMITTED IN PARTIAL FULFILLMENT OF THE REQUIREMENTS  
FOR THE DEGREE OF

DOCTOR OF PHILOSOPHY

in

The Faculty of Graduate and Postdoctoral Studies

(Land and Food Systems)

THE UNIVERSITY OF BRITISH COLUMBIA

(Vancouver)

April 2017

© Sean Patrick Kearney, 2017

# Abstract

Agriculture now covers over a third of the Earth's terrestrial surface, and smallholder farmers alone manage over a billion hectares globally. As stewards of the land, smallholders do much more for human well-being than just harvest useful products. However, a conventionally narrow focus on productivity over the last half-century now threatens ecosystem health and long-term agricultural production, particularly as global climate change accelerates. Agroecological and 'climate-smart' agricultural (CSA) practices have been proposed to both mitigate climate change and build resilience by enhancing multiple ecosystem services (ES), and policies are emerging to incentivize the adoption of such practices. In order to (1) better understand how agroecological and CSA management alternatives impact multiple ES, and (2) contribute to operationalizing monitoring of ES in smallholder landscapes, I present research from El Salvador combining field methods and remote sensing analysis to evaluate multiple ES.

Using data from on-farm field trials, I developed composite ES indices to demonstrate distinct benefits and synergies among multiple ES from agroforestry and, to a lesser extent, organic management (i.e., CSA) compared to conventional management. I also identified a subset of easy-to-measure field proxies that correlate well with multiple ES, and proposed an improved method to compare relative erosion resulting from different land management practices.

At the landscape scale, I focused on emerging techniques to map aboveground woody biomass (AGWB) – a large terrestrial carbon sink and indicator of agroforestry management – using high-spatial-resolution satellite imagery and airborne laser scanning (ALS). I showed how satellite data could be used to quantify AGWB at the watershed to landscape scale with uncertainties of less than 5%, and suggest that a singular focus on plot-scale uncertainty limits the operationalization of satellite-based approaches to monitor AGWB. I also present a novel approach to using ALS that improves the accuracy of measuring AGWB in trees outside of forests (e.g., agroforestry, hedgerows) and apply it to show that these trees contain substantial AGWB within smallholder landscapes, further demonstrating the ES benefits of agroforestry.

This dissertation contributes to designing simple and cost-effective monitoring strategies to help operationalize policies promoting management practices that enhance multiple ES in smallholder agriculture.

## Lay abstract

Agriculture today covers more than a third of the Earth's land surface, and smallholder farmers manage about 25% of all agricultural land. Over the last half-century, a narrow focus on increasing agricultural production at the expense of other benefits that nature provides (often called 'ecosystem services') now threatens global environmental health and long-term agricultural production. The key goals of this dissertation were to (1) better understand how agricultural management alternatives impact ecosystem services, and (2) contribute to practical methods for monitoring these services in smallholder landscapes. I present research from El Salvador combining field methods and remote sensing (e.g., satellite imagery) to evaluate the impacts of agroforestry and organic management on multiple ecosystem services, and show that these alternatives provide distinct benefits compared to conventional management. My methods contribute to designing simple and cost-effective monitoring strategies to operationalize policies promoting management that enhances multiple ecosystem services from smallholder agriculture.

# Preface

This dissertation is structured as a series of four manuscripts (Chapters 3 – 6) written for publication in peer-reviewed journals, contextualized and tied together with an introduction (Chapter 1), a description of the study area (Chapter 2) and a conclusion (Chapter 7). I developed the overarching objectives of this dissertation through discussions with my supervisory committee. Manuscript chapters were modified slightly from the versions submitted to journals to avoid redundancy and improve the readability of the dissertation. Writing of individual manuscripts, and the approaches to data analysis and interpretation, are my own work, with critical feedback provided by the co-authors of each manuscript, as listed below:

**Chapter 3:** Kearney, S. P., Fonte, S. J., García, E. D., Siles, P., Chan, K. M. A., & Smukler, S. M. (2017). Evaluation of synergies and trade-offs among multiple ecosystem services in agroforestry systems. [In review]

**Chapter 4:** Kearney, S. P., Fonte, S. J., García, E. D., Siles, P., & Smukler, S. M. (2017). Improving the utility of erosion pins: absolute value of pin height change as an indicator of relative erosion rates. [In review]

**Chapter 5:** Kearney, S. P., Coops, N. C., Chan, K. M. A., Fonte, S. J., Siles, P., & Smukler, S. M. (2017). High-resolution carbon mapping to support investments in 'climate-smart' agriculture: making the case for a landscape approach. [In review]

**Chapter 6:** Kearney, S. P., Coops, N. C., & Smukler, S. M. (2017). A simplified approach to mapping tree biomass in heterogeneous landscapes with airborne laser scanning. [In prep]

In the process of preparing the chapters included in this dissertation, I also wrote a related chapter for an edited book published put together by the Climate Change,

Agriculture and Food Security research program within the CGIAR (Consultative Group for International Agricultural Research). This chapter, cited within my dissertation, is listed here:

Kearney, S. P., & Smukler, S. M. (2016). Determining Greenhouse Gas Emissions and Removals Associated with Land-Use and Land-Cover Change. In T. S. Rosenstock, M. C. Rufino, K. Butterbach-Bahl, E. Wollenberg, & M. Richards (Eds.), *Methods for Measuring Greenhouse Gas Balances and Evaluating Migration Options in Smallholder Agriculture*. Springer. [https://doi.org/10.1007/978-3-319-29794-1\\_3](https://doi.org/10.1007/978-3-319-29794-1_3)

# Table of Contents

<b>Abstract</b> .....	<b>ii</b>
<b>Lay abstract</b> .....	<b>iv</b>
<b>Preface</b> .....	<b>v</b>
<b>Table of Contents</b> .....	<b>vii</b>
<b>List of Tables</b> .....	<b>xi</b>
<b>List of Figures</b> .....	<b>xii</b>
<b>List of Abbreviations</b> .....	<b>xiii</b>
<b>Acknowledgements</b> .....	<b>xvi</b>
<b>Dedication</b> .....	<b>xx</b>
<b>1 Introduction</b> .....	<b>1</b>
<b>1.1 Background and motivation</b> .....	<b>1</b>
1.1.1 Agriculture as a global force and the concept of ecosystem services .....	1
1.1.2 Promoting ‘climate-smart’ agriculture among smallholders using payments for ecosystem services .....	4
1.1.3 Key challenges to quantifying ecosystem services in smallholder landscapes....	6
<b>1.2 Research objectives and goals</b> .....	<b>9</b>
<b>1.3 Dissertation overview</b> .....	<b>11</b>
<b>2 Study area</b> .....	<b>15</b>
<b>2.1 La Mancomunidad La Montañona, El Salvador</b> .....	<b>15</b>
<b>2.2 The SMAS field trials</b> .....	<b>17</b>
<b>2.3 The QuickBird study area</b> .....	<b>17</b>
<b>3 Evaluation of synergies and trade-offs among multiple ecosystem services in agroforestry systems</b> .....	<b>20</b>
<b>3.1 Background and introduction</b> .....	<b>20</b>
3.1.1 ‘Climate-smart’ agriculture and payments for ecosystem services .....	20
3.1.2 Agroforestry and the ‘slash-and-mulch’ system .....	22
<b>3.2 Methods</b> .....	<b>26</b>
3.2.1 Experimental design.....	26
3.2.2 Framework for measuring multiple ES .....	29
3.2.3 Provisioning services .....	30
3.2.4 Regulation and Maintenance services.....	31

3.2.5	Biodiversity .....	35
3.2.6	Statistical analysis .....	37
<b>3.3</b>	<b>Results .....</b>	<b>40</b>
3.3.1	Individual ES indicator variables .....	40
3.3.2	Composite ES indices .....	44
3.3.3	PCA of ES indices and correlation with field proxies .....	45
<b>3.4</b>	<b>Discussion.....</b>	<b>48</b>
3.4.1	ES indicators and indices.....	48
3.4.2	ES synergies and trade-offs .....	57
3.4.3	Field proxies for multiple ES.....	59
3.4.4	Implications for management, ES monitoring and PES .....	60
<b>3.5</b>	<b>Conclusions .....</b>	<b>66</b>
<b>4</b>	<b>Improving the utility of erosion pins: absolute value of pin height change as an indicator of relative erosion rates.....</b>	<b>68</b>
<b>4.1</b>	<b>Background and introduction.....</b>	<b>68</b>
<b>4.2</b>	<b>Methods.....</b>	<b>71</b>
4.2.1	Erosion pin installation and measurement.....	71
4.2.2	Correlating erosion pins with modeled and measured erosion.....	75
4.2.3	Statistical analysis of management effects on erosion.....	77
<b>4.3</b>	<b>Results .....</b>	<b>78</b>
<b>4.4</b>	<b>Discussion.....</b>	<b>82</b>
<b>5</b>	<b>High-resolution carbon mapping to support investments in ‘climate-smart’ agriculture: making the case for a landscape approach .....</b>	<b>86</b>
<b>5.1</b>	<b>Background and introduction.....</b>	<b>86</b>
<b>5.2</b>	<b>Methods.....</b>	<b>90</b>
5.2.1	Data collection.....	91
5.2.2	Mapping AGWB-C .....	92
5.2.3	Estimating map uncertainty.....	96
5.2.4	Predicting changes in AGWB-C with CSA adoption and potential C revenues ...	99
<b>5.3</b>	<b>Results .....</b>	<b>103</b>
5.3.1	Mapping AGWB-C .....	103
5.3.2	Estimating map uncertainty.....	107
5.3.3	Predicting changes in AGWB-C with CSA adoption and potential C revenues	109
<b>5.4</b>	<b>Discussion.....</b>	<b>112</b>
5.4.1	Mapping AGWB-C .....	112
5.4.2	Predicting changes in AGWB-C with CSA adoption and potential C revenues	116
<b>5.5</b>	<b>Conclusions .....</b>	<b>117</b>

<b>6</b>	<b>A simplified approach to mapping tree biomass in heterogeneous landscapes with airborne laser scanning .....</b>	<b>119</b>
6.1	<b>Background and introduction.....</b>	<b>119</b>
6.2	<b>Methods.....</b>	<b>123</b>
6.2.1	Study area .....	123
6.2.2	Field data collection.....	124
6.2.3	ALS data acquisition and processing .....	125
6.2.4	Model Validation .....	131
6.2.5	Total AGWB by vegetation type .....	131
6.3	<b>Results .....</b>	<b>133</b>
6.3.1	Accuracy of AGWB predictions using ALS .....	133
6.3.2	Total AGWB by woody vegetation type .....	137
6.4	<b>Discussion.....</b>	<b>139</b>
6.4.1	Accuracy of AGWB predictions using ALS .....	139
6.4.2	Total AGWB by woody vegetation type .....	140
6.4.3	Strengths, limitations and future directions.....	141
6.5	<b>Conclusions .....</b>	<b>144</b>
<b>7</b>	<b>Overall conclusions.....</b>	<b>146</b>
7.1	<b>Key research findings and contributions.....</b>	<b>146</b>
7.1.1	Overarching research objectives.....	146
7.1.2	Field-scale research findings .....	147
7.1.3	Landscape-scale research findings.....	150
7.2	<b>Limitations .....</b>	<b>154</b>
7.2.1	Field-scale research limitations.....	154
7.2.2	Landscape-scale research limitations .....	157
7.3	<b>Potential applications .....</b>	<b>158</b>
7.3.1	Applications of field-scale research .....	158
7.3.2	Applications of landscape-scale research.....	160
7.4	<b>Future research directions.....</b>	<b>162</b>
7.4.1	Field-scale research directions .....	162
7.4.2	Landscape-scale research directions.....	163
7.5	<b>Final reflections.....</b>	<b>165</b>
	<b>References.....</b>	<b>167</b>
	<b>Appendices.....</b>	<b>190</b>
	<b>Appendix A.....</b>	<b>190</b>
	Description of indicator development methods for the water regulation index used in Chapter 2 .....	190

Supplementary Tables for Chapter 2 .....	193
Supplementary Figures for Chapter 2 .....	195
<b>Appendix B</b> .....	<b>199</b>
Allometric equations used to derive aboveground woody biomass.....	199
Supplementary Tables for Chapter 5 .....	204
<b>Appendix C</b> .....	<b>210</b>
Supplementary Table for Chapter 6.....	210

# List of Tables

Table 3.1 Ecosystem service (ES) groups used for index development .....	30
Table 3.3 Results of statistical analysis of individual ecosystem service indicators by treatment.....	43
Table 3.4 Ecosystem service composite index values by treatment .....	45
Table 4.1 Correlation of erosion pin measurements with individual RUSLE factors.....	79
Table 5.1 Potential predictor variables tested by stepwise multivariate linear regression ..	95
Table 5.3 Results of the final regression model to predict AGWB-C .....	104
Table 5.4 Total predicted AGWB-C by land use/land cover (LULC) class.....	106
Table 5.5 Potential gains in AGWB-C with 100% adoption of CSA .....	110
Table 5.6 Projected revenue of C payments for CSA adoption over 15 years .....	111
Table 6.1 Validation of AGWB prediction results for area- and CHM-based models .....	134
Table 6.2 Total landscape aboveground woody biomass (AGWB) for the study area by forest fragmentation class.....	138
Table A - 1. Descriptive statistics by treatment for field proxies measured in individual plots .....	193
Table A - 2. Select results from principal component analysis of ecosystem service indices .....	194
Table A - 3. Expected benefits, costs and net profit of each maize-bean production system .....	194
Table B - 1. Allometric equations used to derive aboveground woody biomass .....	204
Table B - 2. Result of analysis of potential diameter-height regression models for large trees (DBH $\geq$ 10 cm).....	206
Table B - 3. Result of analysis of potential diameter-height regression models for small trees (DBH $1 <$ 10 cm) .....	207
Table B - 4. Results for validation and grid simulation analysis of AGWB-C map uncertainty .....	208
Table C - 1. Plot metrics used in random forest modeling to predict AGWB with the area-based approach.....	210

# List of Figures

Figure 2.1 Map of the study area with ground sampling and field trial locations .....	18
Figure 3.1 Co-variation among ecosystem services indices for cultivated treatments .....	46
Figure 3.2 Correlation matrix of field proxies and ecosystem service indices .....	48
Figure 3.3 Radar chart of non-production ecosystem services.....	63
Figure 4.1 Diagram of erosion pin setup.....	72
Figure 4.2 Graphical depiction of installed erosion pin measured with a digital depth gauge .....	74
Figure 4.3 RUSLE-modeled and pin-measured erosion by management systems and cover class.....	81
Figure 5.1 Top 10 most frequently chosen regression model variables.....	105
Figure 5.2 Final map of AGWB-C predicted from QuickBird satellite imagery.....	106
Figure 5.3 Uncertainty map of AGWB-C predictions from QuickBird satellite imagery .....	108
Figure 5.4 Uncertainty of AGWB-C predictions by aggregation unit size .....	109
Figure 5.5 Map of average expected AGWB-C gains with CSA adoption.....	112
Figure 6.1 Schematic diagram of the generalized CHM-based approach.....	129
Figure 6.2 Visual representation of the forest fragmentation index model.....	133
Figure 6.3 Predicted vs. field-measured AGWB for area- and CHM-based models.....	135
Figure 6.4 Select results of mapped AGWB using different approaches and spatial resolutions.....	136
Figure 6.5 Map showing woody vegetation types based on fragmentation classes for a select area .....	138
Figure A - 1. Correlation between weed biomass and soil mulch cover .....	195
Figure A - 2. Co-variation of soil properties by treatment and farm location .....	196
Figure A - 3. Correlation between SOM and infiltration rates.....	197
Figure A - 4. Co-variation of non-production ES indices by treatment .....	198
Figure B - 1. Spatial autocorrelation of AGWB-C prediction uncertainty.....	209

# List of Abbreviations

ABES - Agroforestry for Biodiversity and Ecosystem Services

AGWB - Aboveground Woody Biomass

ALS - Airborne Laser Scanning (also called LiDAR)

ARI2 - Anthocyanin Reflectance Index 2

ARVI - Atmospherically Resistant Vegetation Index

ASTER - Advanced Spaceborne Thermal Emission and Reflection

BIC - Bayesian Information Criterion

BLF - Broadleaf Forest

C - Carbon

CA - Crown Area

CENTA – Centro Nacional de Tecnología Agropecuaria y Forestal

CHM - Canopy Height Model

CGIAR – Consultative Group for International Agricultural Research

CO<sub>2</sub> - Carbon Dioxide

CO<sub>2</sub>-Eq. - Carbon Dioxide Equivalent

CROP - Cropland

CSA - Climate-Smart Agriculture

CV - Coefficient of Variation (or Cross-Validation when used in context)

DBH - Diameter at Breast Height (1.3 m)

DEM - Digital Elevation Model

ES - Ecosystem Service(s)

EU - European Union

EVI - Enhanced Vegetation Index

FAO - Food and Agriculture Organization (of the United Nations)

GHG - Greenhouse Gas

GLCM - Grey Level Co-occurrence Matrix

IPCC - International Panel on Climate Change

LDSF – Land Degradation Surveillance Framework

LiDAR - Light Detection and Ranging (also called ALS)

LOOCV - Leave One Out Cross Validation

LULC - Land Use / Land Cover

MARN – Ministry of Environment and Natural Resources, El Salvador

MPF - Mixed Pine Forest

MUHNES – Natural History Museum of El Salvador

NASA - National Aeronautics and Space Administration (of the United States)

NDVI - Normalized Difference Vegetation Index

NIR - Near Infrared

OSAVI - Optimized Soil Adjusted Vegetation Index

PAST - Pasture

PC - Principal Component

PCA - Principal Component Analysis

PES - Payment(s) for Ecosystem Service(s)

PRISMA – Programa Regional de Investigación sobre Desarrollo y Medio Ambiente

RMSE - Root Mean Squared Error

SMAS - Slash and Mulch Agroforestry System

SR - Simple Ratio (Vegetation Index)

TC - Tasselled Cap

TOF - Trees Outside Forests

TWI - Topographic Wetness Index

UBC – University of British Columbia

UES – University of El Salvador

US - United States

USAID - United States Agency for International Development

USD - Dollars (United States)

VIF - Variance Inflation Factor

# Acknowledgements

This research was made possible with funding from the United States Agency for International Development (USAID) through the “Agroforestry for Biodiversity and Ecosystem Services” (ABES) project, under the leadership of Dr. Sean Smukler, Dr. Steve Fonte, Dr. Aracely Castro and Dr. Pablo Siles and in collaboration with the Earth Institute at Columbia University, the International Center for Tropical Agriculture (CIAT) and the Programa Regional de Investigación sobre Desarrollo y Medio Ambiente (PRISMA). Special thanks to USAID staff in El Salvador, especially Mary and Jason, for your support, encouragement and efforts to connect this research with other projects. The Ministry of Environment and Natural Resources (MARN), El Salvador, also provided insight and cooperation to broaden the scope and applicability of this research, including sharing airborne laser scanning (ALS) data. Additional financial support was provided by the Public Scholars Initiative and the David and Mary Macaree Fellowship through the University of British Columbia (UBC).

I would like to thank my colleagues and partnering organizations in El Salvador for your support and extensive contributions the fieldwork behind much of this research. The majors’ offices and the Association of Municipalities of La Mancomunidad La Montañona, especially director Juan Arnulfo Alberto, were integral in facilitating safe and community-engaged access to field sites and helping

me to better understand the social, political and environmental contexts in which this research was conducted. Thank you to the Natural History Museum of El Salvador (MUHNES), especially Jenny Menjivar and Gabriel Cerén, for your expertise in tree species identification, and your patient training of the field crew and myself.

I would like to acknowledge the profound and untiring contribution of the field crew to develop a robust landscape dataset by measuring thousands of trees, taking hundreds of soil samples and climbing to all corners of La Montañona. Special thanks to the crew from El Zapotal and Las Vueltas, especially Victor, and the many students and faculty from the University of El Salvador (UES), especially Brenda García and Dr. Reynaldo López. The soils laboratory at UES, along with the Centro Nacional de Tecnología Agropecuaria y Forestal (CENTA), also conducted soil analyses used in this study.

Edwin García provided invaluable oversight and coordination of the three-year field trials used as the basis for Chapters 2 and 3 – this was no small feat! Thank you to Ricardo, Celia, Juan and Porfirio – the farmers on whose land these trials were conducted. I appreciate your gracious commitment of time, energy and expertise to conduct experiments on your farms. I would also like to acknowledge the hard work provided by the field crew, especially Edgar, to help establish and manage these trials and collect such a wide array of data with the utmost attention to detail.

This work would not have been possible without the coordination of Dr. Rolando Barillas, whose contributions in bringing together such a wide array of individuals and institutions are too numerous to mention here. Thank you for all your professional and personal support.

Special thanks to the Sustainable Agricultural Landscapes Laboratory at UBC for your continued friendship and academic support, especially Dr. Sean Smukler for your mentorship and confidence in my abilities, and Khalil Walji for your determined work in the field, in the lab, at the office and on the pitch. Also, thank you to the members of the Integrated Remote Sensing Studio at UBC for your technical guidance processing ALS data, as well as the occasional lakeside debauchery.

Thank you to my supervisor, Dr. Sean Smukler, my committee members, Dr. Kai Chan and Dr. Nicholas Coops, my co-authors, Dr. Steve Fonte, Edwin García and Dr. Pablo Siles, for your critical feedback and intellectual guidance in writing. A special thank you as well to Susanna Klassen for providing valuable and constructive comment on countless iterations of nearly every chapter of this dissertation – you make me a better writer and continue to catalyze my intellectual curiosity.

Much of what led to this dissertation would not have possible without the support of countless teachers, colleagues and friends. You are too numerous to name, but thank you for your wisdom and inspiration along the way (in all its forms), and for your

efforts to keep me well-balanced and well-fed. Most importantly, thank you to my family, for always creating for me a place in which I had every opportunity to thrive.

# Dedication

*For...*

*...my grandparents, Marie and Jack Kearney –  
whether you knew it or not, you introduced me  
to agriculture.*

*...my parents, Lori and Patrick Kearney – you  
are the smartest and kindest people I know,  
and continue to inspire me in so many ways.*

*...farmers and farmworkers everywhere  
that seek to nourish people, build  
community and sustain ecosystems for  
generations to come – that your heroic  
service is not overlooked.*

# 1 Introduction

## 1.1 Background and motivation

### 1.1.1 *Agriculture as a global force and the concept of ecosystem services*

Agriculture has become a dominant feature of the land cover of our planet, with cropland and pasture combined covering about a third of Earth's land surface (Ramankutty et al., 2008). Agricultural production provides humans with the food we need to survive, fibre for clothes and other materials and, increasingly, a host of other products ranging from rubber to cosmetics to biofuels. However, there is no question that agriculture's prolific presence is also having a profound impact on the environment, progressively weakening the ability of ecosystems to support life (Barnosky et al., 2014; Foley et al., 2005; Millennium Ecosystem Assessment, 2005). The impacts are being felt at multiple spatial scales: land degradation from soil erosion and nutrient depletion is threatening long-term agricultural productivity within individual fields and watershed (Dixon et al., 2001); we are witnessing an unprecedented loss of wildlife habitat and biodiversity across landscapes and eco-regions, largely due to agricultural expansion and intensification (Green, 2005) and; agricultural production and land use change together account for about 20 – 25% of global anthropogenic greenhouse gas (GHG) emissions (Edenhofer et al., 2014; Tubiello et al., 2015). An international effort is underway to develop innovative policy mechanisms to address these issues and others, but designing such policies

requires greater understanding of how alternative land management strategies would mediate environmental impacts, as well as cost-effective and accurate methods to monitor changes in impacts over time (de Groot et al., 2010; Kremen and Ostfeld, 2005; Naeem et al., 2015).

Research demonstrates that, as stewards of the land, farmers do much more for human wellbeing than just harvest useful products, and that the manner in which agricultural land is managed greatly influences environmental impacts (Foley et al., 2005; Power, 2010; Robertson et al., 2014). Ecological and social research over the last few decades have led to a growing understanding that humans derive a whole range of real and measureable benefits from healthy, functioning ecosystems (Chan et al., 2006; Costanza et al., 1998; Daily, 1997; Luck et al., 2009; Millennium Ecosystem Assessment, 2005). These benefits, termed *ecosystem services* (ES), can be broadly divided into three categories (Haines-Young and Potschin, 2013; Palomo et al., 2016): (1) provisioning services – the direct output of consumable products (e.g., food, fibre, fuel); (2) regulating services – the processes that mediate or moderate the environment upon which humans rely (e.g., water filtration and storage by soil, C cycling and storage by trees) and; (3) cultural services – the non-material outputs that affect human physical and mental well-being (e.g., spiritual and experiential interactions).

All ecosystems provide these services in differing proportions, and changes in land management inevitably lead to changes in the proportions of ES provided (Foley et

al., 2005). Agroecosystems are of particular importance in that they support food production more intensively than any other system, but the emergence of new technologies combined with agricultural commercialization, a growing population, increased per capita consumption and a strong demand for cheap products has led to a disproportionate emphasis on provisioning services, often at the expense of the regulating ES<sup>1</sup> that agroecosystems also provide (Foley et al., 2005; Hunter et al., 2017; Kareiva et al., 2007; Power, 2010).

Production is obviously vital to feed the global population (there are few pure hunter-gatherers left!) and to support farmers, of which there are many – roughly 1 out of every 3 people on the planet relies on agriculture for their livelihood (FAO, 2013a), and approximately 0.5 billion smallholder<sup>2</sup> farmers rely directly on agriculture to feed their families (FAO, 2016). However, the loss of regulating ES threatens the well-being of farmers and non-farmers alike, and there is mounting

---

<sup>1</sup> While this dissertation focuses exclusively on provisioning and regulating ES, I would like to acknowledge that cultural services have also been heavily impacted by a prioritization of provisioning ES. The relationships of many peoples with the land, indigenous peoples and smallholder farmers in particular, have been undermined by a narrow focus on productivity and resulting industrialization (e.g., Wittman et al., 2015), at times unknowingly but often in the presence of outspoken resistance (e.g., La Via Campesina, 2014; Lang and Barling, 2012).

<sup>2</sup> Smallholders are generally understood to be family owned farmers of small land holdings, often defined as less than 2 ha, but there is a lack of consensus on the precise definition (e.g., see Graeub et al., 2016).

concern about the impact of disruptions to regulating ES (e.g., climate change, soil degradation) on long-term agricultural production (FAO, 2016; Foley et al., 2005; Titttonell and Giller, 2013). While in some cases, human technology and ingenuity may be able to overcome the loss of regulating ES, in many instances it is impossible, too costly or undesirable to do so utilizing strictly non-natural capital, and steps must be taken to ensure that ecosystems are able to continue functioning to provide a variety of services in tandem with human intervention (Palomo et al., 2016).

### ***1.1.2 Promoting 'climate-smart' agriculture among smallholders using payments for ecosystem services***

There is a growing body of evidence demonstrating that agricultural management strategies exist that provide a suite of regulating ES while also maintaining long-term productivity (Foley et al., 2005; The World Bank, 2008). A subset of these management strategies is referred to as 'climate-smart' agriculture (CSA), where practices serve to both mitigate climate change and increase long term agricultural resilience to an already changing climate. This is done by enhancing regulating ES, for example through increased C storage, reduced greenhouse gas emissions, and improved nutrient and water cycling (Steenwerth et al., 2014; Verchot et al., 2007). As political will for climate action grows, there have been widespread calls to

incorporate ES concepts generally, and CSA specifically, into agricultural policies (Engel and Muller, 2016; Steenwerth et al., 2014)<sup>3</sup>.

A variety of policy levers exist to encourage CSA and other ES-enhancing agricultural practices, including: regulations, standards, certifications, environmental taxes, tradable permits and payments for ES (PES). Among these, PES has garnered special attention as a mechanism to support the adoption of ES-enhancing management by low-income smallholder farmers. While imposing taxes or other 'polluter pays' policies on smallholders raises equity concerns, PES has been proposed as a method to both protect ES and alleviate poverty (Engel and Muller, 2016; Jack et al., 2008), although concerns do exist about the ability to optimize both and whether PES might exacerbate power asymmetries and inequality (Daw et al., 2011; Wittman et al., 2015; Wunder, 2008). However, under the right circumstances, PES may be a particularly well-suited policy to encourage

---

<sup>3</sup> The term 'climate-smart agriculture' arose only in the last decade and its definition remains broad (Nagothu, 2016). The term has been criticized for being poorly defined and co-opted to promote industrial agriculture, ignoring issues of power dynamics, access and inequality (La Via Campesina, 2014; Nagothu, 2016) . It is used here primarily as an example of the recent shift in international attention toward broader agricultural development efforts that consider sustainability goals, including enhancing regulating ES provided by agriculture. It is further deemed an apt example due to recent efforts to evaluate incentive-based policies to support CSA adoption (e.g., Engel and Muller, 2016), which would require ES monitoring, the topic of this dissertation. Other terms such as 'agroecological', 'sustainable' or 'eco-friendly' have also been used to describe similar practices, without the explicit focus on global climate change.

CSA adoption with smallholders by covering short-term implementation costs and improving long-term profitability (Engel and Muller, 2016), while potentially providing additional benefits for smallholders (e.g., land-tenure security; Wunder, 2008).

Agricultural PES programs are emerging at the global (e.g., Groom and Palmer, 2012), regional (e.g., Pagiola et al., 2007) and local (e.g., Kosoy et al., 2007) scales; however, PES policy remains nascent, in part due to the challenges associated with quantifying and monitoring ES provision (de Groot et al., 2010). It is widely agreed that a central feature of PES is ‘conditionality’ – the concept that payments are tied to measurable ES provision (Wunder, 2008). Therefore, developing methods to measure the delivery of ES is a critical step for any PES program.

### ***1.1.3 Key challenges to quantifying ecosystem services in smallholder landscapes***

About 20% of the world’s agricultural population are smallholder farmers – a group that manages over a billion hectares of agricultural production, yet remains among the poorest and most food insecure (Dixon et al., 2001; FAO, 2016; Palm et al., 2005). As interest grows to promote CSA for both poverty alleviation and environmental conservation, it is becoming increasingly desirable to quantify ES in smallholder contexts. Such quantification is particularly challenging due to the extreme spatiotemporal heterogeneity arising from small land uses, shifting cultivation, integrated crop-livestock systems, complex agroforestry management,

and other factors (Kearney and Smukler, 2016; Stringer et al., 2012). Effectively promoting CSA would require simultaneously measuring multiple ES in order to demonstrate mitigation and adaptation benefits of CSA, and, compared with measuring individual services, would further compound monitoring challenges. In fact, there has been a call to consider multiple ES across all ecosystems in order to identify trade-offs and synergies among them (Kareiva et al., 2007; Kremen and Miles, 2012; Naeem et al., 2015) and explore opportunities for bundling ES as opposed to tying incentives exclusively to a single ES, which may undermine the adoption of diversified farming systems (Wendland et al., 2010).

As such, there is a significant need for scientifically sound methods to measure multiple ES at various spatial scales in complex landscapes with small and heterogeneous land uses (de Groot et al., 2010; Naeem et al., 2015). At the field scale, studies are needed to better understand the interactions between ES and the relative expected ES benefits of various land management options. Recent research has begun to develop methods to better quantify ES and their interactions (e.g., Kremen and Miles, 2012; Mitchell et al., 2014; Smukler et al., 2010), but this work has largely been conducted in temperate agroecosystems and outside of the smallholder context. More work is needed to apply these methods to tropical smallholder landscapes and to continue operationalizing ES monitoring by lowering costs (e.g., through the use of proxy indicators).

There is also a need to scale ES measurements up to policy-relevant geographical regions, requiring analysis across large areas. Remote sensing provides the ability to acquire spatially explicit data over the Earth's surface and is one of the most promising tools to measure the extent of multiple ES at the scale of landscapes, nations and continents (Ayanu et al., 2012; Feng et al., 2010). Recent advances in sensor technology, computer processing power and analytical methods are enabling the quantification of ES indicators with unprecedented accuracy and spatial resolution. However, much of this work has been conducted in comparatively 'data-rich' industrialized countries (e.g., Chan et al., 2006; Nelson et al., 2009) or applied to relatively homogenous and intact forest landscapes (e.g., Asner et al., 2013; Castillo-Santiago et al., 2010; Levick et al., 2016; Lin et al., 2016), once again leaving gaps in research to measure ES in smallholder landscapes (Leh et al., 2013).

Finally, in order to develop operational monitoring methods, we need to understand the limitations of ES measurements at all scales, which requires that method uncertainty also be quantified and communicated (Gregr and Chan, 2014; Grêt-Regamey et al., 2013). This will help inform decision-makers about if and how to use such tools, and contribute to a more complete picture of potential trade-offs between ES, and how likely they are to occur.

## **1.2 Research objectives and goals**

In my research, I sought to evaluate the supply of both provisioning and regulating ES in CSA compared to conventional management within a smallholder context. I wanted to quantify these services in order to better understand what is driving ES supply and the interactions that may exist between different services, as well as to support decisions about how PES could be used to overcome potential short-term trade-offs between provisioning services (for which a market often already exists) and regulating services (for which farmers are rarely compensated). I also recognized that some ES are notoriously challenging to quantify, and so an additional focus of my research was to further develop methods to measure individual indicators of ES at both the field and landscape scales.

I chose to address these research priorities within Latin America, where PES programs are rapidly emerging (Balvanera et al., 2012; Kosoy et al., 2008). Specifically, I conducted this research within the context of the Mesoamerican maize-bean system, currently practiced by some 11 million smallholders across 65 million ha from Mexico to Nicaragua (Dixon et al., 2001). The system is characterized by subsistence maize and bean production on steep hillsides and marginal lands, which, combined with increasing populations, the continued use of slash-and-burn practices and the rising use of agrochemicals, is leading to concerns about widespread degradation of ES and human well-being (Dixon et al., 2001; Morris et al., 2013).

In response, a CSA practice known as the ‘slash-and-mulch’ agroforestry system (SMAS) has been proposed as an alternative management practice, both within Central America (where it originated) and other tropical hillslope agricultural systems worldwide (Castro et al., 2009; Hellin et al., 1999; The World Bank, 2008). The SMAS is a flexible management system based on three general principles: (1) eliminating burning during field preparation, (2) maintaining a permanent vegetative soil cover or ‘mulch’ (e.g., tree prunings, crop residues) and, (3) intercropping maize and beans with diverse tree species (Castro et al., 2009; Hellin et al., 1999). The SMAS has been shown to provide multiple ES benefits (Fonte et al., 2010; Fonte and Six, 2010; Pauli et al., 2011; Welches and Cherrett, 2002) and increase farm profitability, and it has been proposed that PES could be a good mechanism to overcome short-term implementation costs and promote widespread adoption (Castro et al., 2009; The World Bank, 2008).

To date, most of the work on the SMAS has been limited to Honduras and focused on evaluating just one or a few ES at the field scale, and there is a need to study the adaptability of the SMAS to new regions, assess multiple ES impacts of the system and scale this assessment to the landscape in order to explore the potential impacts of widespread adoption. In 2012, a four-year USAID-funded project in El Salvador titled “Agroforestry for Biodiversity and Ecosystem Services” (ABES) was initiated to assess the adaptability of the SMAS to a new area and better understand its impacts on multiple ES. Utilizing resources and datasets available through the ABES

project, I combined data from field trials, ground surveys and remote sensing to address three overarching scientific research objectives:

- (1) Develop, test and validate new methods to quantify multiple ES and individual ES indicators related to agricultural management at the field scale
- (2) Evaluate trade-offs and synergies among ES within the SMAS compared to other management options for smallholders
- (3) Innovate upon existing methods to map ES indicators and uncertainty in heterogeneous smallholder landscapes, and apply those methods to address questions about the potential impacts of widespread SMAS adoption and the implications for policy design

Through addressing these objectives in the context of smallholder agriculture in El Salvador, I hoped to contribute to a broader understanding of ES and how to measure them in heterogeneous landscapes; I also sought to discuss how ES dynamics and measurement challenges might inform policies such as PES. In the following section, I elaborate on these overarching objectives by highlighting the specific research I conducted for each chapter of my dissertation.

### **1.3 Dissertation overview**

Chapter 2 begins with a description of the study area in northern El Salvador. The general region in which this research was conducted is first broadly described, followed by more specific descriptions of where research activities were carried out

for individual chapters. A map is provided showing the locations of all data collection activities.

Chapter 3, is an assessment of multiple ES measured within on-farm field trials comparing the SMAS to conventional and organic management and a forest-fallow reference site. This chapter highlights methods for simultaneously assessing multiple ES in order to determine trade-offs and synergies associated with CSA and smallholder agroforestry. Here I also evaluate whether simple field-proxies correlate well with multiple ES in an effort to move toward cost-effective ES monitoring tools.

Chapter 4 focuses on improving the measurement of single ES indicator: relative erosion rates. Erosion is an important indicator of various ES (e.g., soil conservation, water quality), but is particularly challenging to monitor accurately and cost-effectively. In this chapter I propose a new innovative method to utilize measurements from erosion pins to evaluate relative erosion rates between land management alternatives. I compared this method to the conventional (and often unsuccessful) approach of assessing erosion pin data.

In Chapters 5 and 6, I shift into monitoring C at the landscape scale, focusing on emerging techniques to map aboveground woody biomass (AGWB) at high spatial resolution using recent advances in remote sensing technology. I focus on AGWB as an individual ES indicator for several reasons. First, AGWB provides a large store of

terrestrial C (Pan et al., 2011), and C monitoring across space and time is a key component for nations working to meet international climate change mitigation goals, and those participating in C-related PES programs (Goetz and Dubayah, 2011). Second, vegetation components such as AGWB are among the ES indicators most 'directly' measureable by satellite and airborne sensors, and can likely be quantified with better accuracy compared to other indicators related to soil or water. Finally, measuring AGWB across landscapes could be utilized to identify and monitor areas under agroforestry management such as the SMAS; however, distribution of C-storing land uses such as agroforestry remain highly uncertain in tropical smallholder landscapes, largely due to substantial spatiotemporal heterogeneity, fine-scale spatial patterning and associated monitoring challenges (Achard et al., 2002; Kearney and Smukler, 2016).

In Chapter 5, I employ the use of very high spatial resolution satellite imagery to map AGWB-C and predict expected changes for several scenarios of CSA adoption. I evaluate map accuracy compared to other studies, with particular attention paid to quantifying map uncertainty at various scales of aggregation in order to examine the utility of such maps for decision makers. I then explore the potential value of that C at various credit prices and discuss the implications of developing C contracts with communities (i.e., at the landscape scale) rather compared to with individual farmers.

Chapter 6 utilizes airborne laser scanning (ALS; also called Light Detection and Ranging or LiDAR) to quantify AGWB in forests and trees outside forests (TOF; i.e., agroforestry, hedgerows, other agricultural land uses). ALS uses pulses of light emitted from aircraft and unmanned aerial vehicles to measure three dimensional vegetation attributes (Lefsky et al., 2002; Lin et al., 2016) and is one of the most promising technologies for accurate and high spatial resolution AGWB mapping (Zolkos et al., 2013). However, to date, much of the research applying ALS to quantify AGWB stocks has focused on intact forest landscapes, and current methods are not well suited for capturing TOF in heterogeneous landscapes. Monitoring AGWB in TOF will be a key component of policies supporting smallholder agroforestry and other tree-based CSA practices.

In Chapter 7, I discuss the key conclusions of my research and reflect upon strengths and limitations of my methods for measuring ES in smallholder agriculture. I examine the applications of my methods to answer key questions, and the contribution that answering these questions may provide for PES and other policies designed to promote sustainable land management within smallholder landscapes.

## 2 Study area

### 2.1 La Mancomunidad La Montañona, El Salvador

This research was conducted in northern El Salvador, a rural and mountainous smallholder landscape. The area is typical of the Mesoamerican dry upland corridor stretching from central Mexico south to Panama, across which an estimated 11 million smallholders cultivate maize and beans, primarily for subsistence (Dixon et al., 2001). Land holdings across the Mesoamerican region are typically small, especially in El Salvador where, with the highest population density of any non-island nation in the western hemisphere (The World Bank, 2016), maize-bean farms average less than 2 ha (Dixon et al., 2001).

Specifically, this research was carried out within an association of seven municipalities covering about 32,000 ha in the department of Chalatenango, along the Honduran border (Figure 2.1). These municipalities, known as La Mancomunidad La Montañona (hereafter referred to as La Mancomunidad), were identified by the Ministry of Environment and Natural Resources of El Salvador (MARN) as a priority region for testing and promoting improved agricultural management due to the predominance of basic grain farming and small-scale extensive livestock grazing on steep slopes near a protected forest area.

Elevations in La Mancomunidad range from 265 – 1575 m and the region has a sub-humid tropical climate with a mean annual temperature of 22 – 26°C and mean annual rainfall of about 1985 mm (MARN, 2013). Rainfall occurs mostly between the months of May and October with a pronounced dry season from November to April, averaging less than 10 mm month<sup>-1</sup> between December and February.

The municipalities of La Mancomunidad have prioritized the conservation of an approximately 1,500-ha area of primary pine (*Pinus oocarpa*) and oak (*Quercus insignis*) forest threatened by deforestation and frequent wildfire from surrounding smallholder agriculture. These mixed-pine forests are found above about 900 m elevation in sparse patches along ridge tops and within the “natural protected area” of La Montañona (shown in Figure 2.1 as the forested area where the municipalities of La Laguna, El Carrizal, Ojos de Agua, Las Vueltas and Concepcion-Quetzaltepeque converge in the north-central region of the study area).

The remaining land is a complex mosaic of farms cultivating basic grains (maize, beans and sorghum), extensive pastures, bush-fallows, secondary forest patches, narrow riparian forests and settlements. Farms and pastures in La Mancomunidad are frequently less than one ha in size and regularly contain highly managed woody perennials in the form of intercropped trees and live fences (i.e., TOF). Shifting cultivation is common practice, resulting in widespread bush-fallows that are highly variable in age, species composition and structure.

## **2.2 The SMAS field trials**

The field trials analyzed in Chapters 3 and 4 were implemented on five farms within the municipality of Las Vueltas (Figure 2.1). This municipality was specifically targeted by the association of mayors of La Mancomunidad for research due to increasing land degradation from agricultural expansion amidst an active and engaged community with broad support for environmental conservation. Farms within Las Vueltas were chosen based on farmers' willingness to participate as well as farm location, size and land-use composition. Elevation of the experimental plots ranged from 624 to 866 m and slopes ranged from 19 – 40 degrees, typical of the area.

## **2.3 The QuickBird study area**

A 10 x 10 km (100 km<sup>2</sup>) area was established to map AGWB using high spatial resolution QuickBird satellite imagery, as described in Chapter 5. The location of the QuickBird study area encompassed the entire municipality of Las Vueltas in order to include the SMAS field trials and establish a baseline for future monitoring within this municipality (Figure 2.1). The 10 x 10 km design was chosen to correspond with the hierarchical sampling design Land Degradation Surveillance Framework (LDSF) developed by the International Center for Tropical Agriculture (Shepherd et al., 2015; Vågen et al., 2010; Vågen and Winowiecki, 2013).

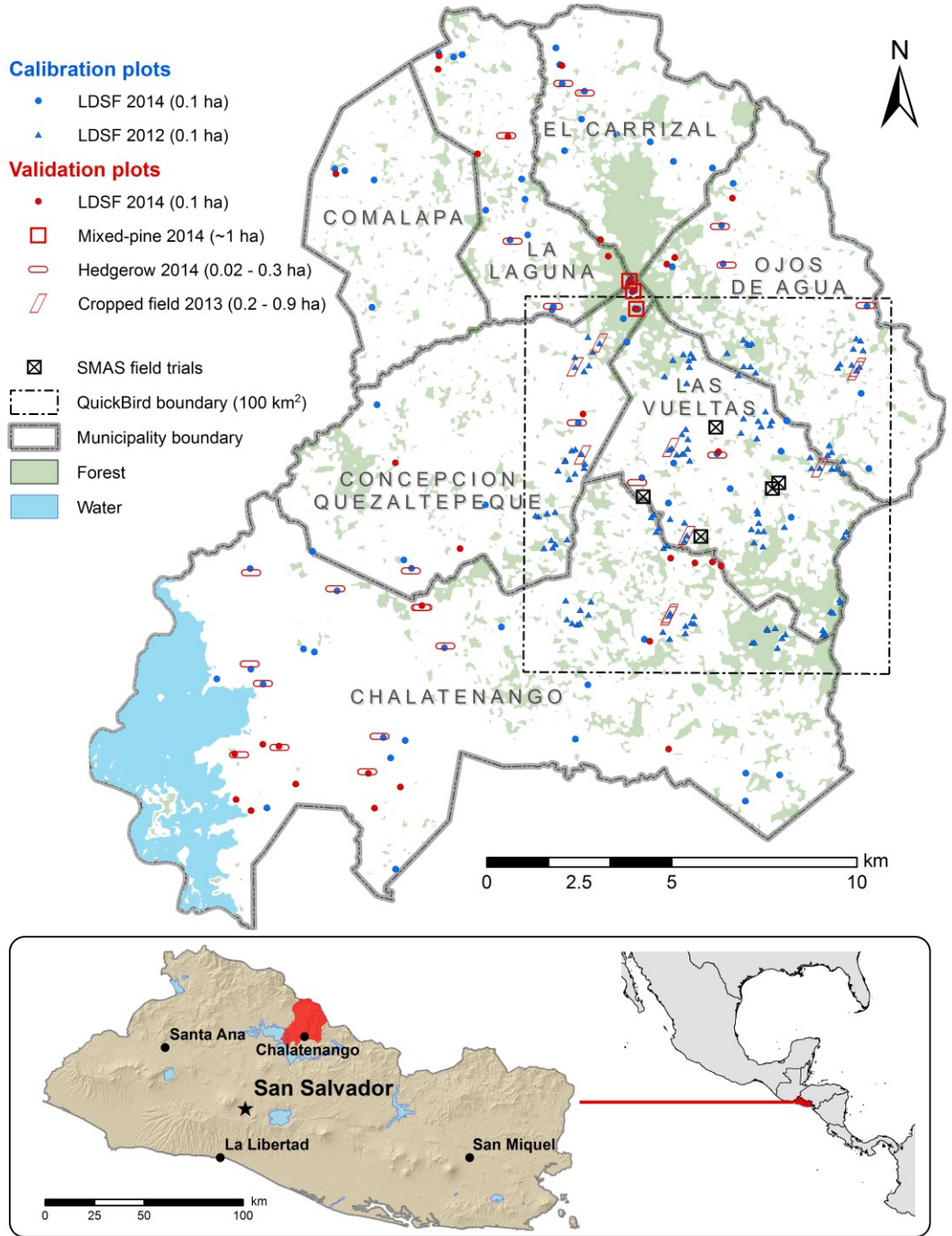


**Figure 2.1 Map of the study area with ground sampling and field trial locations**

The main map shows research plots within the seven municipalities of La Mancomunidad La Montañona, near Chalatenango in northern El Salvador (see inset). Calibration plots sampled using

the Land Degradation Surveillance Framework (LDSF) in 2012 (n = 138) were used to predict aboveground woody biomass (AGWB) from QuickBird satellite imagery (see Chapter 5) and LDSF plots sampled in 2014 (n = 73) used to calibrate airborne laser scanning (ALS) data using an area-based approach (see Chapter 6). Validation plots include randomly selected LDSF plots from 2014 (n = 34), cropped fields (n = 10) and hedgerows (n = 22) and large closed-canopy mixed-pine forest (MPF) inventory plots (n = 3). All 69 validation plots were used to validate ALS-predicted AGWB maps, while the 10 cropped fields and one of the MPF plots were used for QuickBird validation. The slash-and-mulch agroforestry system (SMAS) field trials (n = 5) within the municipality of Las Vueltas are also shown (see Chapters 3 and 4).

# 3 Evaluation of synergies and trade-offs among multiple ecosystem services in agroforestry systems

## 3.1 Background and introduction

### 3.1.1 *'Climate-smart' agriculture and payments for ecosystem services*

One of the great social and environmental challenges of the 21st century is how to support smallholder farmers on the landscape and simultaneously produce equitable food security and environmental outcomes (FAO, 2016). Globally, smallholders make up about 20% of the world's agricultural population and manage over a billion hectares, yet they remain one of the poorest and most food insecure groups (Dixon et al., 2001; FAO, 2016; Palm et al., 2005). Combined with the recognition that smallholders will be disproportionately impacted by climate change, there has been a call to build resilience among smallholders through 'climate-smart' agriculture (CSA; Rioux et al., 2016), defined as management strategies that enable (1) sustainable increases in agricultural productivity and incomes; (2) increased adaptation and resilience capabilities to climate change and; (3) reduced greenhouse gases emissions (GHG), where possible (FAO, 2013b).

Payments for ecosystem services (PES) have emerged as one tool to overcome socioeconomic barriers to CSA adoption (Engel and Muller, 2016) and account for the fact that many ecosystem service (ES) benefits accrue off-farm and at multiple scales. PES models are based on the principle that those providing services (in this case, farmers) are compensated by those receiving the benefits of those services (Hegde and Bull, 2011; Wunder, 2008). Such models raise concerns about exacerbating power asymmetries (e.g., allowing the wealthiest groups to ‘control’ which ES are provided), but also present opportunities for poverty alleviation and long-term welfare gains (Wunder, 2008). It is also hypothesized that even a relatively small payment to farmers, especially early in the establishment of a new management system, will minimize the timeframe in which sustainable management may impose a net cost, thereby increasing adoption (Engel and Muller, 2016; Pagiola et al., 2007). However, PES policy remains nascent, in part due to the challenges associated with quantifying and monitoring ES provision (de Groot et al., 2010).

A further challenge to implementation lies in the critique that PES oversimplify the complexity of ecosystems by separating ecosystem functions into “discrete units of trade” and focusing on very specific land management strategies (Kosoy and Corbera, 2010). Promoting prescriptive production strategies for individual ES (e.g., biofuels for GHG mitigation) may reinforce systemic causes of poverty by trapping smallholders in long-term contracts for rigid management systems or restricting

access to resources by local communities (Schoon et al., 2015; Wittman et al., 2015). Furthermore, PES programs singling out individual ES (e.g., C trading) may undermine the adoption of diversified farming systems that would better provide multiple ES, enhanced biodiversity and long-term resilience (Kosoy and Corbera, 2010; Palomo et al., 2016; Wittman et al., 2015).

Ideally, PES would encourage practices that are adaptable to farmers needs and beneficial for a basket of ES (Wendland et al., 2010), while accounting for trade-offs and synergies among them (Kremen and Miles, 2012; Naeem et al., 2015). But accomplishing this in practice presents additional challenges to measuring ES provision (e.g., Hegde and Bull, 2011). In this paper I address these challenges within the context of agroforestry, a widely promoted example of CSA with multiple ES benefits.

### ***3.1.2 Agroforestry and the 'slash-and-mulch' system***

Agroforestry systems have been incorporated into discussions around CSA for their ES benefits on-farm (e.g., food, fuelwood, soil fertility, water infiltration) and off-farm (e.g., water conservation, C storage, biodiversity; see Mbow et al., 2014; Rioux et al., 2016; Steenwerth et al., 2014). However, a wide range of well-documented socioeconomic factors have limited widespread agroforestry adoption (e.g., Current et al., 1995a; Hellin et al., 1999; Pattanayak et al., 2003; Pollini, 2009). PES is therefore an attractive option to incentivize agroforestry adoption, and many

agroforestry-related PES programs are emerging (e.g., Groom and Palmer, 2012; Kosoy et al., 2007; Pagiola et al., 2007), but there has been a call to ensure that agroforestry approaches are designed to be flexible, allowing farmers to adapt them to their preferences (Adesina et al., 1999; Pollini, 2009)

Here I consider a 'slash and mulch' agroforestry system (SMAS) gaining popularity in Central America. Also called the Quesungual system, named after the village in western Honduras where it was first documented (Hellin et al., 1999), the SMAS offers an agroforestry alternative to the conventional maize-bean farming system, characterized by slash-and-burn management and currently practiced by some 11 million smallholders (covering 65 million ha) across Mesoamerica (Dixon et al., 2001). The SMAS can be considered flexible and adaptable, as it is based on three general principles (Castro et al., 2009; Hellin et al., 1999):

- (1) Eliminating burning during field preparation
- (2) Maintaining a permanent vegetative soil cover or 'mulch' (e.g., tree prunings, crop residues)
- (3) Intercropping maize and beans with diverse tree species

Intercropped trees can be established by planting, natural regeneration or left in place during conversion of secondary forest to agriculture, and farmers choose which tree species to maintain based on their own objectives (e.g., timber, fuelwood, fodder, fruit). Tree densities can be highly variable and the majority of trees are

heavily pruned to minimize competition with crops and provide a substantial mulch layer of leaves and branches to protect the soil and provide nutrients (Beer et al., 1998; Fonte et al., 2010; García, 2011). Other reported benefits, mostly from western Honduras where the system has been widely adopted, include: improved soil health and biodiversity (Fonte et al., 2010; Fonte and Six, 2010; Pauli et al., 2011); climate change mitigation and C storage (Castro et al., 2009; Fonte and Six, 2010); reduced erosion and improved resilience to drought and hurricanes (The World Bank, 2008; Welches and Cherrett, 2002) and improved yields (Castro et al., 2009; Welches and Cherrett, 2002)

The flexibility of the system could make it appropriate for a wide array of biophysical, socioeconomic and cultural contexts. Furthermore, the multiple ES benefits it provides could align well with emerging PES programs (The World Bank, 2008); however, questions remain to determine if and how the SMAS can be integrated into broader sustainability strategies and how to evaluate ES benefits associated with the SMAS and other similar systems.

First, with respect to the SMAS specifically, are ES benefits observed in western Honduras likely to occur in other contexts – especially the simultaneous increase in yields and other non-provisioning ES? Most of the research to date has been limited to western Honduras, an area where yields were below average for the region and land degradation was at crisis levels (Ayarza et al., 2010). Furthermore, research in Honduras has focused on the implementation of the SMAS during conversion from

forest-fallow, and it is unclear whether ES benefits would accrue if the system were implemented to restore already cleared and largely treeless fields, representative of more degraded areas of the region.

More broadly, can we quantify the multiple ES benefits expected from flexible agroforestry systems such as the SMAS, and do trade-offs or synergies among services exist? Most published studies on the SMAS to date have tended to focus on only one or a few ES, mostly related to soil biological health and nutrient cycling (Castro et al., 2010; Fonte et al., 2010; Fonte and Six, 2010; Pauli et al., 2011).

Finally, it would be useful to identify simple field proxies that represent multiple ES, to simplify monitoring efforts and support payments for a basket of ES.

In order to address these questions, I established on-farm trials with two variations of the SMAS in El Salvador with three objectives: (1) evaluate the field-scale impact of the SMAS on a suite of individual ES and biodiversity indicators as compared to other land management options; (2) develop ES indices in order to evaluate the impact of the SMAS on multiple ES indicators and determine if trade-offs and synergies exist and; (3) identify simple and measureable field proxies that demonstrate the principles of the SMAS and could serve as proxies for ES in a monitoring program.

## 3.2 Methods

### 3.2.1 Experimental design

Experimental trials were established in April 2012 on 12 m x 20 m plots on five farms (replicate blocks) located within the municipality of Las Vueltas (see Section 2.2 and Figure 2.1). Each farm was managed for three growing seasons (ending in 2015) and consisted of five treatments (5 treatments x 5 farms; n = 25). Treatments were developed in coordination with MARN, local officials and farmers and included: conventional management (CONV); organic management (ORG); the SMAS established from a plot previously under conventional management (SMAS-1); the SMAS established from a forest-fallow, similar to the Quesungual approach (SMAS-2) and; a forest-fallow reference plot (FOR). The treatments CONV, SMAS-1 and ORG were randomly allocated to previously deforested plots of land under agricultural production, while SMAS-2 and FOR plots were selected from adjacent areas of secondary forest on each farm.

The CONV treatment was managed according to prevailing farmer practices in the region, similar to those described in the introduction and observed elsewhere in El Salvador (e.g., Morris et al., 2013). Maize (*Zea mays*, local variety “H5-G”) was planted each year in May in rows spaced 90 cm apart, with two seeds sown every 45 cm. Beans (*Phaseolus vulgaris*, local variety “Curaneteño”) were planted each year in July/August in rows spaced 45 cm apart, with two seeds sown every 30 cm. A

mixture of ammonium sulphate (21-0-0-24S) and formula (16-20-0) were applied to maize at 10 and 40 days after planting, equivalent to 164 kg N ha<sup>-1</sup>, 39 kg P ha<sup>-1</sup> and 100 kg S ha<sup>-1</sup>. The formula fertilizer was applied to beans at rates equivalent to 60 kg N ha<sup>-1</sup> and 28 kg P ha<sup>-1</sup>. Herbicides and pesticides were applied according to common practice for the area. One notable departure of the CONV treatment from conventional farmer practice is that plots were not burned prior to planting at the behest of local officials since burning is technically outlawed, although rarely enforced. However, manual weeding with machetes prior to planting largely eliminated tree saplings and crop residues were removed with the harvest to simulate the loss of soil mulch cover that occurs with burning or with feeding of residues to livestock.

The SMAS-1 treatment was designed to test the adaptability of the SMAS to situations where land access is limited and forest loss, degradation or laws prohibiting forest clearing may constrain farmers' ability to implement the Quesungual (SMAS-2) system. Trees were planted from seedlings and from cuttings to achieve a final density of roughly 1,000 to 1,400 trees ha<sup>-1</sup> (accounting for anticipated mortality rates of up to 50%), the approximate density of trees observed in the Quesungual system in Honduras (García, 2011; Ordonez Barragan, 2004; Pauli et al., 2011). Tree species were chosen through participatory workshops with farmers to identify species of interest to them and included fruit-bearing species, namely *jocote* (*Spondias mombin*). All crop residues were left in the field and natural

regeneration of saplings was managed to encourage the regrowth of priority tree species. Apart from that, SMAS-1 plots were managed in the same manner as CONV plots.

The SMAS-2 treatment was managed similar to SMAS-1, with the main difference being that it was established directly from a forest-fallow (FOR), following the Quesungual approach (Castro et al., 2009; Hellin et al., 1999). As a result, the SMAS-2 tended to have a higher proportion of mature trees and slightly different species composition, reflecting the previous forest-fallow for that site and the preferences of each farmer. The FOR treatment was an unmanaged reference plot of secondary forest-fallow, approximately 10 – 20 years old. It was located adjacent to the SMAS-2 at each farm and was the land-use from which the SMAS-2 was converted.

The ORG treatment was included to explore the potential benefits and trade-offs associated with chemical-free management associated with proposed legislation in many parts of Central America. Management was similar to the SMAS-1 except no trees were planted and no agrochemicals used. Instead, “bocchachi” (a composted chicken manure rich in microorganisms) was added in split applications at a rate of 7.4 Mg ha<sup>-1</sup> (128 kg N and 66 kg P ha<sup>-1</sup>) for maize and 3.7 Mg ha<sup>-1</sup> (64 kg N and 33 kg P ha<sup>-1</sup>) for beans. Two organic foliar sprays, known locally as *FOREFUN* and *Sulfocalcio*, were prepared on-farm and applied 3 times during the growing season to manage for pests and diseases.

### **3.2.2 Framework for measuring multiple ES**

I measured a suite of indicators of ES supply and biodiversity in each of the 25 plots between July 2015 and February 2016 (during and following the third year of production). Ecosystem services were classified into groups (Table 3.1), largely based on the Common International Classification of Ecosystem Services (CICES) developed by the European Environmental Agency (Haines-Young and Potschin, 2013). For this study, I focused on two CICES sections: Provisioning services and Regulation and Maintenance services. I also include indicators of biodiversity as it is a major focal point for conservation at the local, national and international scale across Latin America (Balvanera et al., 2012) and has been linked to the supply of ES in multiple contexts (Kremen and Miles, 2012; Richards and Méndez, 2014). I present methods for developing and measuring individual ES indicators in Sections 3.2.3 – 3.2.5 (see Table 3.3 for a complete list of indicators), and discuss my approach to statistically analyze indicators and develop and evaluate composite indices in Section 3.2.6.

**Table 3.1 Ecosystem service (ES) groups used for index development**

Final ES groups were defined by the authors, but categorized by CICES Section and Division. A list of individual ES indicators can be found in Table 3.3.

CICES Section	CICES Division	ES Groups
Provisioning	Nutrition	Crop production
	Energy	Fuelwood production
Regulation and Maintenance	Mediation of Flows	Erosion Control Water Regulation
	Maintenance of physical, chemical, and biological conditions	Pest & Disease Control Soil Composition Carbon (C) Storage
	Biodiversity <sup>†</sup>	Aboveground Biodiversity <sup>†</sup> Belowground Biodiversity <sup>†</sup>

<sup>†</sup> Note that biodiversity is not specifically defined as a section by CICES. For more information see Haines-Young and Potschin (2013)

### **3.2.3 Provisioning services**

I estimated the quantity and value of cultivated crops and fuelwood produced in each of the managed plots as indicators of provisioning services. Timber production was excluded since participating farmers stated that wood extraction is primarily for fuelwood, not timber, and estimates of standing timber would overlap with estimates of biomass C, leading to double counting.

#### **3.2.3.1 Crop production**

Maize and beans were harvested in November 2015 after being left in the field to dry as per farmer practice. Maize was harvested from 5 equidistant rows, leaving a 1 m buffer to avoid edge-effects, while beans were harvested from a 5 m x 10 m subplot in the center of each plot. Grain was oven dried and final yields corrected to

11% moisture content. The value of maize and bean production was based on the average annual consumer price, as reported by the Ministry of Agriculture and Livestock of El Salvador (MAG, 2016).

#### *3.2.3.2 Fuelwood provision*

Fuelwood yields were estimated in May 2015 during field preparation and tree pruning, prior to planting. All deadwood and tree prunings were collected as fuelwood following common local practice and yields were calculated in *cargas* – the visually estimated merchantable unit used in the region for selling fuelwood (approximately 25 – 35 kg). Fuelwood from each managed treatment was piled into *cargas* and the total number counted to the nearest one-third *carga*. Even though many farmers harvest some fuelwood from forests and forest-fallows, no fuelwood was harvested from the FOR plots monitored in this study in order to leave these plots as an unmanaged reference treatment. Fuelwood value was set at \$4.00 per *carga* based on local prices.

#### **3.2.4 Regulation and Maintenance services**

##### *3.2.4.1 Erosion control*

Comparative erosion rates were estimated using pins (0.6 cm diameter, 40 cm length) installed in late May 2012 before maize planting. Pin placement was laid out in a grid pattern of 3 columns and 6 rows at 3 m x 3 m spacing for a total of 18 pins per plot. Pins were hammered into the soil perpendicular to the slope, leaving

approximately 10 cm protruding from the soil surface. Pin protrusion was measured 5 times during the 2015 rainy season using a digital depth gauge (0.02 mm precision) and checked for damage or disturbance. Pins that remained undisturbed for the entire season were used to calculate the absolute value of the change in pin height as an indicator of soil movement and erosive activity, as described in Chapter 4 (also see Couper et al., 2002; Luffman et al., 2015).

Soil mulch cover (non-living vegetative biomass) was also measured as an indicator of soil conservation in February 2016. All mulch was collected in five 1-m<sup>2</sup> quadrats randomly located in each plot, dried in an oven at 65° C for 48 hours, weighed and converted to kg ha<sup>-1</sup>.

#### *3.2.4.2 Water regulation*

I chose four indicators to estimate the effects of management on water flows: water infiltration rate, runoff, deep percolation and water stress during the 2015 rainy season. I measured infiltration as unsaturated hydraulic conductivity using a mini-disk infiltrometer from Decagon Devices (Pullman, WA, USA). The infiltration rate provides an indication of how quickly water can move into dry soil and is calculated in mm hr<sup>-1</sup>.

Runoff during the 2015 rainy season was estimated using hourly precipitation data, canopy cover and the measured infiltration rate for each plot. Precipitation data was collected at each farm using an automatic tipping bucket rain gauge from Davis

Instruments (Hayward, CA, USA; Model No. 7857) set up to measure rainfall at 10-minute intervals. Hourly precipitation intensity was calculated for each rain gauge location and then discounted by the canopy cover (% closure, see Table 3.2) to account for canopy interception. Hourly *Hortonian* runoff (Horton, 1933) was then estimated in mm as the difference between the discounted rainfall intensity and plot-measured infiltration rates when rainfall intensity exceeded infiltration rates. The sum of all runoff over the growing season was taken for each plot to estimate expected runoff. Deep percolation and water stress were estimated with crop water models developed by the FAO using the Penman-Monteith method (Allen et al., 1998), calibrated with biweekly soil moisture readings. A detailed explanation of daily water balance and deep percolation calculation methods is provided in Appendix A.

#### 3.2.4.3 *Pest and disease control*

Weed presence and indicators of the effects of pests and diseases were measured in each of the cultivated plots. Damage from pests and disease incidence was monitored in beans approximately 6 weeks after planting in late September, when pest pressures tend to be highest<sup>4</sup>. Forty plants were randomly selected and visually

---

<sup>4</sup> Due to resource constraints, only a single sampling could be performed for pest and disease incidence. Beans tend to be more susceptible to pests and diseases than maize, and pressures tend to be highest in late September; thus this was the chosen sampling approach. However, it should be noted that a single sampling may miss events due to temporal variability within seasons and between

inspected for pests and diseases in each plot and the severity of impact was ranked as none (0), low (1), medium (2) or high (3). Pest damage and disease incidence were ranked separately and the average value for each plot was taken to give two separate continuous scores (0-3) for each plot. Weed presence was measured in February 2016 using the same quadrats and methods used to measure soil mulch cover. Pest and disease incidence and weed presence were not evaluated in FOR plots since I was only interested in the impact of these on crops. Therefore, zero values were assigned for each of these indicators for the purpose of developing the Pest and Disease Control composite index (see Section 3.2.6.2).

#### *3.2.4.4 Soil composition*

Soil samples were collected in February 2016, taken from the 0-20 cm depth at four points in each of two subplots established within each experimental plot. Sub-samples from each subplot were composited for analysis and the results averaged to give a single value for each plot. Soils were air-dried and passed through a 2mm sieve prior to analysis of texture, pH (in H<sub>2</sub>O), total soil organic matter (SOM; Walkley and Black, 1934) and total nitrogen (N), available phosphorus, potassium (K), calcium (Ca) and magnesium (Mg) using the Mehlich-3 method (Mehlich, 1984) at the CENTA (Centro Nacional de Tecnología Agropecuaria y Forestal) laboratory in

---

years. While pest and disease did not appear to be an issue in the 2015 maize crop, it could be a concern in other years.

El Salvador. I used soil cores (7.25 cm diameter x 7.65 cm length) to calculate bulk density at 0-10 and 10-20 cm in four of the sub-sample points and an average value (0-20 cm) was taken for each plot.

#### *3.2.4.5 C storage*

I calculated C stored in aboveground woody biomass (AGWB) and topsoil (0-20 cm) as indicators of climate regulation services. In order to estimate AGWB I measured all trees and shrubs with a diameter at breast height (DBH, approximately 1.3 m) of at least 1 cm. All trees and shrubs were identified to the genus and species (when possible) and height and DBH measured in order to estimate AGWB from allometric equations (see Appendix B). I estimated C content as 49% of AGWB based on studies conducted in similar regions in Central America (Gómez-Castro et al., 2010; Hughes et al., 1999a; Suárez, 2002) and converted all values to Mg ha<sup>-1</sup>. SOM was converted to total organic C using a factor of 0.5 based on calculated ratios from a subset of the data and following recommendations made by Pribyl (2010). I then calculated topsoil C density by multiplying percent organic C by soil bulk density and converting values to Mg ha<sup>-1</sup>.

### **3.2.5 Biodiversity**

#### *3.2.5.1 Aboveground biodiversity*

I calculated species richness and the Shannon index (Shannon, 1948) for all trees with DBH ≥ 1 cm as indicators of aboveground biodiversity. Species richness was

calculated as the total number of uniquely identifiable species found in each plot in February 2016. The Shannon index was used as a measure of biodiversity to take into account the proportions of species found in a plot using the equation:

$$H = - \sum_{i=1}^S p_i \ln p_i \quad \text{[Equation 1]}$$

where  $H$  is the Shannon index,  $S$  is the total number of unique species observed within a plot and  $p_i$  is the proportion of  $S$  made up by the  $i$ th species (Magurran, 1988).

#### *3.2.5.2 Belowground biodiversity*

Macrofauna present in the soil were measured in July 2015 to develop four indicators of belowground biodiversity. Following the Tropical Soil Biology and Fertility (TSFB) method (Anderson and Ingram, 1993), soil pits (25 x 25 cm) were excavated to a depth of 30 cm and soil invertebrates (>2 mm) were hand sorted and stored in alcohol for subsequent identification of individuals to the level of species (when possible) in the laboratory at the National University of El Salvador. Two indicators of abundance were calculated as the number of individuals per m<sup>2</sup> based on the number of arthropods and earthworms, respectively, found in each pit. I also calculated macrofauna species richness and the Shannon index (see Equation 1) at the 'order' level of taxonomic rank.

### **3.2.6 Statistical analysis**

#### *3.2.6.1 Individual ES indicator variables*

I first compared treatment effects on each of the individual ES and biodiversity indicators described in Sections 3.2.3 – 3.2.5. I used a linear mixed effects model from the *nlme* package (Pinheiro et al., 2013) in R (R Core Team, 2013) with each indicator used, in turn, as the response variable, treatment as the fixed effect and farm location as the random effect. Distributional assumptions for each model were evaluated following Pinheiro and Bates (2000). When necessary, the response variable was transformed to achieve normality of within-group errors and random effects, and the '*varIdent*' variance function used to allow for non-constant variance among farm locations, following the approach utilized by Davis et al. (2012). Tukey's pairwise comparisons were made on models with a statistically significant treatment effect. Treatment effects and pairwise comparisons were considered statistically significant at  $p < 0.05$ .

#### *3.2.6.2 Composite indices*

In order to better compare and visualize the impacts of management on multiple ES, I developed composite indices of ES groups using an approach similar to that utilized by Velasquez et al. (2007) and others (e.g., Mukherjee and Lal, 2014) to develop soil quality indices. First, I converted the values of individual ES indicators to a common scoring unit ranging from 0.1 – 1 using the homothetic transformation

$$Y_i = 0.1 + \left( \frac{x_i - b_i}{a_i - b_i} \right) \times 0.9 \quad \text{[Equation 2]}$$

where  $Y$  is transformed value of the variable  $i$ ,  $x$  is the original variable value, and  $a$  and  $b$  are the maximum and minimum observed values of variable, respectively. In order to set all variables on a 'more-is-better' scale, variables originally on a 'more-is-worse' scale (e.g., pest presence and runoff) were converted using the reverse transformation

$$Y_i = 1.1 - \left( 0.1 + \left( \frac{x_i - b_i}{a_i - b_i} \right) \times 0.9 \right). \quad \text{[Equation 3]}$$

These transformations were performed on all individual variables except the provisioning and C storage services, which could already be combined using standardized units. In the case of provisioning services, I first calculated the total production value in USD as the sum of the quantity of each product multiplied by its average unit price. For C storage, above- and below-ground C stocks were summed to give total C stocks in Mg ha<sup>-1</sup>. Equation 2 was then applied directly to these two ES groups to develop their respective composite indices.

For all other ES groups, composite indices were calculated as the weighted sum of all transformed variables within each group. Weights were applied based on each variable's relative contribution to the variance within an ES group based on principle component analysis (PCA). The respective factor scores for each variable in the first two axes were used as weights, such that the final index was calculated as

$$CI = \sum Y_i w_{i,PC1} + Y_i w_{i,PC2} \quad [\text{Equation 4}]$$

where  $CI$  is the composite index,  $Y_i$  is the transformed value from Equation 2 or 3 for each variable  $i$ , and  $w$  is the factor score from the first and second principal component axes, respectively. Finally, each composite index was again reduced to the range 0.1 – 1 using Equation 2.

### *3.2.6.3 PCA of ES composite indices and correlation with field proxies*

For the four cultivated treatments (non-FOR), I assessed potential trade-offs and synergies between ES composite indices using PCA. This analysis was limited to cultivated plots since I was primarily interested in evaluating synergies and trade-offs between provisioning and regulating services within production management systems. In an effort to identify simple and measureable field proxies for multiple ES, I also explored relationships between proxies that can easily be measured in the field (Table 3.2) and the ES composite indices using Pearson's correlation analysis, again limiting analysis to cultivated plots.

**Table 3.2 Field proxies expected to correlate with multiple ecosystem services**

Category	Proxy	Description	Units
Trees	Stem Count (All)	The total number of boles	trees ha <sup>-1</sup>
	Stem Count (DBH < 10)	The number of boles with a DBH < 10 cm	trees ha <sup>-1</sup>
	Stem Count (DBH 10+)	The number of boles with a DBH of 10 cm or more	trees ha <sup>-1</sup>
	Canopy Cover	Binary visual assessment of canopy cover at 60 points along 3 transects using a periscope densiometer	Percent (%)
Mulch	Soil Mulch Cover (Visible)	Binary visual assessment of non-living vegetative soil cover at 60 points along 3 transects	Percent (%)
	Soil Mulch Cover (Biomass)	Oven-dry biomass of non-living vegetation collected from five 1-m <sup>2</sup> quadrats	kg ha <sup>-1</sup>
Soil	Infiltration	Unsaturated hydraulic conductivity measured with a Decagon mini-disk infiltrometer	mm hr <sup>-1</sup>
	Soil Organic Matter	Soil organic matter content (Walkley and Black, 1934)	%
	Bulk Density	Soil bulk density measured using ring (7.25 x 7.65 cm)	g cm <sup>-3</sup>

### 3.3 Results

#### 3.3.1 Individual ES indicator variables

##### 3.3.1.1 Provisioning services

Maize yields for all plots were lower than the 2007 national average of 3,200 kg ha<sup>-1</sup>, while bean yields were comparable to the national average of 900 kg<sup>-1</sup> (IICA, 2009). Both maize and bean yields tended to be highest under CONV and SMAS-1 management. Significant differences were only found between CONV and SMAS-2 for maize (Table 3.3), but maize yields in the ORG treatment averaged about half that for CONV and SMAS-1. Fuelwood production was about 300% and 50% higher in the SMAS-2 and SMAS-1 treatments, respectively, compared to CONV and ORG.

While fuelwood production increases were substantial, their value relative to crop production was low. Based on current prices, the value of increased fuelwood production in the SMAS-2 is \$44.00 ha<sup>-1</sup> yr<sup>-1</sup>, or about 8% of average farm revenue under CONV management.

#### *3.3.1.2 Regulation and maintenance services*

Soil mulch biomass was highest in the FOR and significantly higher under agroforestry management (SMAS-1 and SMAS-2) compared to management with fewer trees (CONV and ORG). Change in erosion pin height was inversely correlated with soil mulch cover, suggesting that increased soil mulch cover contributed to reduced erosion (see Chapter 4). However, statistically significant differences in erosion pin height could not be detected between any treatments.

FOR tended to have higher rates of water infiltration, although no significant differences were found between any treatments. The SMAS-2 and FOR treatments had the best values of the modeled indicators of water flows (increased deep percolation and reduced runoff and drought stress). Weed biomass was significantly reduced in the SMAS treatments compared to CONV and was negatively correlated with soil mulch cover (see Appendix A, Figure A - 1). Pest and disease presence also tended to be lower in the two agroforestry treatments, although significant differences were only detected for pest presence between SMAS-2 and ORG.

Soil properties varied more by farm than by treatment (Figure A - 2) and I found no obvious trends or significant differences between treatments for individual properties. FOR stored significantly more AGWB-C than all other treatments, and nearly 10 times as much as CONV. The SMAS-2 system maintained about half the AGWB-C stored in FOR and four times as much as CONV, while the SMAS-1 treatment doubled AGWB-C compared to CONV. However, differences among production systems were not statistically significant for either C pool.

#### *3.3.1.3 Biodiversity*

Tree species diversity (both for richness and the Shannon index) was significantly increased with agroforestry management. The tree species diversity of the SMAS-1 and SMAS-2 systems nearly matched that of FOR and maintained twice as many species compared to CONV, but was not significantly different from ORG. Overall macrofauna abundance tended to be higher in cultivated plots than in FOR while macrofauna diversity showed the opposite trend. Earthworm abundance tended to be highest in the ORG and SMAS-1 plots; however, no statistically significant differences were found for any of the belowground biodiversity indicators measured.

**Table 3.3 Results of statistical analysis of individual ecosystem service indicators by treatment**

Mean value for ecosystem service (ES) indicators by treatment. P-value denotes the significance of the fixed-effect (i.e., treatment) in the linear mixed effects model. Different letters denote significant differences ( $p < 0.05$ ) between treatments based on Tukey pairwise comparisons. N/A signifies data was not collected for that treatment and it was not included in statistical analysis. CONV = conventional management; ORG = organic (conventional management without chemical inputs); SMAS-1 = the slash-and-mulch agroforestry system, converted from CONV; SMAS-2 = the same as SMAS-1, but converted from FOR and; FOR = forest-fallow.

ES Group	ES Indicator	Unit	p-value	CONV	ORG	SMAS-1	SMAS-2	FOR
<i>Provisioning</i>								
Crop production	Maize yield <sup>†</sup>	kg ha <sup>-1</sup>	0.002	2392 b	1033 b	1937 b	457 a	N/A
	Bean yield	kg ha <sup>-1</sup>	0.088	978	891	793	503	N/A
	Jocote yield	# ha <sup>-1</sup>	0.022	0.0 a	0 a	1133 b	0 a	N/A
Fuelwood production	Fuelwood harvest	cargas ha <sup>-1</sup>	0.029	5.50 a	6.05 a	8.25 ab	16.50 b	N/A
<i>Regulation and Maintenance</i>								
Erosion Control	Erosion	mm	0.487	11.7	12.2	9.7	10.2	9.3
	Soil mulch cover <sup>§</sup>	kg ha <sup>-1</sup>	< 0.001	4628 a	4312 a	6191 b	7288 c	6848 c
Water Regulation	Drought stress	prop. of days	0.149	0.42	0.40	0.39	0.36	N/A
	Runoff <sup>†</sup>	mm	< 0.001	257 b	159 b	173 b	5 a	0 a
	Deep percolation	mm	< 0.001	193 a	234 a	235 a	367 b	420 b
	Infiltration <sup>†</sup>	mm hr <sup>-1</sup>	0.128	5.52	11.31	8.99	16.02	18.98
Pest & Disease Control	Weed cover	kg ha <sup>-1</sup>	0.012	2337 b	1770 ab	1094 a	872 a	N/A
	Pest presence	score (0-3)	0.024	1.24 ab	1.34 b	1.04 ab	0.99 a	N/A
	Disease presence <sup>†</sup>	score (0-3)	0.035	1.24 ab	1.57 b	1.24 ab	0.81 a	N/A
Soil Composition	pH	pH units	0.846	5.59	5.56	5.41	5.59	5.64
	Phosphorus (P) <sup>†</sup>	mg kg <sup>-1</sup>	0.992	22.63	15.29	22.65	29.97	44.87
	Potassium (K)	mg kg <sup>-1</sup>	0.996	235	225	227	221	226
	Calcium (Ca)	cmolc kg <sup>-1</sup>	0.863	12.42	11.29	13.08	11.83	11.49
	Magnesium (Mg)	cmolc kg <sup>-1</sup>	0.930	4.52	3.87	4.31	4.12	4.05
	SOM	%	0.709	4.29	4.10	4.35	4.54	4.76
Carbon (C) Storage	AGWB-C <sup>†</sup>	Mg ha <sup>-1</sup>	0.001	3.9 a	9.6 ab	8.2 ab	16.9 bc	34.3 c
	Soil C	Mg ha <sup>-1</sup>	0.715	28.8	24.9	28.1	30.5	31.4
Aboveground biodiversity	Tree/shrub richness	# of species	< 0.001	6 a	7 ab	13 bc	14 cd	20 d
	Tree/shrub diversity <sup>†</sup>	Shannon index	0.001	1.36 a	1.61 ab	2.12 bc	2.19 c	2.36 c
Belowground biodiversity	Arthropod presence <sup>†</sup>	# of individuals	0.713	1903	1188	2823	1664	1449
	Earthworm presence <sup>§</sup>	# of individuals	< 0.001	86 a	138 bc	153 c	142 c	96 ab
	Macrofauna richness	# of species	0.329	13	13	14	12	16
	Macrofauna diversity	Shannon index	0.393	1.80	1.77	1.42	1.47	1.85

<sup>†</sup> Denotes that the ES indicator variable was transformed to meet model assumptions.

<sup>§</sup> Denotes that non-constant variance among farms was detected and incorporated into the model.

### **3.3.2 Composite ES indices**

The treatments with more trees (i.e., SMAS and FOR) tended to have higher values for most ES indices, with the exception of Production Value, Soil Composition and Belowground Biodiversity (Table 3.4). At the end of the three-year study period, tree densities in the SMAS treatments ranged from 1,700 to 3,600 trees ha<sup>-1</sup>, averaging about half that of the FOR treatment (mean = 3,883 trees ha<sup>-1</sup>) and more than double the densities of the CONV and ORG treatments, which averaged 517 and 867 trees ha<sup>-1</sup>, respectively (Table A - 1). The mean Production Value index for CONV was nearly double that for SMAS-2, but results were highly variable between sites and no statistically significant differences were found (Table 3.4). Pest and Disease Control was significantly higher in the SMAS-2 treatment compared to CONV and ORG, with SMAS-1 falling in the middle.

Erosion Control was lowest for ORG and CONV and highest for FOR, and index values for SMAS-2 and SMAS-1 were not significantly different from FOR. Water Regulation and Aboveground Biodiversity followed similar trends and SMAS-2 was not significantly different from FOR for either index. C Storage in FOR was 2-3 times higher than CONV, ORG, and SMAS-1, but again not significantly different from SMAS-2. No significant differences were found between treatments for the Soil Composition and Belowground Biodiversity indices, although FOR tended to provide higher values for these ES.

**Table 3.4 Ecosystem service composite index values by treatment**

Mean index value by treatment. P-value denotes ANOVA of the LME model and letters denote significant differences ( $p < 0.05$ ) between treatments based on Tukey pairwise comparisons. CONV = conventional management; ORG = organic (conventional management without chemical inputs); SMAS-1 = the slash-and-mulch agroforestry system, converted from CONV and; SMAS-2 = the same as SMAS-1, but converted from FOR and; FOR = forest-fallow.

ES Composite Index	p-value	CONV	ORG	SMAS-1	SMAS-2	FOR
<i>Provisioning</i>						
Production Value	0.105	0.56	0.41	0.53	0.32	
Pest & Disease Control	< 0.001	0.34 a	0.35 a	0.53 ab	0.64 b	1.00 c
<i>Regulation and Maintenance</i>						
Erosion Control	0.006	0.36 a	0.31 a	0.59 ab	0.60 ab	0.71 b
Water Regulation	0.007	0.23 a	0.25 a	0.25 a	0.31 ab	0.53 b
Soil Composition	0.832	0.55	0.48	0.54	0.51	0.61
Carbon (C) Storage	0.003	0.25 a	0.26 a	0.28 a	0.42 ab	0.66 b
<i>Biodiversity</i>						
Aboveground Biodiversity	< 0.001	0.45 a	0.53 ab	0.73 bc	0.76 c	0.89 c
Belowground Biodiversity	0.520	0.54	0.55	0.54	0.34	0.65

### 3.3.3 PCA of ES indices and correlation with field proxies

The first two principle components explain 48.1% of the variance in the composite indices, and a distance biplot shows the relationships between ES (Figure 3.1).

Along the first axis (PC1), negative relationships exist between Production Value in one direction and Erosion Control and Aboveground Biodiversity in the other (see Table A - 2 for relative contribution of indices to each axis). Positive relationships were found between Production Value, Water Regulation, Pest and Disease Control, Soil Composition and Belowground Biodiversity. Along the second axis (PC2), however, all ES indicators are moving in the same direction, indicating potential synergies between all indicators. The two SMAS treatments had comparable scores and score distributions, as represented by the overlapping and similarly shaped

ellipses in Figure 3.1. Scores for the CONV treatment were tightly grouped, distributed primarily along the first axis, while scores for ORG were more variable.

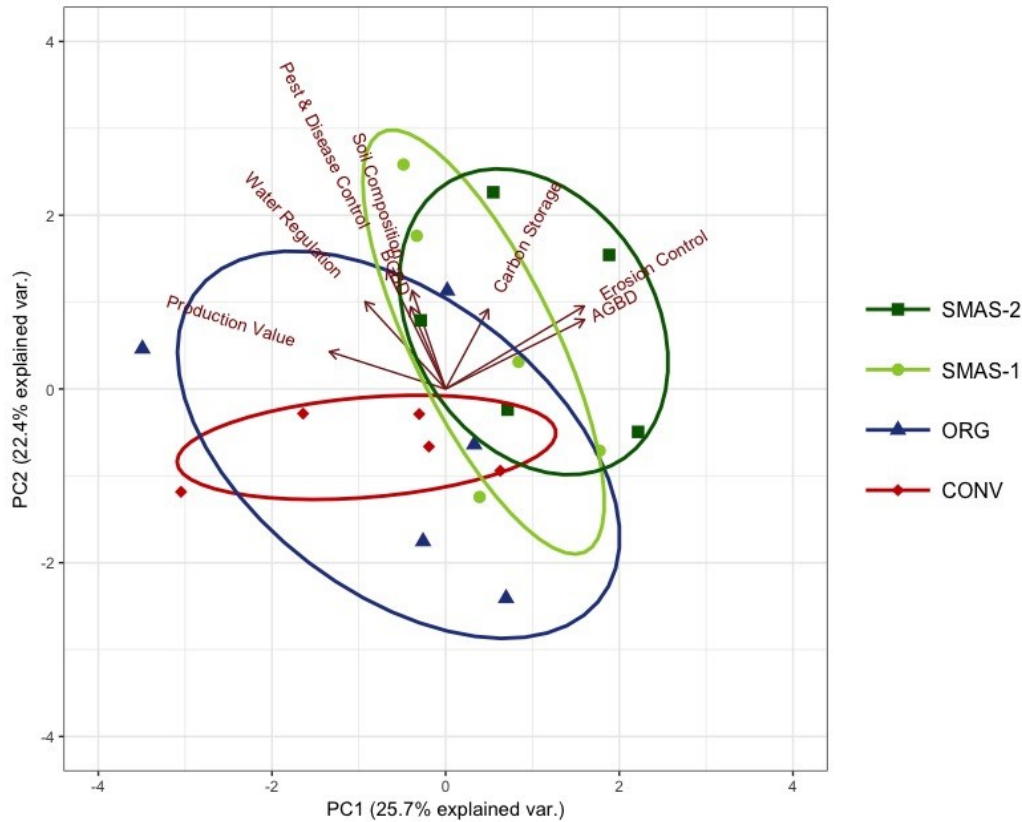


**Figure 3.1 Co-variation among ecosystem services indices for cultivated treatments**

Distance biplot of the (scaled) first two principal components of all ecosystem service composite indices for cultivated treatments: CONV = conventional management; ORG = organic (conventional management without chemical inputs); SMAS-1 = the slash-and-mulch agroforestry system, converted from CONV and; SMAS-2 = the same as SMAS-1, but converted from forest-fallow. AGBD and BGBD are aboveground and belowground biodiversity, respectively. See Table A - 2 for the relative contributions of indices to each principal component.

In exploring potential field proxies, significant correlations were found with at least one field proxy for all ES indices in cultivated treatments, but no one field proxy was indicative of all 8 (Figure 3.2). Stem count of large trees (DBH 10+ cm) was significantly correlated with the greatest number of composite indices, with positive correlations with Pest and Disease Control, greater Erosion Control and Aboveground Biodiversity and a negative correlation with Belowground Biodiversity. The number of large trees was more highly associated with the C Storage index, while measuring small trees (DBH < 10 cm) better captured Aboveground Biodiversity. Canopy cover, soil mulch cover and soil organic matter all were significantly correlated with half of the indices, with some overlap among them.

A mass-based measurement of soil mulch cover was more highly correlated with ES indices compared to a visual estimation. Infiltration was significantly correlated with Pest and Disease Control and was the only proxy associated with Water Regulation. Soil organic matter was positively correlated with increased Production Value and Pest and Disease Control.

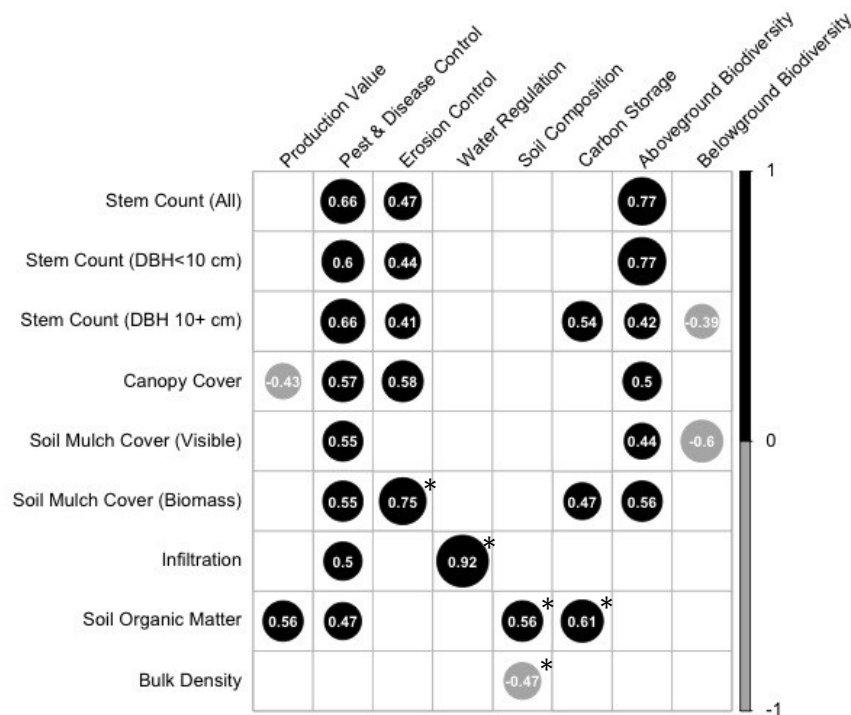


**Figure 3.2 Correlation matrix of field proxies and ecosystem service indices**

Pearson's correlation results for field proxies (rows) and ES composite indices (columns). Dark circles represent positive correlations and light-grey circles negative correlations. Larger circles indicate a stronger correlation. Only significant correlations ( $p < 0.10$ ) are shown. \* Denotes field proxies are directly included in the development of the ES composite index.

## 3.4 Discussion

### 3.4.1 ES indicators and indices

#### 3.4.1.1 Production of crops and fuelwood

Results of this study indicate that the SMAS can provide multiple ES, with potentially minimal reductions in farm productivity. Crop yields in the SMAS-1 were

comparable to CONV and ORG while also producing fruit and fuelwood, demonstrating that strategic management of trees can diversify production without compromising overall crop production value in these systems. However, production did not increase under SMAS management, as was found in neighbouring Honduras (Castro et al., 2009; FAO, 2005). There are several possible reasons for this.

First, El Salvador has the highest average maize yields in Central America, more than double that of Honduras (IICA, 2009). Low yields under conventional management in Honduras are likely the result of lower incomes that are associated with reduced use of fertilizers and improved seed. Thus, the productivity gains from the SMAS observed in Honduras may be unique to local circumstances, especially when compared to El Salvador where yields are nearer to their biophysical potential.

Meanwhile, bean yields under both SMAS treatments and maize yields under SMAS-1 were similar to those achieved with the SMAS in Honduras (Castro et al., 2009).

Maize yields in the SMAS-2 were substantially lower and it is suspected that lateral shading from the surrounding forest may have had an impact. It was difficult to find large enough swaths of FOR in suitable sites to clear a buffer around the treatment, and SMAS-2 plots were often bordered by forest on 2 or 3 sides, resulting in substantial shading that appeared to negatively impact crop yields. I suspect this would not be an issue in the case where an entire farm field was managed as SMAS-2. However, canopy cover was negatively correlated with the Production Value

index in cropped treatments (Figure 3.2), indicating that careful management of trees is important to minimize light competition (Beer et al., 1998).

While maize yields under ORG management were less than half that of CONV, average bean yields were comparable to CONV. The contrasting results for maize and beans highlight that N supply may be an issue in the ORG treatment, since beans can supply a substantial portion of their N requirements through fixation.

Additionally, the ORG treatment may be improving micronutrient availability and buffering pH, allowing beans to do well in this treatment despite having lower inputs of labile N and P. Beans are especially sensitive to soil acidity, which can increase with the application of ammonium sulphate. Yield impacts on beans may be especially important to producers as prices for beans in Central America generally, and in El Salvador specifically, have been rising steadily and tend to be more volatile than maize prices (IICA, 2009).

Increased fuelwood and timber production is often cited as a benefit of agroforestry systems that may incentivize farmers to adopt practices such as the SMAS (e.g., Current et al., 1995b; de Sousa et al., 2016). While fuelwood production in the SMAS-2 treatment was triple that for CONV, fuelwood value was low relative to crop value (about 8% of farm revenue, see Table A - 3). It is unclear whether the value of fuelwood alone would be sufficient to incentivize farmers to adopt the SMAS, especially if profitability is diminished by reduced yields or increased labor costs. It is also unclear how fuelwood production in the SMAS compares to potential

production in FOR. While farmers often harvest fuelwood from forest-fallows, I did not attempt to measure fuelwood production in FOR and recognize that this would increase the Production Value index for FOR. Further research on fuelwood harvesting and household consumption is needed to understand to what degree the SMAS might offset fuelwood collection in forests and fallows.

#### *3.4.1.2 Pest and disease control*

Results from this study may alleviate concerns expressed by some farmers and technicians in the area that the SMAS and organic management would result in increased pest and disease pressures. The pest control methods used in the ORG treatment performed as well as CONV management and the two SMAS treatments showed reduced presence of pests, weeds and disease, suggesting the SMAS might enhance control. Other studies have shown that diverse non-crop habitat can harbor pest predators, resulting in improved pest control (Bianchi et al., 2006; Karp et al., 2013). Weed control is likely a result of suppressed weed emergence caused by increased mulch cover in the SMAS (Schipanski et al., 2014), as demonstrated by a strong negative correlation between mulch and weed presence (Figure A - 1).

Disease control may be a result of multiple plant-soil interactions such as improved infiltration (Abawi and Corrales, 1990), enhanced soil biological diversity (Kremen and Miles, 2012) and better plant nutrition (e.g., Zörb et al., 2014).

#### *3.4.1.3 Erosion control*

The two SMAS treatments increased soil mulch cover, which appears to be leading to reduced soil erosion. Soil mulch cover and absolute change in erosion pin height were significantly correlated across treatments (see Chapter 4), probably resulting from both direct (e.g., raindrop interception and reduced runoff velocity) and indirect (e.g., increased SOM leading to improved soil structure and infiltration) mechanisms (Elwell and Stocking, 1976). I used absolute change in erosion pin height as an indicator of relative erosion as it was significantly correlated with slope and sediment captured in erosion pits installed on a subset of the plots (see Chapter 4). Soil losses (sediment < 2 mm) in pits ranged from 300 to 1,200 kg ha<sup>-1</sup> yr<sup>-1</sup>. Studies quantifying soil loss in Central America are scant, but a study from Jamaica (a slightly wetter climate) found sediment losses of 2,000 to 3,000 kg ha<sup>-1</sup> yr<sup>-1</sup> and also demonstrated reduced erosion with agroforestry management (McDonald et al., 2002). My findings strengthen the link between agroforestry, soil mulch cover and erosion control, and can support erosion modeling and risk mapping for landscape planning (Delgado and Canters, 2012).

#### *3.4.1.4 Water regulation*

Infiltration rates were similar to those found in other studies in Central America (e.g., Tully et al., 2012) and there was a strong tendency for increased infiltration on non-CONV treatments receiving elevated inputs of organic matter from trees and composted manure. Decomposition of organic material can increase SOM, which is

commonly associated with increased soil aggregation and infiltration (Craswell and Lefroy, 2001; Franzluebbers, 2002), and indeed positive correlations exist between SOM and infiltration rates (Figure A - 3). While significant differences in infiltration rates were not detected between treatments, I did find significant results for indicators derived from water balance modeling, suggesting that the compounding effects of infiltration with other site parameters may lead to even more substantial off-site impacts for water quality and quantity.

For example, increased infiltration rates combined with rainfall captured by the tree canopy and increased evapotranspiration from trees have a multiplicative effect to reduce runoff (Bruijnzeel, 2004). In this study, modeled runoff was near zero for FOR and SMAS-2, demonstrating the potentially dramatic ES benefits for downstream water quality and flood protection. As a result, forests and agroforestry systems also enhance groundwater recharge, and deep percolation was approximately doubled in FOR and SMAS-2 compared to CONV.

#### *3.4.1.5 Soil composition*

The 3-year duration of this study likely was not sufficient to observe changes in soil properties with land management. Furthermore, there was significant spatial variability in soil properties (Figure A - 2), which can complicate analysis of land-use impacts (Holmes et al., 2005). But some trends in my results do suggest that increased tree density may improve soil quality.

FOR had the highest mean index value for Soil Composition, driven by higher available P, SOM and pH, and lower bulk density. These are among the most important chemical and physical soil properties for cultivation in tropical climates (Velasquez et al., 2007), and studies from other regions show that management following the SMAS principles can mediate these properties over time (e.g., Kremen and Miles, 2012; Nziguheba et al., 2005; Thomazini et al., 2015). However, longer trials are needed to evaluate the long-term impacts of the SMAS on these soil properties in the Mesoamerican maize-bean context.

#### *3.4.1.6 C storage*

Total C storage in the SMAS was similar to that found for other crop and silvopasture agroforestry systems (e.g., Henry et al., 2009; Luedeling et al., 2011), but lower than that generally found for fruit, timber or coffee agroforestry (e.g., Kirby and Potvin, 2007). Results of this study indicate that adoption of the SMAS-2 could increase C stocks by an average of 14.8 Mg ha<sup>-1</sup> over CONV management. This amount is likely an underestimate since it does not account for belowground biomass C (e.g., root biomass), which can contain 20 to 30% (or more) of AGBW (Brown, 2002). However, I chose not to include belowground biomass as it is highly variable, especially in agricultural landscapes (Kuyah et al., 2012), and may confound validation of biomass C predictions from remote sensing, the focus of Chapters 5 and 6.

It is difficult to determine from this study whether this amount of C would be sufficient to enable participation in C markets, as this would depend heavily on C prices, transaction costs and the time over which this change in C is averaged, which would be determined by the duration of the rotation with FOR. However, my findings show that regional C storage potential is substantial. There are an estimated 6 million hectares under active maize-bean cultivation in Central America alone (Dixon et al., 2001), indicating that C storage could be increased by up to 89 million tons with widespread implementation of the SMAS.

Increased C storage is expected to come primarily from AGWB as I found no significant differences in soil C stocks between treatments, although the same issues of study duration and spatial variability discussed in Section 3.4.1.5 apply here. However, maintaining regular inputs of organic matter to the soil is especially important in the tropics due to rapid decomposition and SOM turnover, and it is possible that soil C stocks under CONV management would decrease over time (Fonte et al., 2010). The ORG treatment did receive elevated inputs of organic matter in the form of composted manure, but transport of such materials in steep landscapes is challenging.

Despite the high density of small trees in the SMAS, AGWB-C was principally driven by the number of large trees (DBH > 10 cm) within a plot. Others have noted the disproportionate contribution of large trees not only to C storage (e.g., Chave et al., 2001) but also to wildlife habitat and cultural values in smallholder systems

(Marinidou et al., 2013). Management of large trees is therefore requisite if C sequestration is to be a primary objective of the SMAS, and would likely enhance other ES not measured in this study.

#### *3.4.1.7 Biodiversity*

Both SMAS approaches maintained species richness comparable to that found by other agroforestry studies in Central America using similar sized plots (Ferguson et al., 2003; Richards and Méndez, 2014). Species richness in the SMAS approached levels observed in FOR, which was low relative to forests in more humid tropical climates (e.g., Chave et al., 2001; Finegan and Delgado, 2000), although differing plot sizes and species assemblages makes comparison difficult without further analysis (Gotelli and Colwell, 2001). Many of the trees in the SMAS came from natural regeneration, as observed in other agroforestry systems in Central America (e.g., de Sousa et al., 2016). However, planting trees, as was done in the SMAS-1 treatment, may help to more quickly achieve biodiversity goals, especially if converting low diversity conventional fields to the SMAS. Planting also provides an opportunity for farmers to select species and diversify production (e.g., fruit trees and fodder), thereby increasing the relative value of biodiversity to farmers.

The tendency for increased macrofauna abundance in cultivated plots compared to FOR aligns with findings from studies on the SMAS in neighbouring Honduras (Fonte et al., 2010; Pauli et al., 2011). The Honduran studies found that secondary

forest plots contained lower macrofaunal abundance than agroforestry plots, perhaps due to lower quality litter in forests, which consist primarily of senesced leaves rather than pruned mulch (Fonte et al., 2010). While cultivation appeared to increase overall macrofauna abundance, I found lower species diversity in cultivated plots, which may reflect the dominance of hardy and adaptable fauna, and the loss of more sensitive taxa that can occur with forest conversion (Pauli et al., 2011; Rousseau et al., 2013). Finally, the lack of statistically significant differences for Belowground Biodiversity indicators between management practices may again reflect the high spatial variability of soil properties (Figure A - 2) and relatively short treatment period.

#### **3.4.2 ES synergies and trade-offs**

A PCA analysis of the relationships between ES by treatment showed that the SMAS better demonstrates potential ES synergies compared to CONV. The upper left quadrant of the distance biplot in Figure 3.1 (positive loading along the PC-2 axis and negative loading on the PC-1 axis) represents potential synergies between Production Value, Water Regulation, Pest and Disease Control, Soil Composition and Belowground Biodiversity. The tight directional grouping of Soil Composition, Water Regulation and Pest and Disease Control suggests synergies with strong theoretical underpinnings. For example, increased SOM is associated with higher infiltration rates, which in turn can reduce the incidence of bean diseases favored by high soil moisture content (Abawi and Corrales, 1990). The parallel loading for

Belowground Biodiversity may indicate further mediation of pests or diseases from host dilution (Kremen and Miles, 2012). The loading for Production Value runs in a similar direction, suggesting that these synergies among regulating services are translating into increased production.

All of the points lying within the synergistic portion of the biplot described above are from SMAS-1, SMAS-2 and ORG plots, showing that the plots with the highest values of multiple ES belong to these treatments. The directional spread of plots within each treatment (indicated by the ellipses in Figure 3.1) demonstrates the types of trade-offs or synergies occurring within each management system.

Groupings for the SMAS-1 and SMAS-2 plots are spread along the upper-left to lower-right diagonal, suggesting that the synergistic regulating ES mentioned above are more likely to translate into higher productivity for these plots, and low productivity occurs when provision for these ES is also low.

On the other hand, CONV plots tended to have a lower occurrence of synergies between multiple ES and instead showed trade-offs between Production Value and non-production ES, as indicated by negative loadings on the PC-2 axis and a directional spread along the PC-1 axis. Others have found similar trade-offs between provisioning and regulating ES in intensified agricultural landscapes (Kremen and Miles, 2012; Nelson et al., 2009; Pilgrim et al., 2010; Raudsepp-hearne et al., 2010; Schipanski et al., 2014), while trade-offs among regulating services were rarely observed (Pilgrim et al., 2010; Schipanski et al., 2014). ORG plots were more

variable as indicated by the wide ellipse and fell between the SMAS and CONV plots, suggesting that the best management within the conventional (non-tree-based) system may improve synergies slightly, but that the tree-based principles of the SMAS are central for the ES evaluated in this study.

### **3.4.3 *Field proxies for multiple ES***

By measuring just three field proxies – SOM and stem counts of small and large trees – one could ostensibly estimate the provision of all ES measured in this study except Water Regulation (Figure 3.2). Infiltration was the only field proxy significantly correlated with the Water Regulation index, and direct monitoring of infiltration rates may be required to ensure that water-related ES are accruing. However, given that many of the ES indicators used to develop the Water Regulation index were modeled rather than measured, it is possible that the model does not fully capture the complexity of hydrologic factors and therefore difficult to conclude that other proxies aren't associated with water-related ES. For example, SOM was significantly correlated with infiltration (Figure A - 3), but not the Water Regulation index.

The findings of this study emphasize the importance of monitoring trees of all sizes. Small trees are an important source of mulch, contribute to biodiversity and indicate the sustainability of the SMAS, since they represent healthy regeneration required to replace larger trees that may have a shortened lifespan due to pruning. Larger trees are critical for AGWB-C storage (Stephenson et al., 2014) and their abundance

does not correlate with lower yields, but strategic management to minimize canopy cover is required to avoid yield reductions (Figure 3.2).

While increased stem counts were correlated with several ES indices, the diversity of these trees may also be important, and measuring aboveground biodiversity may still be desirable. Since all of the SMAS plots in this study contained a diverse mix of tree species by design, it was impossible to compare against an agroforestry system with high stem counts and low diversity; but some studies have suggested that synergies exist between tree diversity and ES benefits (e.g., Richards and Méndez, 2014). Soil mulch cover appears to be an important field proxy for multiple ES, especially erosion control, although visible estimation may be a less reliable monitoring approach than biomass sampling (Figure 3.2).

#### ***3.4.4 Implications for management, ES monitoring and PES***

This study demonstrates that agroforestry can increase multiple non-production ES benefits compared to either CONV or ORG management, approaching the services provided by secondary forest-fallows in the study area (Figure 3.3 and Figure A - 4). In this 3-year study, I found no clear impacts of management on belowground biodiversity or soil composition, however it is noteworthy that these two indices were highly correlated (Figure 3.1 and Figure A - 4), supporting the growing evidence that biological, biophysical and biochemical interactions influence soil health (Brussaard et al., 2007).

For illustrative purposes I quantified the overall ES provision by summing all the ES composite indices for each treatment (Figure 3.3, inset). This value is highest for FOR (4.1 out of a maximum possible of 6.0), while the SMAS-2 and SMAS-1 treatments had intermediate values (about 25% lower than FOR) and the CONV and ORG treatments had the lowest values (about 45-50% lower than FOR).

Quantifying overall service provision could be a simple way to compare land management strategies, and is indeed the goal of some ES evaluation tools (Bagstad et al., 2013). However, such a quantitative approach presents several issues. First, the selection of ES indicators and indices can never be exhaustive and is by necessity arbitrary, constrained by methods, data availability, resources and evaluation objectives. For example, in this study, comparisons to the ORG system may be limited. The ES indicators measured were chosen primarily to test the expected benefits of tree-based systems. In the ORG treatment, agrochemical inputs were replaced with organic options, but the SMAS principles commonly associated with agroforestry and conservation agriculture were not implemented. It is possible that ORG management provides other ES benefits not measured in the study, such as increased mycorrhizal colonization and its associated benefits (Gosling et al., 2006) or enhanced crop pollination (Kennedy et al., 2013; Kremen et al., 2002).

Second, deciding how important individual indicators are to overall ES provision is not straightforward. I used PCA in an effort to objectively determine indicator weights for construction of the composite indices, but did not weight composite

indices for the overall provisioning index. Therefore, the relative weights (or importance) attributed to ES indicators determined the final ES index value, but ES indices equally contributed to the overall provisioning index. In practice, neither indicators nor indices can be weighted 'objectively', as different stakeholders have different perceptions of the relative value of services (Chan et al., 2016; Hauck et al., 2013), and demand for services varies over space and time (Chan et al., 2006). Weighting is problematic and controversial (Satterfield et al., 2013), but regional ES indices show promise as a strategy to rank ES provision and scale PES within a given context (e.g., Marinidou et al., 2013; Pagiola et al., 2007), and participatory approaches have begun to incorporate stakeholder values into relative ES weights (Satterfield et al., 2013; The Plan Vivo Foundation, 2013).

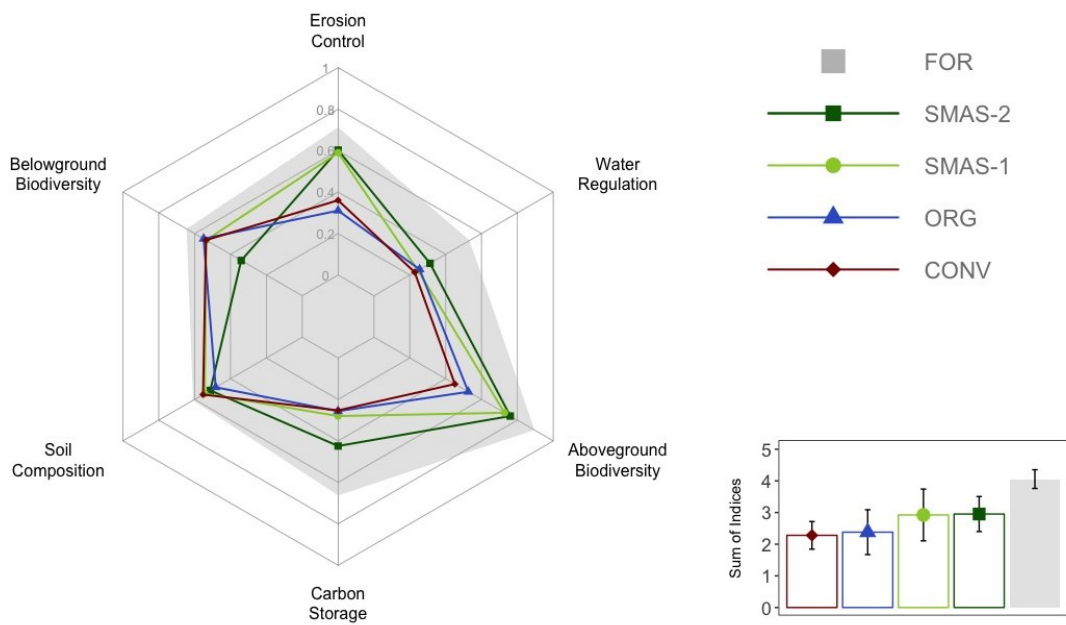


**Figure 3.3 Radar chart of non-production ecosystem services**

Comparison of non-production ecosystem service composite index values (main) and bar chart of total the sum total of all indices (inset; error bars denote standard deviation) by treatment. The shaded area represents the forest-fallow (FOR) reference treatment and lines show the four cultivated treatments: CONV = conventional management; ORG = organic (conventional management without chemical inputs); SMAS-1 = the slash-and-mulch agroforestry system, converted from CONV and; SMAS-2 = the same as SMAS-1, but converted from FOR.

Farmer involvement in this study and varying site conditions led to a wide range of tree densities and species in the SMAS treatments, highlighting the system’s adaptability. This flexibility is important for reasons outlined in Section 3.1, but presents challenges for quantifying the expected contribution of such systems to

individual ES indicators. This quantification is increasingly desired by programs seeking to enhance the provision of individual ES (Naeem et al., 2015). This study was able to provide empirical quantification for some indicators, but more importantly demonstrates a consistent pattern supporting the hypothesis that the principles of the SMAS do, in fact, enhance multiple ES and encourage synergies between them. My findings also suggest that diversification of farming systems and agroecological principles associated with SMAS implementation may be more important for ES supply than simply replacing chemical inputs with organic alternatives.

Finally, incentives such as PES and improved access to credit may be required for widespread adoption of the SMAS or organic management to occur. Profitability of the SMAS-1 was about the same as CONV, while SMAS-2 and ORG were lower (Table A - 3), demonstrating that direct incentives for farmers in the immediate term (e.g., increased fuelwood production, lower input costs and reduced labour) are low, at least in the context of this study area. Other potential benefits to farmers such as improved soil fertility and increased yields were not observed in this three-year study, suggesting they would only accrue in the long-term, and smallholder farmers without access to capital or secure land-tenure may struggle to invest in systems with long-term payoffs (Engel and Muller, 2016).

Incentives need to be combined with supporting policies and continuing collective action to address other issues. For example, Hellin et al. (1999) found that the SMAS

was not adopted where available land area was sufficient to allow shifting slash-and-burn agriculture to continue, and the lack of family labour due to out-migration can be a barrier to adopting new practices (Ayarza et al., 2010). Ayarza and Welchez (2004) noted the importance of policies banning burning and long-term interactions among diverse stakeholders to build knowledge and technical capacity.

Implementation of the SMAS combined with increased community awareness eventually led to a shift in perceptions, and land value under SMAS management in Honduras is now 30% higher than in areas without it (Ayarza et al., 2010).

In summary, I have three general recommendations for ES-related outreach, policy and incentive programs for hillside smallholder maize-bean growing regions:

- (1) Promote the *principles* of the SMAS (eliminating burning, maintaining a permanent vegetative soil cover or 'mulch', and; intercropping with diverse tree species)
- (2) Focus on *multiple* ES groups rather than tying incentives or regulations to a single ES
- (3) Design monitoring programs to measure field proxies (e.g., tree stem counts, SOM) that relate to multiple ES and reflect the principles of the SMAS, rather than seeking out binary definitions of agroforestry

### 3.5 Conclusions

Using controlled on-farm experiments, I empirically demonstrated that the SMAS improves some indicators of non-provisioning ES compared to conventional and organic management systems without trees. Results show that substantial ES benefits can accrue within just three years of conversion from conventional management (SMAS-1), comparable to those found for traditional SMAS establishment from a forest-fallow (SMAS-2). These ES increases can potentially be achieved without significant reductions to overall crop production value, although challenges with the study design (e.g, lateral shading in SMAS-2) make it difficult to determine the exact impact of mature SMAS on maize and bean yields.

The inherently flexible design of the SMAS addresses some of the critiques of previous agroforestry research, but leads to high variability, potentially limiting the ability to statistically detect ES enhancements in a study of moderate resources. By developing composite indices of multiple ES I was able to identify patterns showing that the SMAS enhances multiple ES and better capitalizes on synergies between regulating and provisioning ES compared to conventional management. Results for organic management were less clear, however the study was designed primarily to evaluate the ES benefits of agroforestry.

I also identified simple field proxies that correlate well with multiple ES, with important implications for management and monitoring strategies. For example,

monitoring schemes should measure both small and large trees, as small trees contribute to biodiversity and system sustainability, while large trees are critical for C storage. However, strategic management of large trees will be necessary to minimize canopy cover and potential negative yield impacts. Policies and incentives focused on multiple ES can support long-term collective action to build farmer knowledge and technical capacity, overcome any yield losses that may occur during transition and develop community awareness around the multiple ES benefits provided.

## **4 Improving the utility of erosion pins: absolute value of pin height change as an indicator of relative erosion rates**

### **4.1 Background and introduction**

Erosion pins are an inexpensive method to estimate hillslope soil erosion and deposition used by numerous studies with varied success (Benito et al., 1992; Diaz-Fierros et al., 1987; Edeso et al., 1999; Haigh, 1977; Hancock and Lowry, 2015; Shi et al., 2011; Sirvent et al., 1997). Typically, narrow metal pins are inserted into the soil to a known depth in a grid or transect pattern along a hillslope, and the length of the pin protruding from the soil is measured at multiple points in time (Haigh, 1977). Most studies calculate annual erosion/deposition rates (also called ground advance/retreat or ground lowering) as the mean net change in pin height for a given experimental unit, usually given in  $\text{mm yr}^{-1}$ . This mean net change value is often then converted to a unit mass per area (e.g.,  $\text{kg ha}^{-1} \text{yr}^{-1}$ ) using the soil bulk density (e.g., Benito et al., 1992).

This approach has the obvious advantage of quantifying erosion/deposition rates at a relatively low cost and intuitively it makes sense. While some studies have found that erosion pin data analyzed in this way is congruent with other erosion estimation methods and related variables (e.g., Edeso et al., 1999), many others have

observed weak or lacking relationships with erosion rates estimated using other methods and with variables that one would expect to be strongly correlated with erosion, such as slope or precipitation. For example, a review by Haigh et al. (1977) reported that several studies found no correlation between erosion pin measurements and topographic variables, including slope. Diaz-Fierros et al. (1987) did not find a relationship between soil erosion estimated from pins and that estimated by the Universal Soil Loss Equation (USLE) in northern Spain, and also noted a lack of correlation with slope. More recently, Hancock et al. (2010) found no apparent relationships between erosion/deposition patterns and hillslope position or soil C concentration at a study site in Australia measured using erosion pins. Likewise, they found no correlation between pin data and caesium-137 ( $^{137}\text{Cs}$ ) radioisotope concentrations (an indicator of soil erosion). Another recent study in Australia did not find statistically significant relationships between erosion pin data and topographic variables derived from high-resolution LiDAR or rainfall data (Hancock and Lowry, 2015).

The incongruence between erosion estimated from pins and other methods, and the lack of correlation with erosion-related variables, calls into question the utility of using the mean net change in pin height for certain applications – for example, when evaluating the treatment effects of different land-management practices. To further elaborate, in a location experiencing large amounts of soil movement, some pins will experience high rates of erosion while others will experience high rates of

deposition between measurements. When the mean net change value is taken for a given experimental unit and measurement period, pins experiencing erosion (a positive change value) and pins experiencing deposition (a negative change value) will offset each other, and the final change value is often near zero (Luffman et al., 2015). This can mask the magnitude of overall soil movement, which could limit the ability evaluate the soil conservation impacts of different land management options and may explain the lack of correlations observed in the aforementioned studies. Some studies have noted that the spatial pattern of erosion pin data is more randomly distributed than that of erosion predicted by other methods (e.g., Shi et al., 2011), suggesting that in an erosive environment individual pins will experience both erosion and deposition at varying and random rates between measurements. In many cases, soil may move downslope in waves, and soil deposited at a pin in a given measurement period may be more available for transport during subsequent rain events (Hancock and Lowry, 2015).

An alternative (or complementary) approach to using the mean net change value that incorporates the 'real number' change in pin height (i.e., both positive and negative change values) is to use the mean absolute value of pin height change to capture the overall magnitude of soil movement and erosive activity (Couper et al., 2002; Luffman et al., 2015). Using the absolute value, rather than net pin height change, assumes that both soil loss and deposition around a pin are part of the erosion process, therefore avoiding some of the challenges mentioned above.

However, to the best of my knowledge, the absolute value has only been utilized in one other pin-based study of hillslope erosion (Luffman et al., 2015), and has only been directly discussed in the context of river bank erosion (Couper et al., 2002).

I propose that the absolute value of pin height change offers a valid and underutilized indicator of hillslope soil erosion that may be especially useful in comparative studies assessing the soil conservation potential of differing land management practices. In order to test this assumption, I compared both the absolute and 'real number' change in erosion pin height against modeled erosion, related factors (e.g., slope and soil cover), and soil loss collected in erosion pits within experimental plots under five hillslope agricultural management systems of varying soil conservation potential.

## **4.2 Methods**

### ***4.2.1 Erosion pin installation and measurement***

This study was conducted across 25 experimental plots (12 x 20 m), separated into five treatments replicated on five farms within the municipality of Las Vueltas (see Section 2.2 and Figure 2.1). The plots were part of the larger study conducted in Chapter 3 comparing ecosystem service provision under four maize-bean production systems – conventional (CONV), organic (ORG) and two 'slash-and-mulch' agroforestry systems (SMAS-1 and SMAS-2) – and a forest-fallow (FOR)

reference site. A complete description of the experiment and its motivations can be found in Section 3.2.

Steel erosion pins (0.6 cm diameter, 40 cm length) were installed in the experimental plots in May 2013, prior to maize planting. Pins were placed in a grid pattern of 3 columns and 6 rows at 3 m x 3 m spacing for a total of 18 pins per plot (Figure 4.1) Pins were hammered into the soil perpendicular to the slope, leaving approximately 10 cm protruding from the soil surface (Figure 4.2), following recommended practices (Haigh, 1977).

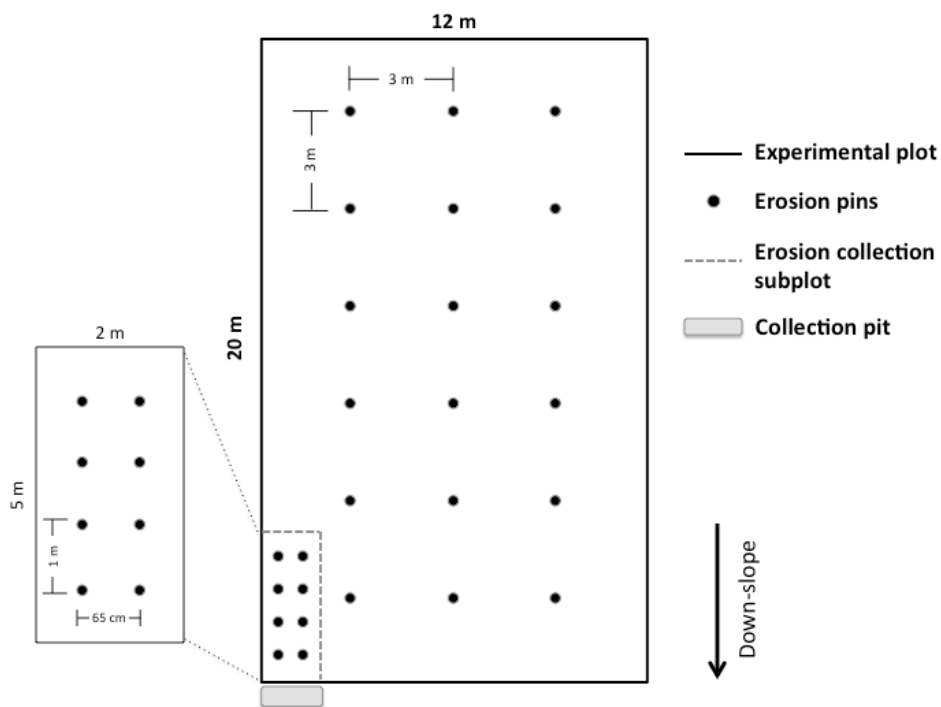


**Figure 4.1 Diagram of erosion pin setup**

The gridded layout of erosion pins within the experimental plot (18 pins) and erosion collection subplots (8 pins, inset).

Eight additional pins were installed in 2 x 5 m erosion collection subplots established within a subset of the larger experimental plots (Figure 4.1). These subplots were installed on 6 of the cultivated treatment plots, 3 under conventional management (CONV) and 3 under one of the 'slash-and-mulch' agroforestry systems (SMAS-1). Each collection subplot was bordered with metal sheeting protruding at least 10cm vertically from the soil surface to prevent overland run-on of water, soil and other debris from upslope. Sediment was collected approximately biweekly from plastic-lined collection pits (approximately 1.8 x 0.5 x 0.5 m) located on the downhill edge of each subplot. Collected sediment was oven-dried for 24 hours at 105° C, sieved to 2 mm, and both the coarse and fine fractions were weighed and converted to Mg ha<sup>-1</sup>. Data from one collection subplot was removed due to a failure of the metal border and substantial run-on into the collection pit from outside the subplot.

For this study, pin protrusion was measured 7 times between April 2015 and February 2016 (covering the entire 2015 rainy season) using a digital depth gauge (0.02 mm precision; Figure 4.2), and each pin was checked for damage or disturbance during every measurement. Only pins that remained undisturbed for the entire study period were used to calculate the mean overall change in pin height for each plot (n = 25) and subplot (n = 5), calculated as both the real number value and absolute value of pin height change in mm over the 10-month period. The real

number value is the average change in pin height during the measurement period and can be positive or negative. Positive numbers indicate erosion from around the pin (increased pin protrusion) and negative numbers indicate deposition. The absolute value (always positive) indicates the magnitude of both erosion and deposition, but does not distinguish between the two. Pin data was cleaned prior to analysis by removing extreme values, identified as measurements exceeding three standard deviations of the sample distribution of all undisturbed erosion pins.

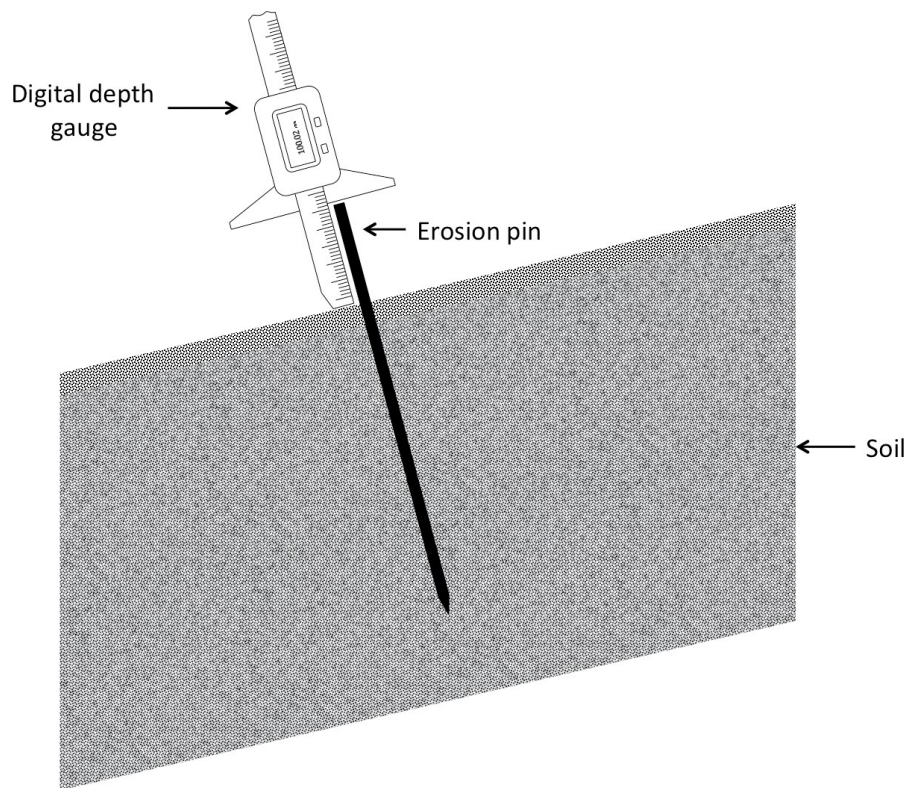


**Figure 4.2 Graphical depiction of installed erosion pin measured with a digital depth gauge**

#### 4.2.2 Correlating erosion pins with modeled and measured erosion

I used data collected from the 240-m<sup>2</sup> experimental plots to develop erosion-prediction factors and model annual soil loss using the RUSLE (Renard et al., 1997) as

$$A = R * K * L * S * C * P \quad \text{[Equation 1]}$$

where  $A$  is annual computed spatial average soil loss, in Mg ha<sup>-1</sup> yr<sup>-1</sup>;  $R$  is a rainfall-runoff erosivity factor;  $K$  is a soil erodibility factor;  $L$  is a slope length factor;  $S$  is a slope steepness factor;  $C$  is a cover management factor and;  $P$  is a support practice factor.

The  $R$  factor was calculated following Renard et al. (1997) and using the equation from Brown and Foster (1987) cited within. Precipitation data was collected in 10-minute intervals from automatic tipping bucket rain gauges (Davis Instruments; Hayward, CA, USA; Model No. 7857) installed at each farm. The  $K$  factor was developed using the equation provided by Lim et al. (2011), converted to SI units (Renard et al., 1997). This equation requires the percentage of sand, silt and clay present in the soil, which was obtained from soil samples collected in each plot and analyzed at the CENTA (Centro Nacional de Tecnología Agropecuaria y Forestal) laboratory in El Salvador (see Chapter 3). The  $L$  and  $S$  factors were computed from the slope length (20 m) and degree slope of each plot following Renard et al. (1997) and McCool et al. (1987) cited within. Slope was measured in degrees up- and down-

slope from the center of each plot using a clinometer, and the average taken as the overall plot slope.

The *C* factor (cover management) was calculated based on canopy- and surface-cover subfactors (Renard et al., 1997). The canopy-cover subfactor (CC) was developed using the fraction of land surface covered by canopy and the average tree canopy height measured in each plot (see Chapter 3). The surface-cover subfactor (SC) was calculated from the percentage of land area covered by surface cover, using a surface roughness value of 0.80 (representing no-tillage) and a coefficient constant of 0.035, typical for cropland where rill and interill erosion occur (Renard et al., 1997). A P-value of 1.0 was assigned to all plots, since no conservation practices were employed apart from cover management, which was already included in the C-factor.

I compared both the absolute value and net real number value of pin height change in each of the 25 experimental plots (excluding the pins in the collection subplots) to modeled annual erosion (*A*) using Pearson's correlation to assess the likelihood that each pin method is related to expected erosion occurring in the plot. I also checked the correlation with each of the RUSLE erosion-prediction factors to evaluate how strongly each pin assessment method was related to rainfall, soil, topographic and vegetation features.

In addition to comparing pin data to modeled erosion in the experimental plots, I checked correlation with soil loss in the five erosion collection subplots. I calculated the Mg ha<sup>-1</sup> of total soil (coarse and fine fractions combined) and sediment (fine fraction only, < 2 mm) collected in each pit during the 2015 rainy season and compared this with the mean absolute and real number pin height change for the pins located within each collection subplot. For correlation analysis, I used the *stats* package in R (R Core Team, 2013) to compute the Pearson's product-moment correlation coefficient (i.e., Pearson's *r*) and statistical significance of correlation (i.e., the *p*-value) for each variable combination.

#### **4.2.3 Statistical analysis of management effects on erosion**

In order to evaluate the utility of the absolute value and real number value to measure erosion, both were used in statistical analyses to detect differences in erosion between plots, as grouped in two ways: (1) by the five management systems described above and (2) by three cover classes reflecting 'high', 'medium' and 'low' vegetative cover. The three cover classes were defined as the upper, middle and lower quantiles of C-factor classes across plots since vegetative cover was expected to be the strongest management factor affecting erosion.

A linear mixed effects model was run using the *lmer* package in R (R Core Team, 2013), with plot grouping set as the fixed effect and farm location included as a random effect to account for site differences. The same statistical analyses were also

performed using the RUSLE-predicted erosion rates for comparison. All significant differences were tested at  $p < 0.05$ .

### **4.3 Results**

Of the 450 pins initially installed in the experimental plots, 54 were removed due to suspected disturbance and 7 removed as extreme values. This left 389 pins in the final dataset, with each experimental plot retaining an average of 16 pins and no fewer than 11 pins. Only 5 pins were removed from the collection subplots: 4 due to suspected disturbance and 1 as an extreme value.

The absolute value of pin height change was strongly correlated with RUSLE-predicted annual erosion rates in the 25 experimental plots, while no relationship was found for the real number value (Figure 4.3). Looking at the individual factors used in the RUSLE shows a similar pattern. The absolute value of pin height change was significantly correlated with RUSLE factors and sub-factors related to slope and cover (L, S, C, CC, SC), but not rainfall (R) or soil erosivity (K); no statistically significant correlations were found for the real number value (Table 4.1).

**Table 4.1 Correlation of erosion pin measurements with individual RUSLE factors**

Pearson's product moment correlation coefficients for the mean absolute value (ABV) and real number value (RNV) of change in erosion pin height in experimental plots (n = 25) with individual factors from the Revised Universal Soil Loss Equation (RUSLE). P-values of correlation tests between paired samples are denoted as follows: \* = p < 0.10, \*\* = p < 0.05 and, \*\*\* = p < 0.01

Factor Description	Factor	ABV	RNV
Rainfall factor	R	-0.216	0.224
Soil erosivity factor	K	0.064	-0.014
Slope length factor	L	-0.529 ***	-0.063
Slope steepness factor	S	0.521 ***	0.072
Cover-management factor	C	0.535 ***	-0.17
Canopy-cover sub-factor	CC	0.393 *	0.115
Surface-cover sub-factor	SC	0.398 **	-0.235
Annual erosion (Mg ha <sup>-1</sup> yr <sup>-1</sup> )	A	0.671 ***	-0.084

For the five erosion collection plots, stronger correlations were also found for the absolute value of pin height change for both total soil loss and sediment (< 2mm) loss (Table 4.2), although they were only significant at p < 0.10. A negative relationship was observed for the real number value change, but correlations were not statistically significant (Table 4.2).

Erosion rates ranging between 23 – 76 Mg ha<sup>-1</sup> yr<sup>-1</sup> were predicted using the RUSLE in the experimental plots (240 m<sup>2</sup>) and measured erosion of 0.6 – 2.1 Mg ha<sup>-1</sup> in collection subplots (10 m<sup>2</sup>), more than an order of magnitude difference. The smaller size of the subplots makes comparison with RUSLE-predicted erosion in the experimental plots difficult due to differing slope lengths. When I changed the slope length of the RUSLE to reflect the subplot size, predicted erosion ranged from 3.3 – 7.3 Mg ha<sup>-1</sup> yr<sup>-1</sup> in the subplots (data not shown), closer to the rates estimated from

sediment collection but still not overlapping. The protected design of the collection subplots may be responsible for the remaining discrepancy.

Erosion and deposition rate estimates calculated from the real number change in pin height and soil bulk density in experimental plots ranged from a loss (erosion) of 107 Mg ha<sup>-1</sup> yr<sup>-1</sup> to a gain (deposition) of 40 Mg ha<sup>-1</sup> yr<sup>-1</sup>, and were not correlated with predicted erosion (data not shown).

**Table 4.2 Correlation of erosion pin measurements with soil and sediment loss**

Pearson's product moment correlation coefficients for the mean absolute value (ABV) and real number value (RNV) of change in erosion pin height in subplots (n = 5) soil and sediment collected in pits. P-values of correlation tests between paired samples are denoted as follows: \* = p < 0.10, \*\* = p < 0.05 and, \*\*\* = p < 0.01

Material	Range (Mg ha <sup>-1</sup> )	ABV	RNV
Soil	0.6 – 2.1	0.815 *	-0.338
Fine sediment (< 2mm)	0.3 – 1.1	0.822 *	-0.374

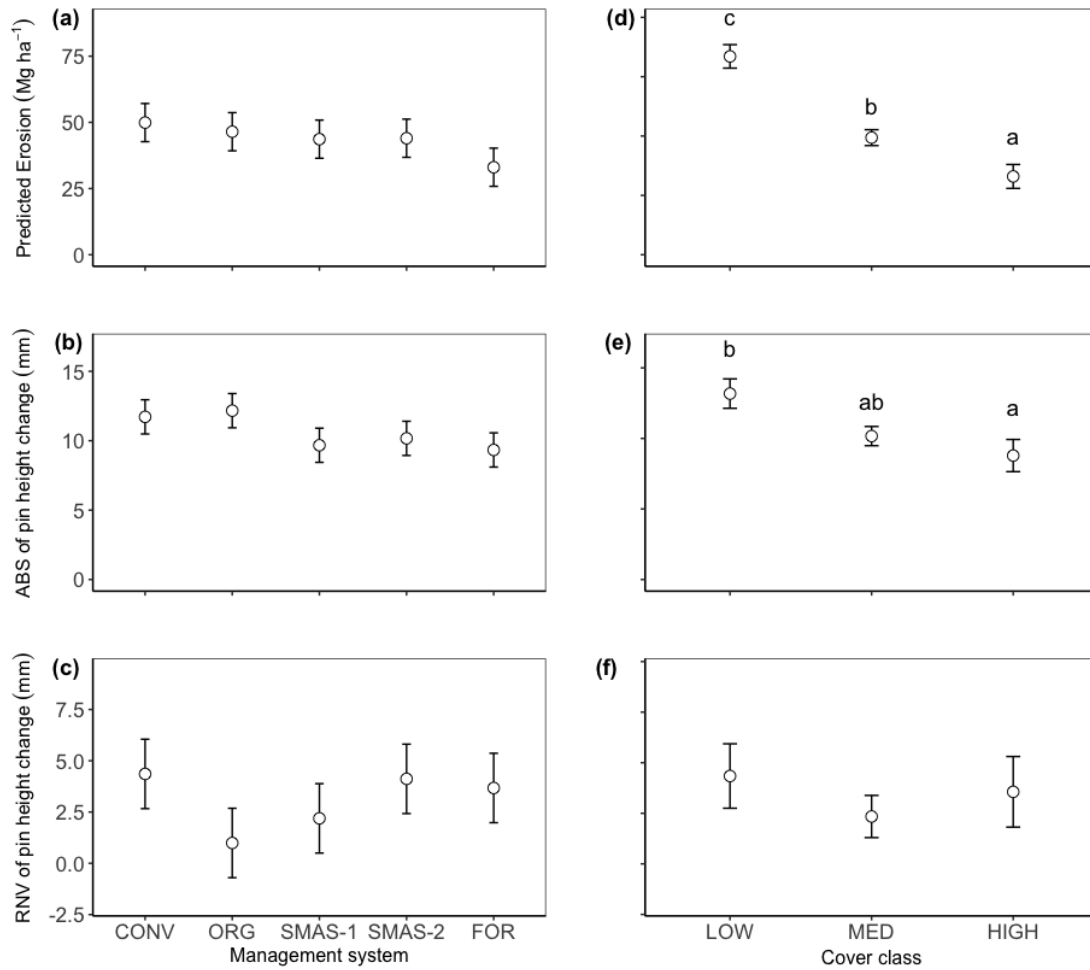


**Figure 4.3 RUSLE-modeled and pin-measured erosion by management systems and cover class**

Relative erosion comparisons between management systems (plots (a) – (c)) and cover classes (plots (d) – (f)), using erosion predicted by the Revised Universal Soil Loss Equation (top row), the absolute value (ABV) of change in erosion pin height (middle row) and the real number value (RNV) of change in pin erosion pin height. Error bars represent one standard error. Significant differences ( $p < 0.05$ ) between categorical x variables are denoted by different letters. Points with the same letters are not significantly different and plots without letters had no significant differences. See text for an explanation of acronyms.

No significant differences were found between management systems, regardless of the method used to predict or measure erosion (Figure 4.3). Significant differences in RUSLE-predicted erosion were found between all three cover classes, and using the absolute value of pin height change, differences were detected between the 'high' and 'low' cover classes, although the 'medium' class could not be statistically distinguished from either of the other classes. No differences were detected between classes using the net real number value change in pin height.

#### **4.4 Discussion**

In this study, I found that the absolute value of pin height change is better able to detect significant differences in erosion between plots expected to have differing rates of soil loss, for example as a result of increased vegetative cover. While no significant differences were found between management systems, there is a pattern of decreasing RUSLE-predicted erosion in tree-based systems (i.e., SMAS and FOR), which were expected to increase soil and canopy cover (Figure 4.3a). This pattern was reflected in the absolute value of pin height change (Figure 4.3b), but disappeared when using the net real number value (Figure 4.3c). Increasing vegetative cover did decrease predicted erosion and the absolute value of pin height change (Figure 4.3d,e), indicating that management systems that increase vegetative cover sufficiently should reduce soil loss. However, this reduction was not detectable when analyzing change in erosion pin height using the net real number value (Figure 4.3f).

The absolute value was strongly correlated with multiple erosion-related factors (in addition to RUSLE-predicted erosion), while the real number value showed no relationship with any factor (Table 4.1). These findings support the few other studies that have used absolute value to compare erosion pin data with erosion-related variables such as hydro-meteorological data (Couper, 2003; Couper et al., 2002; Luffman et al., 2015).

Looking more closely at my results, the absolute value captures interactions between slope and cover management – the variables driving erosion rates in the experimental plots. Absolute value was more strongly correlated with the cover-management factor (C) than with the individual sub-factors used to calculate it (CC and SC), and an even stronger correlation was found for the final predicted annual erosion rate (Table 4.1). This observation that correlation was higher for factors derived from the interaction of other factors or sub-factors further supports my hypothesis that the absolute value of pin height change can serve as a valid indicator of soil erosion.

When using erosion pins for comparative analysis between land management practices or monitoring changes in erosion over time, the absolute value of pin height change is likely a better indicator than the net real number change (i.e., ground advance/retreat) when negative change values are observed. Individual pins experienced both erosion and deposition over time indicating substantial soil movement, but the net change in pin height for any given measurement period

appeared to be episodic and random, thereby masking differences resulting from management. Given a long enough measurement period, the net change in pin height may reflect actual erosion/deposition rates, but this period is unknown a priori and may be impractical for many research and monitoring applications.

One argument against using the absolute value is that the ability to quantify erosion/deposition rates is lost. However, it may be possible to calibrate the absolute value of pin height change to measured erosion rates using other methods (e.g., collection pits or radioisotope concentrations) or modeled erosion rates (e.g., using the RUSLE) from a subset of plots or from suitable reference sites. For example, the relationships between the absolute value of pin height change and RUSLE-predicted erosion, or sediment collected in pits, could be used to predict erosion in similar locations using pin measurements alone. In this study, the strength of these relationships for making such predictions is debatable. The discrepancy between predicted erosion rates in the experimental plots and measured erosion in the subplots highlights that plot size and site conditions should be carefully considered if seeking to extrapolate relationships between erosion rates and pin measurements to other areas.

Additional research is needed to better understand the utility of calibrating erosion pins for accurate low-cost monitoring. Likewise, I encourage other researchers to evaluate the relationship of the absolute value of erosion pin height change with

erosion-related variables on existing and new datasets to corroborate or refute my findings that this method is an improved indicator of relative erosion.

# **5 High-resolution carbon mapping to support investments in ‘climate-smart’ agriculture: making the case for a landscape approach**

## **5.1 Background and introduction**

Multiple benefits can be realized at both the farm and landscape scale when managing for C storage in smallholder agriculture (Harvey et al., 2013). Benefits include reduced erosion, increased habitat and biodiversity, improved nutrient cycling and yield stability (Steenwerth et al., 2014); however, due to a variety of methodological concerns related to C monitoring, international and voluntary agreements on land-use-related C mitigation have largely omitted agriculture, and have instead been restricted to reforestation and afforestation activities (Pelletier et al., 2012). Agroforestry management can store substantial amounts of C in aboveground woody biomass (AGWB; e.g., Henry et al., 2009) and soil (Lorenz and Lal, 2014). It is considered a form of ‘climate-smart agriculture’ (CSA) because it can serve to both mitigate climate change through increased terrestrial C storage and increase the resilience of agricultural systems (e.g., through the benefits mentioned above), thereby improving farmers’ ability to adapt to an already changing climate (Steenwerth et al., 2014; Verchot et al., 2007).

There is growing interest in including CSA practices like agroforestry in C mitigation programs, such as the UN's Reducing Emissions from Deforestation and Forest Degradation (REDD+) program (e.g., Harvey et al., 2013; Steenwerth et al., 2014), and efforts are underway to develop strategies to monitor C sequestration associated with changes in smallholder agricultural land management (Gómez-Castro et al., 2010; Henry et al., 2009; Marinidou et al., 2013; Rosenstock et al., 2016). Small farm sizes, low C sequestration rates per hectare and inaccessibility in smallholder landscapes often result in unacceptably high costs when attempting to monitor C at the farm scale (Cacho et al., 2013). This not only hampers efforts to assess the C mitigation benefits of CSA, but has also led some authors to conclude that agroforestry-based C contracts with individual farmers would likely be impractical at current C prices (Henry et al., 2009; Luedeling et al., 2011).

An alternative is to develop C contracts with groups of landholders or organizations at the landscape scale (e.g. the scale of watersheds, communities, municipalities, etc.), rather than with individual farmers. This approach offers several potential benefits: 1) reduced monitoring and transaction costs and uncertainty if C accounting occurs at more aggregated scales rather than on individual farms; 2) increased flexibility for communities to promote or incentivize CSA for multiple benefits, beyond just C storage (Harley et al., 2012); and 3) the ability to achieve C storage through a suite of interventions (e.g. agroforestry, fire management, afforestation and reforestation), allowing activities to be dynamic and meet the

needs of individual land managers and communities within the same contract (Chhatre and Agrawal, 2009; Harley et al., 2012; Stringer et al., 2012).

A key step to developing landscape-scale C contracts is the development of accurate C monitoring methods at aggregated scales (Scherr et al., 2012), especially for C stored in AGWB. The simplest and most common methods to estimate landscape AGWB-C are inventory-based or 'stratify and multiply' approaches (Goetz et al., 2009). Specifically, these approaches involve assigning a single C value, or a range of values, to individual vegetation, thematic or land use/land cover (LULC) classes and then multiplied by class areas estimated from satellite imagery, existing maps, census data or other sources. These approaches face challenges for monitoring changes in AGWB-C with CSA adoption, especially in smallholder landscapes (Kearney and Smukler, 2016). For example, CSA practices exist along a gradient, confounding binary definitions of what is and is not CSA, thus complicating assignment of specific C values to each LULC class. Furthermore, calculating LULC class area totals is exceptionally challenging in smallholder landscapes due to small field sizes, highly heterogeneous management practices, shifting cultivation and rapid changes in land use over time.

Monitoring approaches utilizing remote sensing data to develop wall-to-wall AGWB-C maps show promise to overcome the challenges of 'stratify and multiply' approaches in smallholder landscapes, although with limitations (Gibbs et al., 2007). AGWB estimations from passive optical satellite sensors have generally been

considered too uncertain to meaningfully monitor AGWB-C due to a variety of complications such as biomass saturation effects (i.e., small changes at high levels of biomass not being accurately detected by “greenness” remote sensing indicators) and highly heterogeneous landscapes resulting in mixed-pixels (Goetz and Dubayah, 2011; Ravindranath and Ostwald, 2008; Zolkos et al., 2013). However, increasing spatial resolution of imagery and advanced processing techniques are yielding improved accuracy in estimating AGWB-related vegetation parameters from optical satellite imagery. For example, the accuracy of optically-derived AGWB estimations has been improved by incorporating texture variables representing the structural arrangement of surfaces within prediction models (Castillo-Santiago et al., 2010; Eckert, 2012; Fuchs et al., 2009; Kayitakire et al., 2006; Sarker and Nichol, 2011). Texture variables (e.g., contrast, entropy, homogeneity, etc.) are statistical representations of the structural arrangement of surfaces and their surrounding environment and can be easily derived using geographic information system (GIS) software.

While uncertainty of AGWB-C predicted from optical imagery may remain high at the pixel and plot scale, it can be markedly reduced when aggregated across a landscape due to the spatial scaling of uncertainty. For example, several studies have shown that uncertainty of AGWB predictions from remote sensing is lower at more aggregated scales, either as a result of increasing map grain size (Asner et al., 2010; Lusiana et al., 2014; Mascaro et al., 2011a) or by aggregating across larger

areas (Asner et al., 2010; Fazakas et al., 1999; Saatchi et al., 2011). However, little discussion has been given to the overall uncertainty of landscape AGWB totals derived from very high spatial resolution optical imagery and how it relates to monitoring efforts for C payments and CSA.

The aim of this study was to assess how landscape-scale C mapping using high-spatial resolution satellite imagery can overcome monitoring challenges for C contracting in regions dominated by smallholder agriculture, with an application to a mountainous region of El Salvador. My objectives were therefore to (1) investigate the potential for using high resolution optical satellite imagery to quantify AGWB-C stocks in a smallholder landscape at multiple scales, accounting for uncertainty, (2) quantify expected gains in AGWB-C with the adoption of CSA and potential payments for C credits and, (3) explore the benefits of using remote sensing to target low-biomass areas to promote agroforestry in smallholder landscapes.

## **5.2 Methods**

My analytical framework to realize the aforementioned objectives consisted of four main steps. First, I took field measurements of individual trees in 0.1 ha plots to calibrate high-spatial resolution QuickBird satellite imagery acquired coincident with field measurements. Second, I mapped AGWB-C for the entire study area using a multiple linear regression model developed from a suite of potential predictor variable extracted from the QuickBird image and a digital elevation model (DEM).

Third, I estimated the uncertainty of the AGWB-C map at multiple scales using two methods: a simple quadratic scaling approach and an object-weighted approach to account for spatial autocorrelation. Finally, I predicted expected changes in AGWB-C for the study area for several scenarios of CSA adoption and estimate potential gross value of C credits at different market prices. I describe each of these steps in detail below.

### **5.2.1 Data collection**

This study was conducted within a 100-km<sup>2</sup> (10,000 ha) area in the eastern portion of La Mancomunidad, encompassing the municipality of Las Vueltas (see Section 2.3 and Figure 2.1). A total of 138 circular calibration plots, each with a radius of 17.84 m (area of 0.1 ha), were sampled in late 2012 following a modified version of the LDSF hierarchical sampling method (Shepherd et al., 2015; Vågen et al., 2010; Vågen and Winowiecki, 2013). Initial site selection was carried out utilizing the LDSF method, but plot centers were ‘pushed’ a random distance at a randomly chosen angle into the nearest homogenous land use parcel when the plot lay within multiple land uses. Plot centers were then georeferenced using GPS and differentially corrected to permanent base towers, achieving sub-meter accuracy for all locations.

Species, height and diameter at breast height (DBH) were measured for all trees with DBH  $\geq$  10 cm. The same measurements were taken for trees with DBH 1 – 10

cm in a 0.01 ha circular subplot in the plot center. Eleven larger plots in the study area were surveyed in early 2013 as part of a regional landscape survey encompassing all of La Mancomunidad. Ten of these sites were cropped fields ranging in size from 0.19 to 0.89 ha that encompassed randomly selected calibration plots and the eleventh was a 1-ha mixed-pine forest plot. These plots were used as validation sites to compare predicted map uncertainty to observed prediction error (calculated from the difference between map-predicted and field-estimated AGWB-C).

A high-spatial resolution QuickBird satellite image (0.6 m panchromatic, 2.4 m 4-band spectral) of the study area was acquired on December 4, 2012. The ASTER 30-m DEM was also downloaded.

### **5.2.2 Mapping AGWB-C**

AGWB was calculated for each tree within the sample plots from a combination of species-specific and generalized allometric equations using DBH, height and, when necessary, wood-specific gravity values from the literature (see Appendix B).

AGWB-C was estimated as 49% of AGWB based on several studies throughout Central America (Gómez-Castro et al., 2010; Hughes et al., 1999a; Suárez, 2002).

AGWB-C density was calculated in metric tons per hectare ( $\text{Mg ha}^{-1}$ ) by summing the estimated AGWB-C of each tree within the plot and converting to a per-hectare area basis.

I used plot data to develop a contiguous prediction map of AGWB-C for the entire study area using a multivariate linear regression model developed from a suite of potential predictor variables (n=97) derived from the QuickBird and ASTER DEM datasets (Table 5.1). Predictor variables were identified from similar studies using multiple linear regression models to estimate AGWB from optical imagery and include: the plot mean and standard deviation of individual spectral bands, band ratios (Okubo et al., 2010), vegetation indices (Castillo-Santiago et al., 2010; Eckert, 2012), principal component analysis (PCA) and tasselled cap transformations (Fuchs et al., 2009), grey level co-occurrence matrix (GLCM) texture variables developed for each spectral band and the panchromatic band (Castillo-Santiago et al., 2010; Eckert, 2012; Fuchs et al., 2009; Lu et al., 2012; Nichol and Sarker, 2011; Okubo et al., 2010), ratios of texture parameters (Sarker and Nichol, 2011) and terrain variables derived from a 30-m ASTER DEM (Table 5.1). All variables were created in ArcGIS 10.1 (ESRI, 2011) or ENVI 5.1 (Exelis Visual Information Solutions, 2010) and their mean and/or standard deviation values extracted for each 0.1 ha plot.

An exhaustive search was used to test all possible regression model subsets with the *leaps* package (Lumley, 2009) in R, Version 2.9 (R Core Team, 2013). The dependent variable, AGWB-C, was approximately log-normally distributed and was log transformed after adding a constant of 1 to each value to avoid issues with zero values. The maximum number of predictor variables allowed was capped at seven (a

sample size to variable ratio of roughly 20:1) and the 40 best model subsets for each number of independent variables were selected using the Bayesian information criterion (BIC) and adjusted- $R^2$ , resulting in 280 potential models. Finally, the variance inflation factor (VIF) was calculated for each of the 280 potential models and all models with a VIF greater than 10 were removed due to high potential multicollinearity (García et al., 2010; Nichol and Sarker, 2011). Of the remaining models, the one with the lowest BIC and highest adjusted  $R^2$  was selected as the final regression model and checked for heteroscedasticity and normality of residuals.

A correction value was calculated to correct for bias introduced by the log-transformation of the dependent variable following methods described in Sprugel (1983). The cross-validated root mean square error (RMSE-CV) of the final model was then evaluated using leave-one-out cross validation (LOOCV) with the *DAAG* package (Mairdonald and Braun, 2014) in R.

In order to generate the final prediction map, a mean filter using a circular moving window set at a radius of 17.84 m (equal to the plot area of 0.1 ha) was applied to a raster of each independent variable in the final model to account for the fact that the model was built using mean values of 0.1 ha plots. These filtered rasters were used to create a prediction map of log-transformed AGWB-C for each pixel, which was then back-transformed and corrected to produce a final AGWB-C prediction map.

**Table 5.1 Potential predictor variables tested by stepwise multivariate linear regression**

Variable Type	Name	Description/Equation	Data/Equation Source
Individual Bands - Mean & Standard Deviation	Band 1 (Blue)	450-520 nm	DigitalGlobe
	Band 2 (Green)	520-600 nm	
	Band 3 (Red)	630-690 nm	
	Band 4 (NIR)	760-900 nm	
	Panchromatic	450-900 nm	
Band Ratios	NIR/Blue	B4/B1	(Okubo et al., 2010)
	Red/Blue	B3/B1	
	Green/Blue	B2/B1	
	NIR/Green	B4/B2	
	Red/Green	B3/B2	
	NIR/Red	B4/B3	
Vegetation Indices	EVI	$2.5 \frac{NIR - Red}{(NIR + 6 * Red - 7.5 * Blue) + 1}$	(Jensen, 2005)
	NDVI	$\frac{NIR - Red}{NIR + Red}$	(Jensen, 2005)
	ARI2	$NIR \left[ \frac{1}{Green} - \frac{1}{Red} \right]$	(Exelis Visual Information Solutions, 2010)
	ARVI	$\frac{NIR - [Red - (Blue - Red)]}{NIR + [Red - (Blue - Red)]}$	(Jensen, 2005)
	OSAVI	$\frac{1.5 * (NIR - Red)}{(NIR + Red + 0.16)}$	(Exelis Visual Information Solutions, 2010)
	SR	$\frac{Red}{NIR}$	(Jensen, 2005)
Tasseled Cap	TC 1	Brightness	(Yarborough and Easson, 2005)
	TC 2	Greenness	
	TC 3	Wetness	
	TC 4	Fourth Coordinate	
Principal Components	PC 1	Principal components 1 – 4	(Exelis Visual Information Solutions, 2010)
	PC 2		
	PC 3		
	PC 4		
GLCM Texture Variables	Contrast	Individual bands (Bands 1-4 with 11 x 11 pixel window; Panchromatic with 25 x 25 pixel window)	(Exelis Visual Information Solutions, 2010)
	Correlation		
	Dissimilarity		
	Entropy		
	Homogeneity		
	Second Moment Variance		
Ratios of GLCM Texture Variables	Contrast	Band Ratios with 11 x 11 pixel window (B4/B2; B4/B3; B3/B4; B3/B2)	(Sarker and Nichol, 2011)
	Correlation		
	Dissimilarity		
	Entropy		
	Homogeneity		
	Second Moment Variance		
Terrain	Elevation	meters above sea level (m.a.s.l.)	NASA
	Slope	degrees	(ESRI, 2011)
	Insolation	Solar radiation tool, ArcGIS 10.1	(ESRI, 2011)
	TWI	$TWI = \ln \left( \frac{a}{\tan B} \right)$ where, $a$ = upslope contributing area (m <sup>2</sup> ) and $B$ = Slope (degrees).	(Wilson and Gallant, 2000)

### 5.2.3 Estimating map uncertainty

The uncertainty of aggregated AGWB-C was estimated at multiple scales as the 95% confidence interval in Mg of AGWB-C. Uncertainty was first calculated for each pixel using the following equation:

$$C_{Px} \pm U_{Px} = t_{(1-\frac{\alpha}{2}, df)} * SE_{Px} \quad \text{[Equation 1]}$$

where  $C_{Px}$  is the predicted AGWB-C at pixel  $Px$ ,  $U_{Px}$  is the uncertainty at pixel  $Px$ ,  $t$  is the Student  $t$  critical value at a specified alpha ( $\alpha$ ) and degrees of freedom ( $df$ ) (in this case  $\alpha = 0.05$  and  $df = 131$ ) and  $SE$  is the standard error of prediction at pixel  $Px$ . The lower and upper uncertainty values for each predicted AGWB-C value were then calculated by back-transforming the lower and upper  $CI$  limits, respectively, and calculating the difference from the predicted value for each pixel. Due to back-transformation, this results in asymmetrical lower and upper uncertainty values. Therefore, average uncertainty was also calculated for each pixel as the simple average of the two values.

Aggregate uncertainty was calculated in two ways (with and without accounting for spatial autocorrelation) at multiple scales to explore how uncertainty changes as the size of the aggregation unit varies from plot to farm to landscape scale. Lattice grids ranging from approximately 0.01 to 10,000 ha on a logarithmic scale were created for the entire study area and the average aggregate uncertainty calculated for each grid as the mean percent uncertainty of individual grid cells.

Aggregate uncertainty was first calculated for each grid as the quadratic sum of all pixels within an aggregation unit as

$$C_A \pm U_A = \sqrt{\sum_{n=1}^{Px} U_{Px}^2} \quad \text{[Equation 2]}$$

where  $C_A$  is the aggregate AGWB-C (calculated as the sum of predicted pixel values within the aggregation unit),  $U_A$  is the aggregate uncertainty and  $U_{Px}$  is the uncertainty at pixel  $Px$ , as calculated in Eq. (1). This method is a simple way to estimate uncertainty where under- and over-prediction are equally likely for each individual pixel and has been used by others to aggregate uncertainty for AGWB predictions (Asner et al., 2010; Saatchi et al., 2011). However, since the quadratic sum method assumes errors are independent and random (Palmer, 2003), it does not account for potential spatial autocorrelation within the data. While no spatial autocorrelation was detected in the residuals of the 138 calibration plots, it may potentially occur at the pixel scale (i.e. at distances much smaller than that between most calibration plot pairs) and, as a result, an object-weighted approach was developed to account for local spatial autocorrelation.

The object-weighted approach consisted of three basic steps: (1) calculate the effective range of spatial autocorrelation of pixel prediction uncertainty, (2) segment the image into spatial objects with similar uncertainty and (3) weight the

sum of uncertainty based on the average distance between points within each object, up to effective range identified in step 1.

In order to calculate the effective range, a variogram was produced from the prediction uncertainty map using the *gstat* package in R (Pebesma, 2004). The very high-spatial resolution of the uncertainty map made it computationally expensive to compute a variogram for the entire study area at once, therefore the map was resampled to 9.6 m pixels and a bootstrapping approach was used to construct variograms for 1,000 randomly selected subsections of approximately 1 x 1 km each. The results of these 1,000 individual variograms were averaged to produce a single estimate of the semivariance between cells, to which an exponential model was fit. The exponential model yielded an effective range of 281 m, beyond which spatial autocorrelation of uncertainty is assumed to be inconsequential (see Appendix B, Figure B - 1).

The original 2.4 m uncertainty map was then segmented using ENVI 5.0 (Exelis Visual Information Solutions, 2010) and the average distance between cells within each object calculated as

$$D_o = e^{(0.5 \cdot \log(A_o) - 0.6515)} \quad \text{[Equation 3]}$$

where  $D_o$  is the average distance between points within an object ( $o$ ), and  $A_o$  is the area of the object. The sum of prediction uncertainty of pixels within each object

was weighted using a modification of Equation 2, where the exponent is scaled between 1 and 2, such that within each object,

$$C_o \pm U_o = \sqrt[2]{\sum_{n=1}^{Px} U_{Px}^{S_o}} \quad \text{[Equation 4]}$$

and  $S_o$  is calculated as

$$S_o = 1 + D_o \left( \frac{1}{281} \right) \quad \text{[Equation 5]}$$

In this manner, uncertainty of very small objects was aggregated by the near-arithmetic sum (i.e. assuming near-perfect spatial autocorrelation), whereas uncertainty was scaled toward the quadratic sum for very large objects where the average distance between pixels exceeded the effective range of 281 m (i.e. assuming independence of errors). The weighted uncertainty of each object was then summed in quadrature for each aggregation unit according to Equation 2, since objects are by definition assumed to be independent of each other.

#### **5.2.4 Predicting changes in AGWB-C with CSA adoption and potential C values**

Simple scenarios of expected AGWB-C gains with the adoption of CSA practices were created to examine the potential magnitude and value of C storage in the study area. Scenarios were based on the objectives of several recent and ongoing projects in La Mancomunidad to promote CSA for multiple benefits, including storing AGWB-C. Specifically, the CSA practices of interest include the adoption of a slash-and-mulch

agroforestry system (e.g., Hellin et al., 1999) and improved silvopasture management (e.g., Dagang and Nair, 2003), both typified by increasing the number and diversity of managed trees left in fields and pastures, thus increasing AGWB-C stocks.

Predicted gains in AGWB-C with conversion from conventional management to CSA were estimated from expected changes in tree density and size-distribution. Based on recommendations from experts and on-farm trials, the average target tree density and size-distribution for the CSA practices of interest is approximately 100 large trees (DBH 10 – 40 cm) and 1000 small trees (DBH 5 – 10 cm) per hectare, respectively. When converted to basal area, this equates to a target basal area averaging  $9.33 \text{ m}^2 \text{ ha}^{-1}$ , which agrees well with the limited published observations of basal area in mature agroforestry and silvopasture systems in Central America (e.g., Pauli et al., 2011). Using a simple linear regression with data from ground plots in cropland, pasture and broadleaf secondary forest/fallow in this study ( $n = 127$ ), the relationship between basal area and AGWB-C was modeled, yielding an estimated target AGWB-C of  $23.35 \text{ Mg ha}^{-1} \pm 0.69 \text{ Mg ha}^{-1}$  (one standard error) at the target basal area of  $9.33 \text{ m}^2 \text{ ha}^{-1}$ .

A LULC map was overlaid with the predicted AGWB-C map to identify areas currently under cropland, pasture or broadleaf secondary forest/fallow classes where AGWB-C gains would be realized with conversion to CSA (i.e., areas with predicted AGWB-C less than  $22.51 \text{ Mg ha}^{-1}$ ). The predicted AGWB-C gains in

broadleaf secondary forest/fallow classes are likely an underestimate, since I assumed that fallows will retain 22.51 Mg C ha<sup>-1</sup> coming out of agroforestry, ignoring additional gains from tree growth that would come as the fallow matures. For each pixel identified, the predicted gain in AGWB-C with CSA adoption was calculated using a Monte Carlo simulation where, for each iteration,

$$G_i = C_i - T_i \quad \text{[Equation 6]}$$

and  $G_i$  is the predicted gain in AGWB-C in Mg ha<sup>-1</sup> for the  $i^{\text{th}}$  iteration,  $C_i$  is current AGWB-C in Mg ha<sup>-1</sup> randomly chosen from the distribution of possible predicted values for each pixel and  $T_i$  is the target AGWB-C with CSA adoption which was randomly chosen from a normal distribution with a mean of 22.51 Mg ha<sup>-1</sup> and a standard deviation of 0.82 Mg ha<sup>-1</sup> (derived from my model results). Monte Carlo simulations have been used in similar studies to estimate uncertainty of C emissions from land use change (Harris et al., 2012; Lusiana et al., 2014) and are among the methods recommended by the Intergovernmental Panel on Climate Change (IPCC) to meet Tier 1 requirements for monitoring C (Penman et al., 2003). The simulation was conducted 100 times and total AGWB-C gain for the study area was calculated for each iteration. The median was taken as the expected total gain in AGWB-C and the 2.5<sup>th</sup> and 97.5<sup>th</sup> percentiles used to calculate a 95% confidence interval. I took the lower bound of this interval as the minimum expected gain in AGWB-C with conversion from conventional management to CSA across the study area.

I estimated the minimum expected gain in AGWB-C under three adoption scenarios: (1) full adoption (100% of all agricultural land converted to CSA), (2) 50% adoption randomly distributed across agricultural lands and (3) 50% adoption targeting only the most denuded areas (i.e., areas with expected gains of at least 5 Mg C ha<sup>-1</sup>). For each scenario, minimum expected gain was calculated using a probability distribution function (PDF) to estimate the gain that could be monitored with 95% confidence based on the uncertainty of the prediction map.

Finally, the potential value of C-payments for CSA adoption was estimated to contextualize the potential for developing a community-scale C contract over a 15-year period. Gross C value (not accounting for monitoring and transaction costs) was calculated by multiplying the minimum expected gain in AGWB-C (converted to metric tons of CO<sub>2</sub> equivalents) by the market price for C. I did this for three different prices of CO<sub>2</sub> equivalents since prices are highly variable across markets and over time. I chose prices of \$4 per ton (the approximate low for EU Allowance credits in 2013), \$12 per ton (the approximate price of California Carbon Allowance Futures from 2014 to 2016) and \$37 per ton, the 'social' or 'shadow' price of C as estimated by the US Interagency Working Group on the Social Cost of Carbon (US Interagency Working Group on the Social Cost of Carbon, 2015).

## 5.3 Results

### 5.3.1 Mapping AGWB-C

AGWB-C density in the 138 calibration plots ranged from 0 – 92 Mg C ha<sup>-1</sup> and, as anticipated, varied by land use (Table 5.2). Variability was high in all LULC classes, and highest for cropland and pasture, with coefficients of variation (CV) of 1.38 and 0.87, respectively.

**Table 5.2 Select descriptive statistics for AGWB-C in calibration plots**

Grouped by land use/land cover (LULC) classes: CROP = cropland, PAST = pasture, BLF = broadleaf secondary forest/fallow, MPF = mixed-pine forest. n = number of calibration plots in each class.

LULC Class	n	AGWB-C (Mg C ha <sup>-1</sup> )				CV
		Mean	Median	Min	Max	
CROP	29	9.73	3.48	0.00	60.22	1.38
PAST	44	11.3	8.75	0.00	35.62	0.87
BLF	52	27.33	24.77	1.57	70.66	0.66
MPF	13	43.48	40.87	13.08	91.92	0.52
OVERALL	138	20.04	15.26	0.00	91.92	0.93

Of the 280 AGWB-C calibration models, 149 met the model selection criteria. I found that GLCM texture variables, namely *correlation*, *entropy* and *homogeneity* from the panchromatic image and Bands 1 and 3, were the most frequently selected variables (Figure 5.1). The ratio of the Second Moment of Band 4 to Band 3 was the only GLCM texture ratio consistently selected. In general, vegetation indices, terrain

variables, tasselled cap transformations, PCA and ratios of GLCM texture variables were rarely included in model subsets. Models with more variables generally had lower BIC and higher adjusted R<sup>2</sup>. No models with seven variables passed the multicollinearity threshold (VIF < 10). Three models with 6 variables met the VIF threshold but did not pass tests for normality of residuals. Therefore, the final chosen model based on the selection criteria contained 5 variables with an adjusted R<sup>2</sup> of 0.52, RMSE-CV of 16.38 Mg ha<sup>-1</sup> (81.71%) and a correction factor of 1.38 (Table 5.3).

**Table 5.3 Results of the final regression model to predict AGWB-C**

Variable	Coefficient Est.	Std. Error	Pr (>  t )	VIF
Intercept	-1.67985	1.35761	0.218	
Band 1	-0.03174	0.00698	< 0.001	1.92
Entropy (Band 3)	-0.00669	0.00129	< 0.001	2.62
Correlation (Panchromatic)	8.12406	1.19259	< 0.001	2.02
Entropy (Panchromatic)	1.26736	0.27321	< 0.001	3.06
Second Moment (NIR/Red)	5.26955	1.14585	< 0.001	3.89
<b>Adjusted R<sup>2</sup> = 0.52   RMSE-CV = 16.38 Mg ha<sup>-1</sup> (81.71%)   CF<sup>†</sup> = 1.3810</b>				

<sup>†</sup> CF is the correction factor (see Sprugel, 1983)

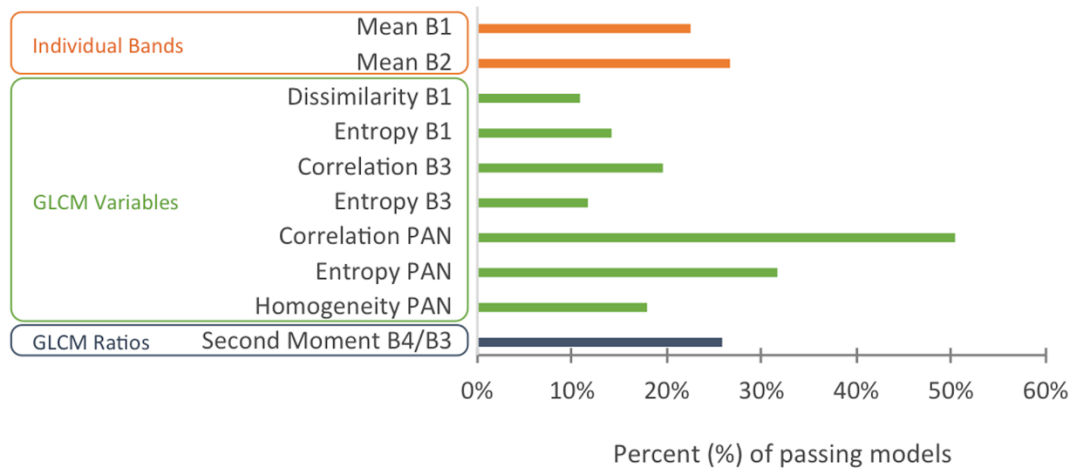


**Figure 5.1 Top 10 most frequently chosen regression model variables**

Variables are grouped by type, where GLCM = grey level co-occurrence matrix; PAN = panchromatic and; B1 = band 1, B2 = band 2, etc. The x-axis shows in what percent of models the variables occurred (limited to models that met the selection criteria; n = 183).

The final map of predicted AGWB-C corresponded well with known areas of high biomass, for example the intact mixed-pine forest in the northwest of the study area, broadleaf riparian zones along rivers and streams and the less-populated highlands in the southeast (Figure 5.2). Map uncertainty (as percent of the prediction value) was typically highest in image-shadowed areas and areas with very low biomass (Figure 5.3). Based on the sum total of all pixels in the prediction map, aggregate AGWB-C for the study area is estimated at 257,360 Mg (Table 5.4). This map-based estimate is about 8.8% higher than a simple plot-based estimate (i.e., a ‘stratify and multiply’ approach calculated by multiplying the area of each LULC class by the

mean AGWB-C measured in field plots of that LULC class). Overall average AGWB-C density was 25.81 Mg ha<sup>-1</sup> and estimates of average AGWB-C density by LULC class were similar to plot-based averages.

**Table 5.4 Total predicted AGWB-C by land use/land cover (LULC) class**

CROP = cropland, PAST = pasture, BLF = broadleaf secondary forest/fallow, MPF = mixed-pine forest

LULC Class	Map Area (ha)	Map-based		Plot-based	
		Total (Mg)	Mean (Mg ha <sup>-1</sup> )	Total (Mg)	Mean (Mg ha <sup>-1</sup> )
CROP	1,680	20,610	12.27	16,360	9.73
PAST	2,217	27,800	12.54	25,410	11.46
BLF	5,218	165,700	31.75	157,270	30.14
MPF	854	43,250	50.65	37,400	43.81
<b>OVERALL</b>	<b>9,970</b>	<b>257,360</b>	<b>25.81</b>	<b>236,440</b>	<b>22.63</b>

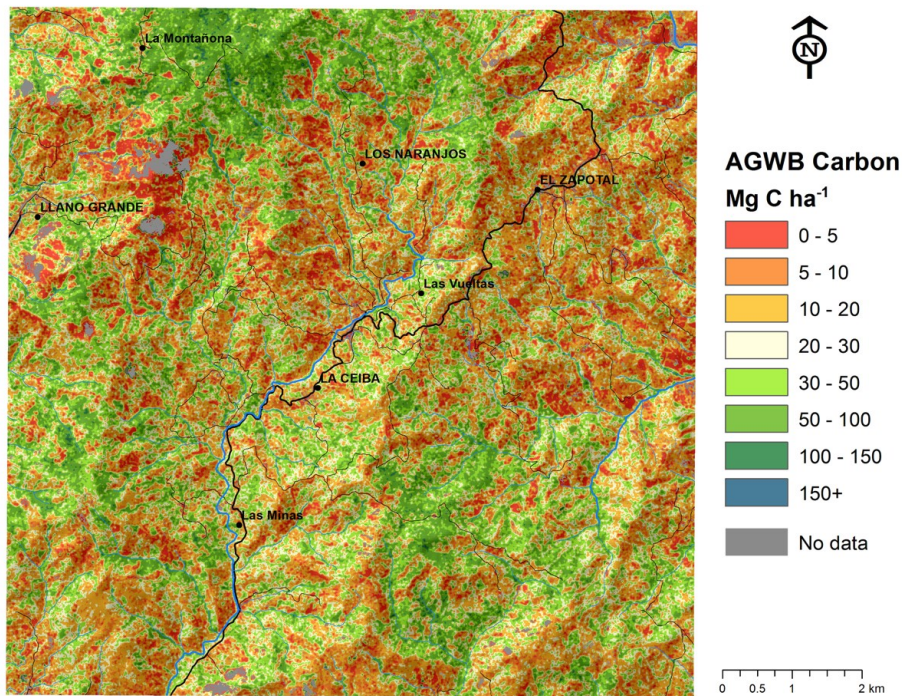


**Figure 5.2 Final map of AGWB-C predicted from QuickBird satellite imagery**

'No data' areas in grey are due to cloud cover. Map resolution is 2.4 m.

### **5.3.2 Estimating map uncertainty**

The grid simulation showed an exponential decay in prediction uncertainty as the size of aggregation units increased for both calculation methods (Figure 5.4).

However, prediction uncertainty for smaller aggregation units was markedly lower using the quadratic sum of individual pixel uncertainty compared to the object-weighted approach.

At the scale of sample plots (0.1 ha) and farms (~1 ha), the object-weighted approach estimated uncertainties of about 50 – 100% (of the predicted value), which was nearer to the range of observed prediction error for most validation plots compared to the quadratic sum (Figure 5.4). It is worth noting that in several of the validation plots with measured AGWB-C less than 2 Mg, percent error was very high despite low gross AGWB-C density error due to dividing by such a small measured value. These values were excluded from Figure 5.4 to improve readability, but are included in Appendix B (Table B - 4).

Object-weighted uncertainty declined below 5% for aggregation units larger than about 250 ha. At the scale of the study area (10,000), uncertainty was less than 1% using both methods.

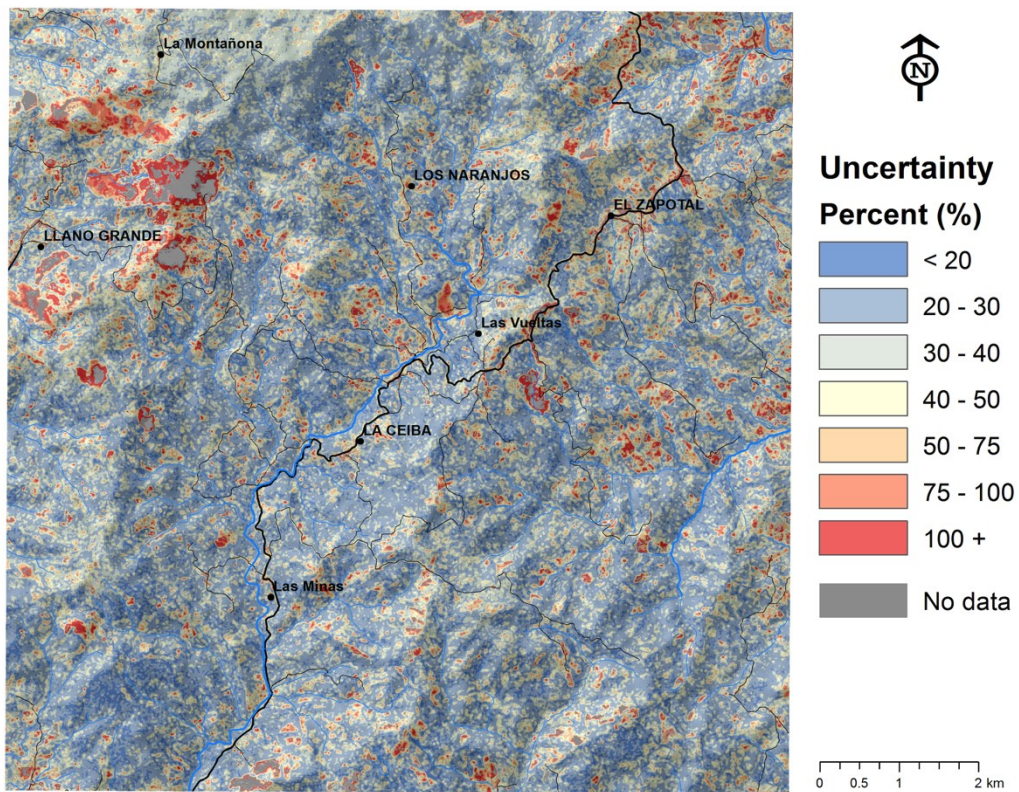


**Figure 5.3 Uncertainty map of AGWB-C predictions from QuickBird satellite imagery**

Calculated as the percent of the predicted AGWB-C value using the average error of the upper and lower bounds of the 95% confidence interval. 'No data' areas in grey are due to cloud cover. Map resolution is 2.4 m.

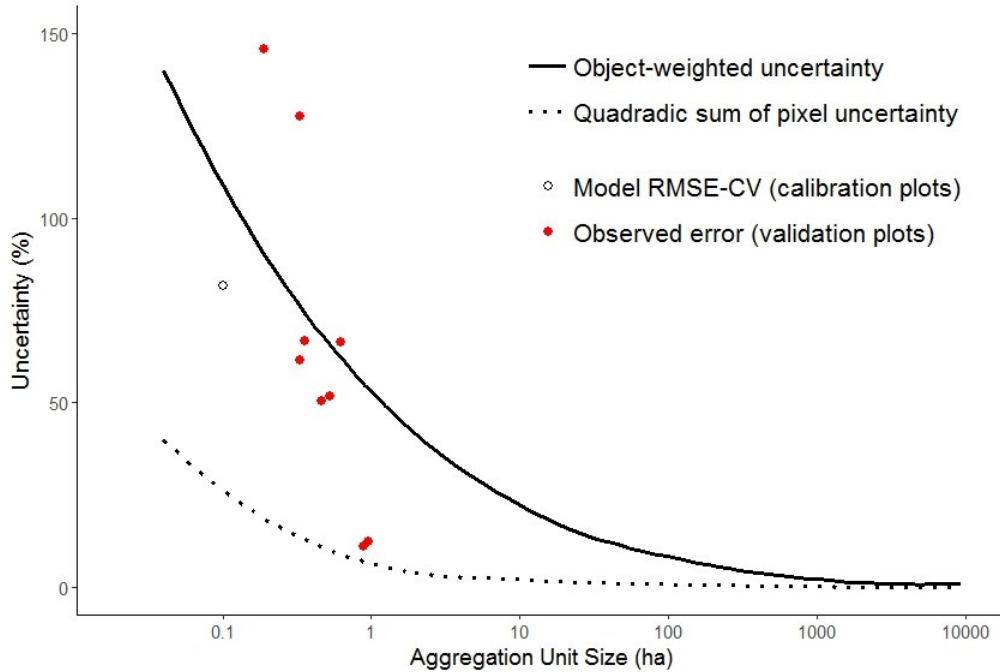


**Figure 5.4 Uncertainty of aboveground woody biomass carbon predictions by aggregation unit size**

The dotted line shows average uncertainty by plot size from the grid simulation calculated as the quadratic sum of pixel uncertainty and the solid line shows the object-weighted uncertainty. The open circle represents the cross-validated root mean squared error (RMSE-CV) from the 0.1 ha calibration plots (n=138), and filled red circles show observed error in validation plots. NOTE: Two of the validation plots were excluded from the figure to improve readability, but are included in Appendix B (Table B - 4). Percent error in these two plots was very high (> 300%) despite low gross prediction error (< 3 Mg) due to dividing by a small measured value for the plot (< 2 Mg).

### **5.3.3 Predicting changes in AGWB-C with CSA adoption and potential C value**

Expected gain in AGWB-C with full conversion to CSA practices within the study area is 58,920 Mg, or about 28% of the estimated current total in managed land uses. Of this potential gain, 19,510 Mg (33%) comes from conversion of cropland to agroforestry, 26,760 Mg (45%) from pasture to silvopasture and 12,650 Mg (21%)

from increased AGWB-C in broadleaf secondary forest/fallow resulting from higher AGWB-C in managed lands entering back into forest/fallow uses (Table 5.5). Overall, nearly 60% of the land area not currently under mixed-pine forest could see gains in AGWB-C with CSA adoption. Nearly all cropland and pasture areas have potential to increase AGWB-C, while gains are expected in 36% of the area classified as broadleaf secondary forest.

**Table 5.5 Potential carbon gains with 100% adoption of climate-smart agriculture**

Grouped by land-use/land-cover (LULC) classes where gains would be expected (CROP = cropland, PAST = pasture, BLF = broadleaf secondary forest/fallow). AGWB-C is aboveground woody biomass carbon.

LULC Class	Area with AGWB-C Gain (ha)	Percent of LULC Class Map Area	Average Density Gain (Mg C ha <sup>-1</sup> )	Expected Total Gain (Mg C)	Percent Gain (compared to current total)*	Percent of Expected Total Gain
CROP	1,560	92.64%	12.53	19,510	94.66%	33.12%
PAST	2,010	90.43%	13.29	26,760	96.25%	45.42%
BLF	1,860	35.61%	6.80	12,650	0.08%	21.46%
<b>OVERALL</b>	<b>5,430</b>	<b>59.47%</b>	<b>10.85</b>	<b>58,920</b>	<b>27.52%</b>	<b>100.00%</b>

\*Based on current totals by LULC class as calculated from the map prediction averages

Combining the uncertainty of the expected gain with the uncertainty of the aggregate AGWB-C, I estimate that a minimum gain of 57,340 Mg could be measured with 95% confidence with 100% adoption of CSA. With 50% adoption by random farms (simulating a non-targeted approach) the expected measurable gain drops to 26,770 Mg. However, the expected AGWB-C gains are not evenly distributed and targeting areas with high potential gain, as shown in the map below (Figure 5.5), was expected to yield substantially higher C gains than a random non-targeted

approach. Indeed, with 50% adoption targeting only the most denuded areas, measureable landscape AGWB-C gains jumped to 39,110 Mg, about 46% higher than the random approach (Table 5.6).

**Table 5.6 Projected value of carbon gains from adoption of climate-smart agriculture**

Expected aboveground woody biomass (AGWB-C) gains across the 100-km<sup>2</sup> study area for three adoption scenarios. The potential gross value (USD) of C over 15 years at three prices is also calculated for each scenario

Adoption scenario	AGWB-C Gain (Mg)*	CO <sub>2</sub> -Eq. (Mg)	at \$4/ton		at \$12/ton		at \$37/ton	
			Total	Annual	Total	Annual	Total	Annual
100%	57,340	210,400	\$841,600	\$56,110	\$2,525,000	\$168,300	\$7,785,000	\$519,000
50% Targeted	39,110	143,500	\$574,000	\$38,270	\$1,722,000	\$114,800	\$5,310,000	\$354,000
50% Random	26,770	98,250	\$393,000	\$26,200	\$1,179,000	\$78,600	\$3,635,000	\$242,300

\* Minimum expected measurable AGWB-C gain after accounting for map uncertainty

The potential value of C payments for CSA adoption at the landscape scale are substantial, but vary strongly with the price of C. I estimate that AGWB-C would increase by nearly 40,000 Mg, or 143,500 tons CO<sub>2</sub> equivalent, with a 50% adoption rate over a 15-year period targeting the most denuded agricultural areas (Table 5.6). Depending on the price per metric ton CO<sub>2</sub> equivalent, the gross value of C gains ranged from \$574,000 (at \$4 per ton) to as much as \$5,310,000 (at \$37 per ton) for the study area. Annual gross value of C per hectare of land converted to CSA ranged from \$13 – 124 ha<sup>-1</sup> yr<sup>-1</sup>, equivalent to between 2.6 and 25.3% of average net on-farm profits in the study area (estimated at \$491 ha<sup>-1</sup> yr<sup>-1</sup>, data not shown).

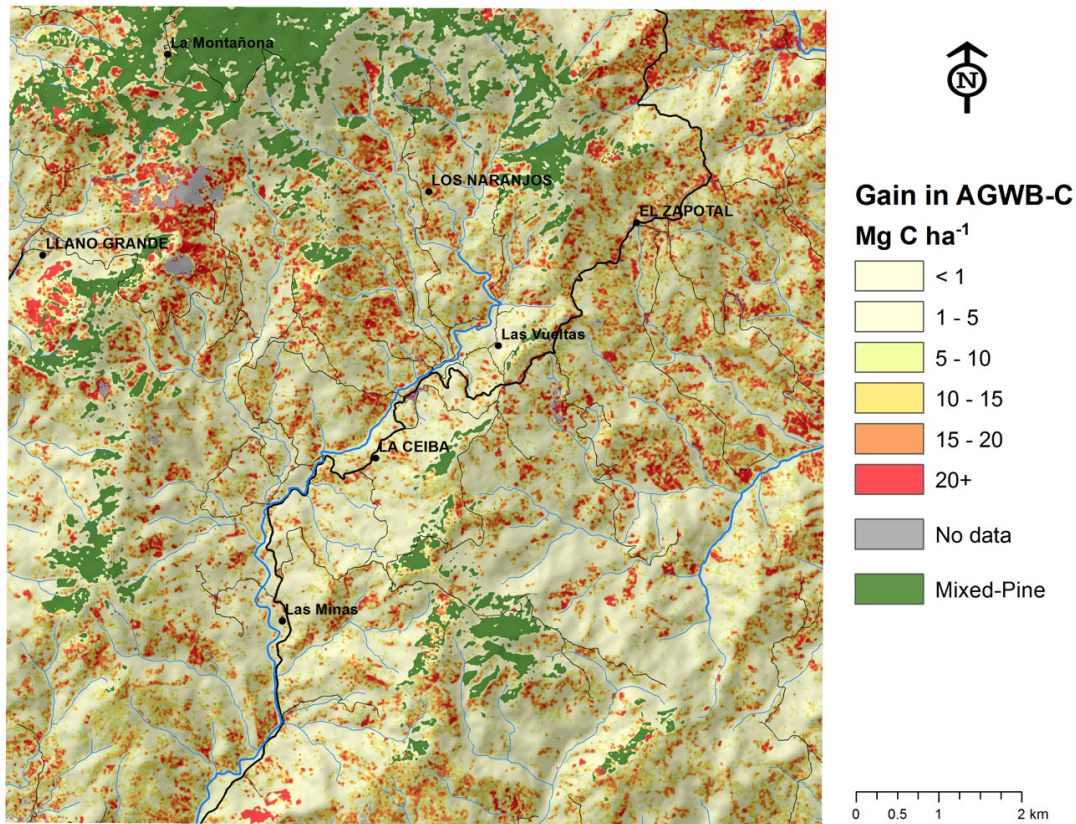


**Figure 5.5** Map of average expected AGWB-C gains with CSA adoption

Map resolution is 2.4 m

## 5.4 Discussion

### 5.4.1 Mapping AGWB-C

AGWB-C in this region is relatively low, consistent with other estimates for degraded tropical landscapes dominated by smallholder agriculture. Saatchi et al. (2011) mapped tropical forest C stocks at the national scale across Latin America, sub-Saharan Africa and Southeast Asia and estimated average AGWB-C density in

forests in El Salvador to be between 39 – 60 Mg C ha<sup>-1</sup>, within the measured range for broadleaf secondary forest and mixed-pine forest in this study. Hughes et al. (1999a) found similar results for secondary forests in a Mexican smallholder landscape. Total AGWB-C ranged from 2 – 50 Mg C ha<sup>-1</sup> in young secondary forests (< 15 yrs) and 44 – 146 Mg C ha<sup>-1</sup> in secondary forests ≥ 15 yrs (assuming that 50% of total AGWB in their study is C).

This study demonstrates that a multiple-linear regression model applied to high-resolution satellite imagery can provide accurate estimates of aggregate AGWB-C for a highly heterogeneous and degraded (low-biomass) smallholder landscape, even with relatively small calibration plots (0.1 ha). Some studies have suggested that AGWB estimates from passive optical imagery alone are too uncertain to satisfy monitoring guidelines (Zolkos et al., 2013). However, my findings show that optical imagery calibrated with a large number of relatively small plots offers a promising option for monitoring AGWB-C aggregated across large areas (> ~250 ha) with very low uncertainty (less than 5%). This is encouraging as small sample plots are not only less costly but in fact necessary in these fragmented landscapes where homogenous land-use units are irregularly shaped and frequently less than 1 ha.

The ranges of map uncertainty and observed errors at the scale of a typical farm (0.1 ~ 1 ha) suggest that monitoring AGWB-C in individual fields may not be feasible using the methodology presented in this study. However, map uncertainty seems to correspond reasonably well with observed error, implying that the predicted 95%

confidence interval for aggregate AGWB-C will usually encompass the true aggregate AGWB-C, even in farm-size plots.

Uncertainty estimates reported in the literature often refer only to the fit of the model used to predict AGWB, usually by the root mean squared error (RMSE) or the mean absolute error (MAE) (Castillo-Santiago et al., 2010; Eckert, 2012; Fuchs et al., 2009; Tsui et al., 2013). The RMSE and MAE are simple and common methods for reporting the uncertainty of a prediction map (Sexton et al., 2015), but they are derived at the scale of the sample unit used to build the model and do not necessarily represent the uncertainty of aggregated total AGWB-C in a landscape (Mascaro et al., 2011b). This study utilized spatially explicit uncertainty estimates and aggregation to demonstrate that the uncertainty of landscape predictions, when correctly calculated, can be quite low, and that for areas less than about 10,000 ha spatial autocorrelation of uncertainty should be incorporated, but for larger areas simple quadratic scaling may be appropriate.

Only a few other studies have explored how uncertainty in AGWB varies with the size of aggregation units. Asner et al. (2010) discussed how map error declines precipitously with increasing sample area and with increasing grain size, falling to 4-5% at 5 ha resolution, and Mascaro et al. (2011b) found similar results for grain sizes ranging from 0.04 ha to 6.25 ha. In a study exploring strategies to efficiently implement REDD+ monitoring activities, Lusiana et al. (2014) showed lower uncertainty of C emissions with larger pixel sizes, dropping from 82% error at 1 ha

resolution to below 5% at 100 ha. Saatchi et al. (2011) found that tropical biomass C estimates aggregated at the national scale had uncertainties around 1% and remained bounded to within  $\pm 5\%$  when aggregated to 10,000 ha using 1 km<sup>2</sup> (100 ha) pixels. Fazakas et al. (1999) mapped forest biomass in Sweden using a Landsat TM image and found that while the RMSE at the plot scale ( $\sim 0.03$  ha) was around 70%, uncertainty fell to  $< 10\%$  when aggregated to the entire 510 ha study area.

These studies show how map uncertainty is reduced as the size of the area of interest increases, although several authors only achieved reduced uncertainty with a loss of spatial resolution. In this study, I demonstrate that focusing monitoring efforts on changes in *aggregate* landscape AGWB-C over time could be an efficient approach to developing C payment programs related to CSA adoption. Furthermore, the methods presented in this paper show that this can be achieved without sacrificing spatial resolution, allowing for assessment of spatial variability with the aggregation area for planning and monitoring purposes. The utility of spatial analysis for project planning is underscored by the finding from this study that targeting areas with higher C storage potential results in 46% larger C gains for the same area converted to CSA, compared to a random approach. However, more complex analysis would be needed to fully assess the utility maps for targeted project planning in practice, and it is likely results would vary by region and context.

#### ***5.4.2 Predicting changes in AGWB-C with CSA adoption and potential C values***

Widespread adoption of CSA in this landscape could substantially increase C stocks. Agriculture is already an important component of AGWB-C storage, comprising 39% of the landscape and storing nearly 20% of all AGWB-C stocks. CSA adoption could potentially double the AGWB-C stored in agricultural land, increasing stocks in the study area by up to 46,270 tons.

Based on current market price ranges (\$4 – 12 per ton CO<sub>2</sub> equivalent), the annual value of C per hectare of land converted to CSA averages \$13 – 40 ha<sup>-1</sup> yr<sup>-1</sup>. Some studies have identified successful programs offering similar payments for watershed enhancement services provided by agroforestry and reforestation (e.g. Kosoy et al., 2007), however others have suggested that per-hectare C payments in this range would be insufficient to incentivize small-scale farmers to adopt CSA, especially once transaction costs for farm-scale monitoring and contracting are included (Cacho et al., 2013; Henry et al., 2009; Luedeling et al., 2011).

While I estimate that per-hectare C values from CSA adoption are low, the value of C aggregated across the study area is substantial. Furthermore, I demonstrated that AGWB-C can be estimated from high-resolution satellite imagery for large areas (greater than ~250 ha) with low uncertainty, which could substantially reduce transaction costs and uncertainty associated with C monitoring across landscapes. These findings support those of other studies suggesting that C-payment programs

for smallholder CSA adoption may need to be developed with groups of landholders, community-based organizations or C aggregators (e.g. Cacho et al., 2013; Henry et al., 2009).

Forming C contracts with organizations rather than individual land owners could also offer a number of additional benefits, especially in the context of CSA projects, such as: increased flexibility in how CSA is promoted and incentivized; the ability to include additional C gains that may occur in non-agricultural lands (e.g. from reduced wildfires and improved fallows); and the possibility to combine C payments with incentives for additional ecosystem services provided by CSA (e.g. water funds) or civic and livelihood projects (Stringer et al., 2012). However, more work is needed to better quantify how C accountability at more aggregated scales may impact transaction costs and land use decisions.

## **5.5 Conclusions**

CSA presents an opportunity to substantially increase C stocks in smallholder landscapes while simultaneously providing additional benefits, including increased resilience to an already changing climate. The per-hectare value of AGWB-C gains from CSA adoption is low, but becomes substantial when aggregated across hundreds or thousands of hectares. Monitoring at this scale using satellite imagery could substantially reduce transaction costs, however a tendency in the literature to report only plot-scale errors (e.g. RMSE) without exploring the aggregated error

AGWB-C maps may be limiting the operationalization of satellite-based monitoring approaches.

My findings demonstrate that high-resolution satellite imagery can be used to accurately monitor aggregate AGWB-C at the watershed to landscape scale (100 – 10,000 ha) in highly heterogeneous smallholder landscapes. Comparing the few studies that have quantified the uncertainty of AGWB-C and C emissions at multiple scales with this study, I conclude that areas of 200-300 ha may be an appropriate minimum scale at which to monitor aggregated C stocks with low uncertainty (i.e., < 5%) using optical satellite imagery. Texture variables are at least as important as vegetation indices to develop AGWB-C prediction models with high spatial resolution passive optical satellite imagery, and mapping AGWB-C at high-resolution could considerably increase C gains per unit area converted to CSA by allowing projects to efficiently target low-biomass areas. .

Landscape-scale accountability of C, supported by satellite-based methods such as that presented in this study, can reduce costs and uncertainty associated with C monitoring. Such an approach can thereby overcome some of the methodological concerns hindering the inclusion of CSA in international and voluntary C agreements, and support both market and non-market mechanisms to incentivize widespread CSA adoption in heterogeneous smallholder landscapes globally.

# **6 A simplified approach to mapping tree biomass in heterogeneous landscapes with airborne laser scanning**

## **6.1 Background and introduction**

As nations work to meet and strengthen climate change mitigation goals, there is growing recognition that terrestrial C stocks associated with land use are a key component (Pan et al., 2011). Much effort has been devoted to quantifying C stocks in aboveground woody biomass (AGWB) – defined here as the mass per unit area of organic matter in woody vegetation (i.e., trees). AGWB is a large C sink readily affected by land management (Brown et al., 1989; Chave et al., 2014; Jucker et al., 2017), and accurate monitoring of AGWB is critical to understanding and measuring the rate of C sequestration or release between terrestrial ecosystems and the atmosphere (Zhang and Ni-meister, 2014).

However monitoring of AGWB in the field is laborious and expensive (Asner et al., 2012), therefore limiting the utility of plot inventory data alone to be used for AGWB accounting at regional, national and global scales required for international cooperation and accounting (Brown, 2002; Sileshi, 2014; Zhang and Ni-meister, 2014). Such challenges are further exacerbated in highly heterogeneous landscapes

requiring additional stratification of plot inventory data, issues with respect to fitting plots within very small land use units and limitations of alternative quantification methods such as flux towers or process-based models (GOF-C-GOLD, 2013; Kearney and Smukler, 2016; Ravindranath and Ostwald, 2008).

Furthermore, plot data is often limited to inventories of forested areas, while there is mounting evidence that TOF hold large amounts of AGWB-C (Guo et al., 2014; Schnell et al., 2015), leading to increased interest in monitoring C associated with non-forest land uses (de Foresta et al., 2013; Rosenstock et al., 2016). For example, measuring AGWB in non-forest lands and TOF is a key component of policies supporting 'climate-smart' agricultural practices, such as smallholder agroforestry systems, to simultaneously sequester C, increase agricultural resilience and alleviate poverty and food insecurity (Mbow et al., 2014; Rioux et al., 2016; Steenwerth et al., 2014; Stringer et al., 2012). Many of these 'climate-smart' practices result in landscape mosaics of highly diversified vegetation (e.g., fields intercropped with trees, hedgerows, riparian buffers and bush-fallow patches), which are desirable for a range of ecosystem service benefits (Harvey et al., 2013; Scherr et al., 2012; Smukler et al., 2010), but present unique challenges for monitoring AGWB (Guo et al., 2014; Lu, 2006; Schnell et al., 2015).

Remote sensing is a demonstrated tool to accurately monitor AGWB-C at broad spatial scales and across diverse land use types (De Sy et al., 2012; Goetz et al., 2009; Lu, 2006; Saatchi et al., 2011; Zhang and Ni-meister, 2014). In particular, the use of

airborne laser scanning (ALS; also called Light Detection and Ranging, or LiDAR), combined with rapidly increasing computer processing power, has recently enabled accurate and high-spatial resolution mapping of vegetated landscapes in 3D using pulses of light emitted from aircraft and unmanned aerial vehicles (Lefsky et al., 2002; Lin et al., 2016). However, to date, much of the research applying ALS to quantify AGWB stocks has focused on temperate conifer, broadleaf and plantation forests (Levick et al., 2016; Lutz et al., 2008; Rana et al., 2013; Tao et al., 2014; Tsui et al., 2013) or intact tropical forest landscapes (Asner et al., 2013, 2012; Lin et al., 2016; Vaglio Laurin et al., 2014) and reliable methods for quantifying AGWB using this type of data in heterogeneous landscapes and TOF are lacking, especially at these broader spatial scales and reporting units (de Foresta et al., 2013; Price et al., 2017).

Current methods for estimating AGWB using ALS generally rely on an area-based approach – developing calibration models from a suite of ALS metrics extracted from fixed-area field plots where AGWB has also been calculated using tree measurements and allometric equations (White et al., 2013). The area-based approach has yielded very accurate results in forested ecosystems (Zolkos et al., 2013), but may be less well suited to heterogeneous landscapes and biomass in TOF for several reasons. For example, the pixel resolution or cell size prediction unit of the final biomass map is generally restricted to the size of calibration plots (Mascaro et al., 2011b; White et al., 2013), presenting a trade-off between the desire for larger

plots to improve calibration (Asner et al., 2012) and the need for very high resolution biomass maps to capture TOF and small land uses (Czerepowicz et al., 2012; Jackson et al., 2013). Additionally, area-based calibration plots must be georeferenced, uniformly sized and representative of the full range of vegetation structure variability (preferably), and field data should be collected as close in time as possible to the acquisition of ALS data, ideally within the same growing season (White et al., 2013). It is therefore difficult to use historical plot inventories which may not meet the above criteria, or to update calibration models with new plot data collected in subsequent seasons or from outside the ALS coverage area. All of these issues are problematic in an operational biomass prediction and mapping context since ALS acquisition is expensive and collection tends to be infrequent and piecemeal (Price et al., 2017).

To address these issues, I propose and develop a simplified method for predicting AGWB from an ALS-derived canopy height model (CHM). These models, generally defined as the difference between the ground surface and the top of vegetation canopy, are easily derived from ALS (Lim et al., 2003). By linking to the CHM, the approach introduced in this study allows estimation of AGWB at the same resolution as the CHM (often  $\leq 1$  m). Moreover, this CHM-based approach is built on allometric relationships between morphological tree variables rather than georeferenced plots (see Section 2.4), meaning that field data could be used that was collected from any point in time and from variable plot sizes.

Therefore, this study sought to address three main objectives: (1) develop a model to predict AGWB from a CHM and compare its accuracy to a traditional area-based approach in a highly heterogeneous landscape; (2) assess the proportions of total landscape AGWB stored in forests and TOF, as predicted by the two approaches; and (3) discuss the strengths and limitations of the CHM-based approach as a tool for AGWB prediction in diverse landscapes.

## **6.2 Methods**

### **6.2.1 Study area**

This research was conducted within the mountainous region of northern El Salvador known as La Mancomunidad La Montañona (hereafter referred to as La Mancomunidad) – a group of seven municipalities spanning about 32,000 ha. La Mancomunidad is organized, in part, around conserving an approximately 1,500-ha area of primary pine (*Pinus oocarpa*) and oak (*Quercus insignis*) forest threatened by deforestation and frequent wildfire from surrounding smallholder agriculture. The remaining land is a complex mosaic of subsistence farms, extensive pastures, bush-fallows and settlements. Farms and pastures in La Mancomunidad are frequently less than one ha in size and regularly contain woody perennials in the form of intercropped trees and live fences (i.e., TOF). Bush-fallows are widespread and highly variable in age, species composition and structure. More information on the study area and species of woody vegetation can be found in Chapter 5.

### **6.2.2 Field data collection**

For this study, I produced and compared ALS-derived AGWB maps for the entire study area of La Mancomunidad (see Section 2.1 and Figure 2.1) using both an area-based approach and a CHM-based approach (Section 6.2.3). AGWB data for model development and validation were compiled from multiple field campaigns conducted between 2012 and 2016. In all years, individual tree measurements were taken from geo-referenced and differentially corrected ground plots ranging in size from 0.02 to 0.97 ha. Tree height and diameter at breast height (DBH; 1.3 m) were measured for all trees with heights  $\geq 1.3$  m and DBH  $\geq 1$  cm. Trees were identified to the species level, when possible, and allometric equations applied to estimate AGWB from DBH for each tree using a combination of species-specific and generalized equations, as described in Chapter 5 and Appendix B. The AGWB of all trees within a plot was summed and divided by the plot area to estimate AGWB density ( $\text{Mg ha}^{-1}$ ) for all plots.

For area-based model calibration, I used data collected in 0.1 ha circular plots sampled in 2014 following methods described in Chapter 5. These circular plots ( $n = 107$ ) were randomly selected, stratified by elevation and four land use/land cover (LULC) classes: cropland (CROP), pasture (PAST), broadleaf forest (BLF) and, mixed-pine forests (MPF). A fifth class, 'OTHER' was later developed to group a small number of plots that did not meet the criteria of the four classes (e.g., teak plantations, old/abandoned coffee agroforests and home gardens). Prior to analysis,

the circular plots were randomly split into two datasets: ~70% for calibration of the area-based approaches (n = 73) and ~30% for independent model validation (n = 34; see Figure 2.1 for plot locations).

I added to the validation dataset all other plot data available from within 1 year of ALS acquisition in order to encompass a broader range of LULC classes (especially those with TOF), geographic area and plot sizes. Additional validation data included: live fences/hedgerows (HR) adjacent to fields and pastures (0.02 – 0.3 ha; n = 22), CROP fields in maize and sorghum with dispersed trees (0.2 – 0.9 ha; n = 10) and, large closed-canopy MPF inventory plots (~1 ha each; n = 3). This resulted in a total of 69 independent validation plots (see Figure 2.1).

Additional data of individual trees from plots sampled in 2012 (Figure 2.1) and revisited in 2016 were included in the final dataset used to develop equations for the CHM-based approach (see Section 6.2.3.3). In total, the dataset consisted of 5,991 broadleaf trees (encompassing all five land use classes) and 90 coniferous trees (MPF class only).

### **6.2.3 ALS data acquisition and processing**

#### *6.2.3.1 ALS data pre-processing*

ALS data was acquired for the entire study area in April 2014 and converted to buffered tiles (390 m tiles; 60 m buffer) in LAStools (Isenburg, 2016). Isolated returns, defined as 15 or fewer points within a 2-m x 2-m x 1-m cell, were removed

from the raw point cloud using the *lasnoise* tool, also in LAStools. A height-normalized point cloud was then produced by first classifying ground returns using *lasground* (default step size of 5 m) and then subtracting the ground elevation from each return. Height-normalized returns greater than 70 m (the maximum expected tree height in this area) were removed as suspected errors or clouds. Further processing of the ALS data to predict AGWB using the area- and CHM-based approaches is described below.

#### 6.2.3.2 Area-based approach

The area-based approach predicts AGWB using ALS-derived vegetation height and density metrics extracted from calibration ground plots (White et al., 2013). Forty-nine standard elevation statistics (see Appendix C, Table C - 1) were developed from height-normalized ALS point clouds extracted from the circular calibration plots (n = 73; size = 0.1 ha) using the *cloudmetrics* command in FUSION (McGaughey, 2014). I then developed a random forest (RF) model to predict total plot AGWB using a two-step process. Among non-parametric methods to develop area-based ALS models, RF is the most common (White et al., 2013), and works by developing an ensemble of regression-based decision trees from bootstrapped training data, and then ‘voting’ for the most popular result (Breiman, 2001).

In order to develop an RF model, all ALS metrics were included as potential predictor variables and an unbiased, conditional RF model was generated in the

*party* package (Strobl et al., 2008) in R (R Core Team, 2013). The number of trees was capped at 500 and the number of variables randomly sampled at each split was set at six, roughly equal to the square root of the number of potential predictor variables (Strobl et al., 2008; Svetnik et al., 2003). Correlated predictor variables (Pearson's  $R > 0.9$ ) were then removed by keeping the variable with the highest conditional variable importance ranking from the full RF model (Strobl et al., 2008). A final RF model was then developed using the reduced set of 12 uncorrelated predictors (see Appendix C, Table C - 1).

Spatial estimations of AGWB were predicted from the final RF model at 5 m and 30 m resolutions. The 30 m estimation was chosen to roughly equal the size of the calibration plots, as suggested by White et al. (2013). I added a 5 m estimation to increase the spatial resolution with the hope of better capturing TOF, and for comparison against the CHM-based approach. A resolution of 5 m was chosen to correspond with RapidEye spectral imagery also available for the study area, and it aligned well with another study using similar methods (Mascaro et al., 2011b).

For the 30 m estimates, ALS metrics were extracted using *gridmetrics* in FUSION (McGaughey, 2014) with the cell size set at 30 m. The RF model was then applied using the metrics of each 30 m cell. For the 5 m estimates, I chose not to reduce the grid size of the metrics since metrics should be extracted from a grid similar in size to the calibration plots and should not be smaller than individual tree crowns (White et al., 2013). Instead, I generated a moving window by running *gridmetrics*

repeatedly at a 30 m cell size and shifting the origin of the output grid in 5 m intervals to the north and east until reaching the origin of the adjacent 30 m cell.

#### *6.2.3.3 CHM-based approach*

To contrast with the conventional area based approach, I developed a new approach to predict AGWB from a CHM produced at 5 m spatial resolution (again corresponding to available RapidEye imagery), recognizing that canopy height is strongly correlated with AGWB and is directly measurable by ALS (Asner and Mascaro, 2014; Zhang and Ni-meister, 2014). The method utilizes allometric relationships between tree height, DBH and AGWB (Figure 6.1) derived from empirical analysis of tree data in this study and published equations (both described below). Using these relationships, the average AGWB per tree can be predicted from its height, and since each CHM pixel represents the average height of the tree canopy within that pixel, the average AGWB per tree can then easily be predicted for each pixel. However, a pixel (in this case, 5 x 5 m) may encompass multiple smaller trees or only parts of larger trees, with the number of trees per pixel unknown. I overcome this unknown factor by estimating the areal AGWB density (e.g.,  $\text{kg m}^{-2}$ ) of a tree at the height of the CHM pixel based on its expected tree crown area. In this way, AGWB per tree can be converted to AGWB per ha (Figure 6.1), allowing landscape level analysis.

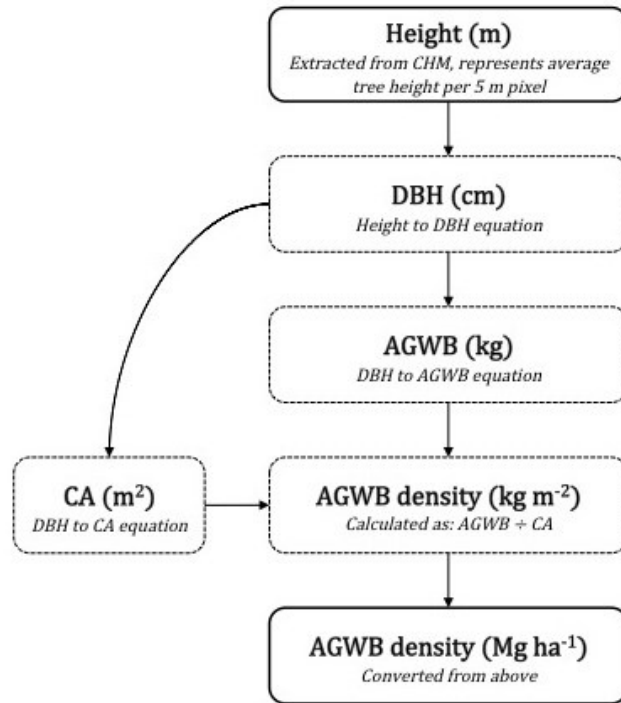


**Figure 6.1 Schematic diagram of the generalized CHM-based approach**

The general steps required to predict areal density of aboveground woody biomass (AGWB) from an ALS-derived canopy height model (CHM) using allometric relationships between tree height, diameter at breast height (DBH) and crown area (CA).

Height-to-DBH and DBH-to-AGWB equations were developed from the individual tree data collected between 2012 and 2016. For broadleaf trees, both height-to-DBH and DBH-to-AGWB equations were developed, whereas for coniferous trees, only height-to-DBH models were developed since all trees were of the same species (*Pinus oocarpa*), enabling the use of an existing model developed by Návar (2009) using destructive techniques.

To derive the height-to-DBH and DBH-to-AGWB equations, logistic models were fit for each tree type using the *nls* function in R (R Core Team, 2013) after binning data by DBH at 5 cm intervals. Binning was performed to overcome issues of non-constant variance and a strongly skewed distribution, with many more observations of smaller trees than larger ones (Jucker et al., 2017). Logistic models were chosen to reflect the non-linear, asymptotic scaling relationships between these three variables (Jucker et al., 2017). A self-starting four-parameter model was first fit using the *SSfpl* function to find reasonable starting parameters for the model. Lower asymptotes were then set at zero (effectively reducing the model to three parameters) and upper asymptotes set at the maximum observed value for each dependent variable in order to avoid extrapolating beyond observed values. A fifth parameter (empirically derived) was added if asymmetrical scaling was suspected based on visual assessment of the fit of the four-parameter model (Paine et al., 2012).

Crown area was estimated from DBH using existing equations developed in similar regions. For broadleaf trees, crown area was estimated from DBH using an equation developed by Muller et al. (2006) from 850 trees in Barro Colorado, Panama. For coniferous trees, I used an equation developed by Nutto et al. (2005) from 400 pine trees across 16 stands in Brazil.

#### **6.2.4 Model Validation**

All three ALS-derived AGWB maps (area-based 30 m and 5 m; CHM-based 5 m) were validated using the 69 independent validation plots. Predicted AGWB for each validation plot was extracted and overall root mean square error (RMSE) calculated for each LULC class in  $\text{Mg ha}^{-1}$  and as percent of the mean field measured value. Model bias was calculated as the median prediction error to explore over and under estimation, and predicted AGWB vs. ground-measured AGWB was graphed to visualize the model fit by plot size and land use type.

#### **6.2.5 Total AGWB by vegetation type**

In order to assess the proportions of total landscape AGWB stored in forests and TOF, as predicted by the two approaches, a forest fragmentation index was developed using a method adapted from Riitters et al. (2000, 2002) to classify woody vegetation into five classes: “core”, “transitional”, “riparian/isolated”, “perforated” and “patch”. The index was created based on the relationship of area density ( $P_f$ ) and connectivity ( $P_{ff}$ ) of forested pixels (Figure 6.2). Forested pixels were identified as those having vegetation exceeding 3 m height using the ALS-derived CHM.  $P_f$  is a measure of the proportion of forested pixels within a surrounding area – in this case a moving window of 21 x 21 pixels, or approximately 1 ha.  $P_{ff}$  measures forest connectivity as the conditional probability that a forested pixel’s neighbouring pixel (in the cardinal directions only) is also forested (Riitters

et al., 2000, 2002). A 9 x 9 pixel window (approximately 0.25 ha) was used for  $P_{ff}$ , as this better captured small linear features such as live fences and riparian corridors.

The core class ( $P_f = P_{ff} = 1.0$ ) thus represents a pixel where all other pixels within ~1 ha are also forested. The transition class represents core forest edges, where a high proportion of pixels are forested and highly connected. The other three classes can be considered representative of TOF. The riparian/isolated class represents wide linear woody vegetation features (e.g., riparian corridors) and isolated forest patches of about 0.25 ~ 1.0 ha. The perforated class generally represents wooded pastures, and the patch class encompasses agroforestry, live fences and settlements, although there is some overlap between these two classes.

Total AGWB by forest fragmentation class for the entire study area was then calculated for both the area-based (5 m) and CHM-based predictions using ArcGIS 10.1 (ESRI, 2011).

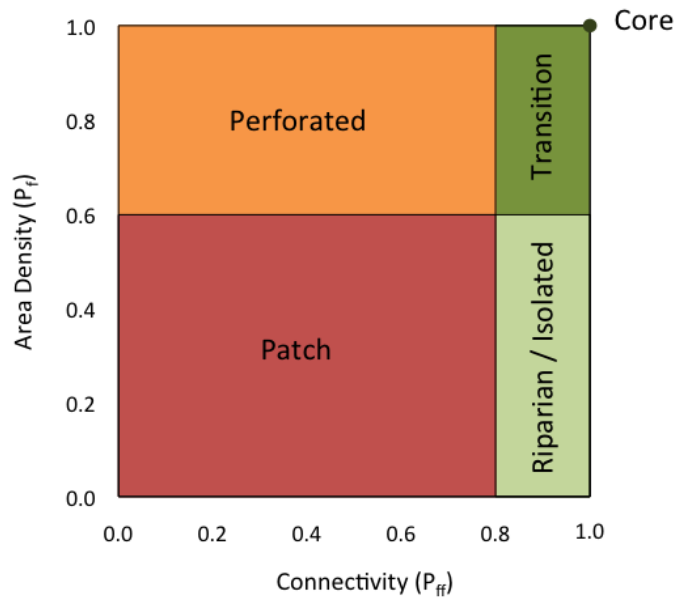


**Figure 6.2 Visual representation of the forest fragmentation index model**

Shows the relative breaks used to identify the five fragmentation classes based on area density ( $P_f$ ) and connectivity ( $P_{ff}$ ) of forested pixels. Adapted from Riitters et al. (2000, 2002), with breaks of  $P_f/P_{ff}$  slightly modified to better represent the study area.

## 6.3 Results

### 6.3.1 Accuracy of AGWB predictions using ALS

Overall accuracy improved using the CHM-based approach compared to the area-based approaches (Table 6.1). Overall bias was low for all models, but both the 5 m and 30 m area-based approaches tended to under-predict AGWB in plots within hedgerows, and over-predict in plots in cropland and broadleaf forests, especially at low AGWB values (Table 6.1 and Figure 6.3). The CHM-based approach increased

the accuracy of hedgerow predictions and showed less bias in all LULC classes except mixed-pine forest.

Using a 30 m grid cell, the area-based approach did a poor job of visually capturing small, isolated and linear woody vegetation features (Figure 6.4c). Increasing the resolution of the area-based approach to 5 m improved the definition of these features, however it still resulted in a marked smoothing effect (Figure 6.4d), while the CHM-based approach better preserved the detail of heterogeneous woody vegetation (Figure 6.4e).

**Table 6.1 Validation of AGWB prediction results for area- and CHM-based models**

Independent validation of the three aboveground woody biomass (AGWB) prediction models by land use/land cover (LULC) class using root mean squared error (RMSE) and the median prediction error (Bias). LULC classes are the following: HR = hedgerows/live fences; CROP = cropland; PAST = pasture; BLF = broadleaf forest; MPF = mixed-pine forest; OTHER = teak, coffee and home gardens. The number of validation plots in each LULC class is indicated by *n*.

LULC Class	n	Area (ha)	Area-Based (30 m)			Area-Based (5 m)			CHM-based (5 m)		
			RMSE			RMSE			RMSE		
			Mg ha <sup>-1</sup>	%	Bias	Mg ha <sup>-1</sup>	%	Bias	Mg ha <sup>-1</sup>	%	Bias
HR	22	0.02 - 0.30	151.0	98.2	-4.3	139.7	90.9	-3.7	119.4	77.7	-2.3
CROP	16	0.10 - 0.89	49.1	224.3	5.9	45.1	206.1	7.3	45.2	206.7	3.9
PAST	10	0.1	128.9	137.8	0.8	137.1	146.6	0.9	148.5	158.8	0.2
BLF	6	0.1	57.1	41.9	4.4	56.0	41.1	4.9	64.7	47.5	3.0
MPF	11	0.1 - 0.97	57.4	31.1	-1.6	58.4	31.6	-1.7	57.8	31.3	-2.7
OTHER	4	0.1	43.0	66.2	3.9	52.9	81.5	5.4	44.8	68.9	3.4
OVERALL	69	0.02 - 0.97	105.6	93.7	0.0	102.0	90.5	-0.2	96.1	85.2	0.0

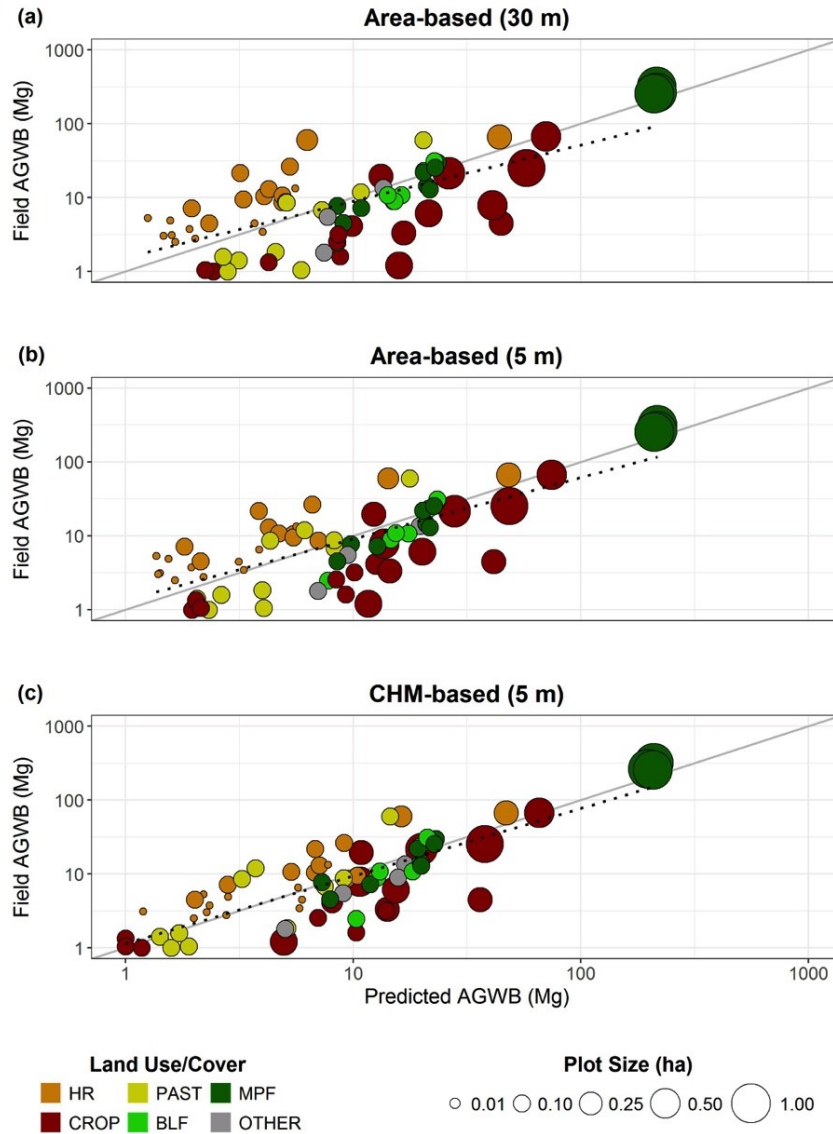


**Figure 6.3 Predicted vs. field-measured AGWB for area- and CHM-based models**

Model fit of predicted aboveground woody biomass (AGWB) for independent validation plots ( $n = 69$ ). Plots (a) and (b) show results from the area-based models with spatial resolutions of 30 m and 5 m (respectively) derived from airborne laser scanning (ALS) plot metrics. Plot (c) shows results of the CHM-based model using a 5 m resolution ALS-derived canopy height model (CHM). The solid grey line shows the 1:1 fit and the dotted line shows the linear regression for predicted vs. field-measured AGWB for each model.

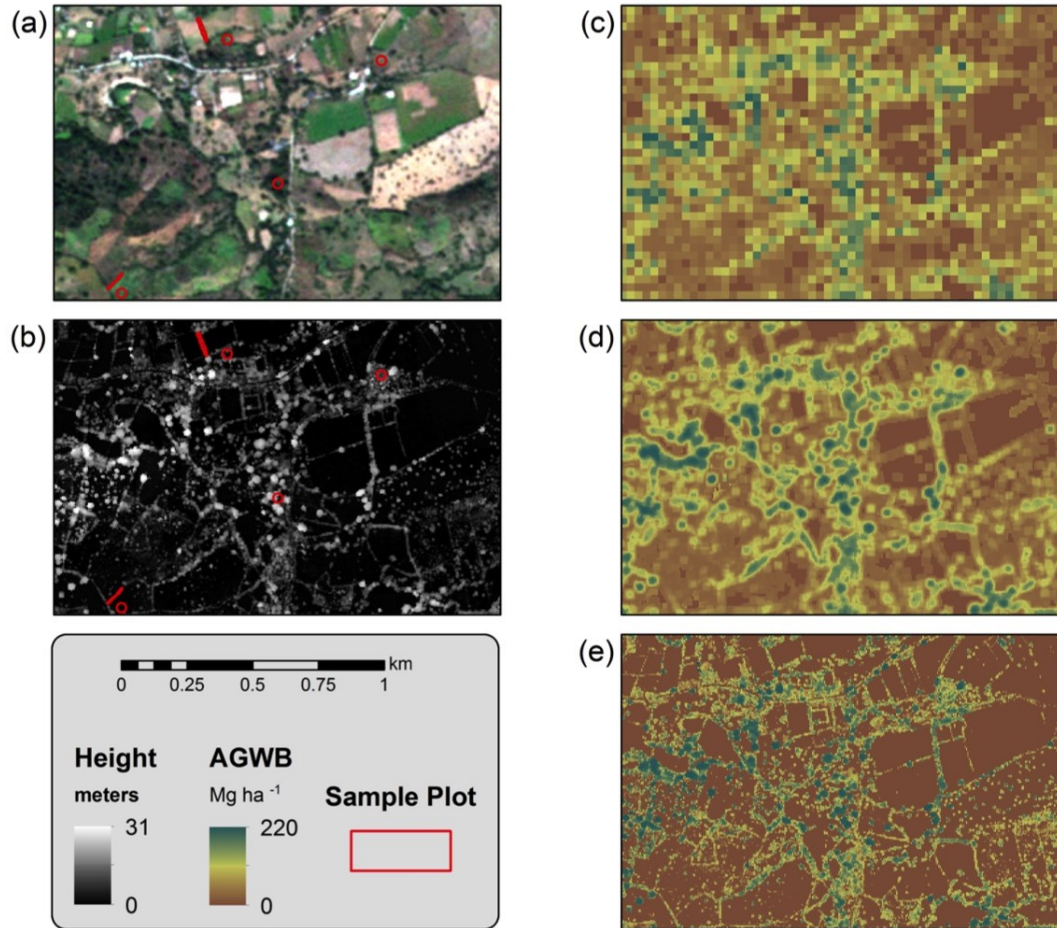


**Figure 6.4 Select results of mapped AGWB using different approaches and spatial resolutions**

Images at 5 m and 30 m resolution of a typical heterogeneous zone within the study area showing (a) satellite image (RapidEye, 5 m); (b) a canopy height model (CHM) derived from airborne laser scanning (ALS) data (5 m); (c) predicted aboveground woody biomass (AGWB) from an area-based model using ALS metrics (30 m); (d) predicted AGWB from an area-based model using ALS metrics and a moving window (5 m); (e) predicted AGWB from a CHM-based model using the ALS-derived CHM (5 m). Examples of sample plots used for calibration or validation are shown in red on images (a) and (b).

### **6.3.2 Total AGWB by woody vegetation type**

The forest fragmentation index represented the different woody vegetation components well (Figure 6.5). A total of 21,328 ha of the study area are covered by woody vegetation  $\geq 3$  m height. About 33% of this vegetated area is in TOF, mostly within perforated or patch fragmentation classes. The remaining 67% is in core or transitional forest classes (Table 6.2).

Between 2.41 – 2.74 million Mg of AGWB are predicted for the study area, depending on which model is used. Both approaches predict similar amounts of AGWB in forest classes, with the area-based approach estimating about 4% more than the CHM-based approach. The area-based approach predicted about 213,000 Mg (8%) of AGWB in areas known to have no woody vegetation and estimated 21% less AGWB in TOF compared to the CHM-based approach (Table 6.2), likely due to the smoothing effect of the area-based approach (see Figure 6.4d). The CHM-based approach predicts that 22% of all AGWB in the study area is stored in TOF, at an average areal density of 77 Mg ha<sup>-1</sup>.

**Table 6.2 Total landscape aboveground woody biomass (AGWB) for the study area by forest fragmentation class**

Fragmentation Class	Area (ha)	AGWB					
		Area-based (5 m)			CHM-based (5 m)		
		Mg	Mg ha <sup>-1</sup>	% of Total	Mg	Mg ha <sup>-1</sup>	% of Total
Core	4,470	731,279	164	27%	677,366	152	28%
Transitional	9,812	1,217,884	124	45%	1,189,158	121	49%
Forest Subtotal	14,282	1,949,163	136	71%	1,866,524	131	78%
Riparian/Isolated	436	51,333	118	2%	56,041	129	2%
Perforated	3,973	245,660	62	9%	291,959	73	12%
Patch	2,637	129,737	49	5%	191,042	72	8%
TOF Subtotal	7,046	426,730	61	16%	539,042	77	22%
Vegetation < 3 m	3,324	147,500	44	5%	1,174	0	0%
Non-Vegetation	7,171	212,711	30	8%	0	0	0%
'Other' Subtotal	10,495	360,211	34	13%	1,174	0	0%
<b>Total</b>	<b>31,823</b>	<b>2,736,104</b>	<b>86</b>	<b>100%</b>	<b>2,406,740</b>	<b>76</b>	<b>100%</b>

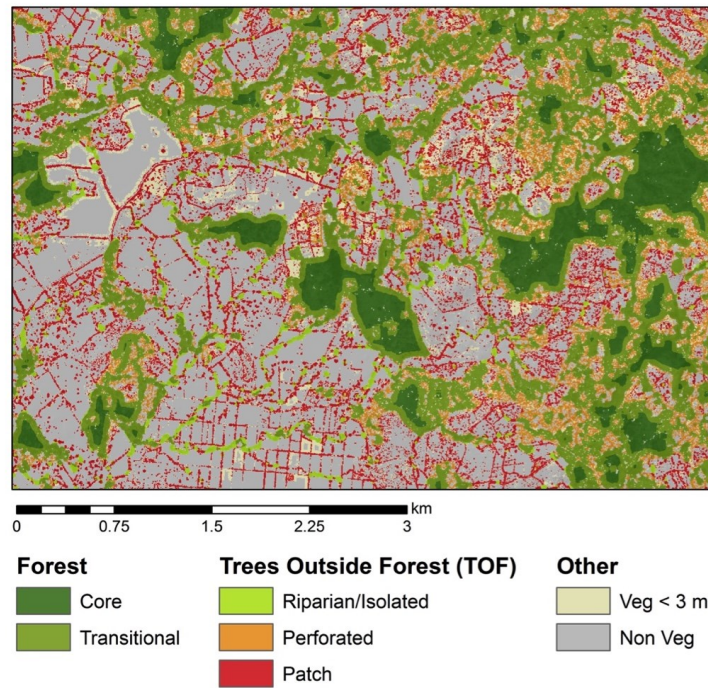


**Figure 6.5 Map showing woody vegetation types based on fragmentation classes for a select area**

## 6.4 Discussion

### 6.4.1 Accuracy of AGWB predictions using ALS

Overall RMSE of prediction from area- and CHM-based models were high, but within the expected range for independently validated AGWB predicted from ALS in a heterogeneous landscape. Lu et al. (2012) used independent validation and found a RMSE of 89% for a mountainous landscape in east China with highly variable AGWB. Other studies report substantially lower RMSE values for ALS-predicted AGWB, but it is difficult to draw comparisons since most studies tend to either occur in more homogenous forest landscapes, use larger plots for validation, use cross-validation methods or simply report the RMSE of model fit.

For example, a study by Asner and Mascaro (2014) used an independent validation dataset for ALS-predicted biomass C and found RMSE values of about 40 – 70% in plots smaller than 0.1 ha, and RMSE values declined toward 10% in plots of 1 ha or greater; however plots were located in mature intact forests with relatively high biomass and low variation. Another study by Lu et al. (2012) of an intact coniferous forest reported an RMSE of 34% for their ALS model, but did not report validation error, independent or otherwise.

A study targeting plots with more variable biomass in Panamá reported a RMSE of about 18% for their ALS model, but also did not report validation error (Mascaro et al., 2011b). A nationwide Swiss study encompassing both forests and TOF obtained

RMSE values of about 40% utilizing a very large number of calibration plots ( $n = 5,562$ ) and leave-one-out cross-validation (Price et al., 2017). Finally, a meta-analysis of 57 studies spanning five different forest types found AGWB errors ranging from around 10 – 60%, although most studies did not use a reserved independent dataset for model validation (Zolkos et al., 2013).

Accuracies become similar to other studies if model fit is reported (rather than validation), cross-validation methods are used, or if error is assessed only for forest sites or larger plots. Looking at just the model fit for the area-based approach, I found a RMSE of 78% for the 0.1 ha calibration plots (essentially the same error as that achieved from the satellite-based methods used in Chapter 5). Using leave-one-out-cross-validation on the 0.1 ha forest plots alone, RMSE reduced to 59%, within the range found by Zolkos et al. (2013). Looking at independent validation on just the large plots in this study ( $> 0.5$  ha;  $n = 6$ ), RMSE reduced to 30% for both the pixel and area-based approaches. This comparison demonstrates the influence of how error is calculated, and highlights the importance of using independent validation.

#### **6.4.2 Total AGWB by woody vegetation type**

In this landscape, typical of much of Central America, I estimate that TOF contains about 29% of the AGWB found in forests, similar to values found for other regions (e.g., Guo et al., 2014). Accurately quantifying AGWB in TOF is a critical component for monitoring ecological, economic and social functions of trees (e.g., from

agroforestry). TOF are becoming an increasing large component of AGWB in many landscapes (Guo et al., 2014; Price et al., 2017) and many international environmental organizations require TOF information in their reporting requirements (Schnell et al., 2015).

By developing a CHM-based approach to predict AGWB, I was able to better predict AGWB in TOF (i.e., hedgerows and agroforestry) compared to an area-based approach. The area-based approach tended to generalize over vegetation edges, of which there are many in smallholder landscapes (Figure 6.4). As a result, the area-based approach appeared to under-predict AGWB in TOF by about 112,000 Mg compared to the CHM-based approach, and to over-predict AGWB in known non-vegetated areas by about 213,000 Mg. Price et al. (2017) also found that area-based ALS models over-predicted AGWB in low-biomass plots compared to national inventory data within a heterogeneous Swiss settlement.

### ***6.4.3 Strengths, limitations and future directions***

In addition to better capturing TOF, the CHM-based approach introduced in this study offers several distinct advantages. First, it is built from allometric relationships rather than relying on georeferenced fixed-area plot data. This means that input data (i.e., individual tree measurements) can be collected at any point in time and updated as new data become available. Furthermore, allometric equations can be developed using data from any applicable region, although local data would

almost certainly improve accuracies, especially if it specifically targets inclusion of TOF (Schnell et al., 2015). Lastly, the CHM-based approach requires little expertise and avoids the need for producing 3D grid metrics, which can be computationally intensive to produce. Thus, this approach shows promise as a simple and transferable approach to predict AGWB from ALS, especially in operational settings where ALS coverage is available across broad areas.

However, more research is needed to validate this approach for other regions and address certain limitations within this study. First, I note that it was not possible to develop empirical relationships between height and crown area for this since crown area measurements were not available. I was able to find DBH-to-crown-area equations from reasonably similar regions, which highlights the flexibility of this approach, but ideally empirical site-based relationships between height and crown area would be developed to better evaluate this method. This supports other recent calls to measure crown area as an important morphological variable for predicting AGWB from both field and remote sensing data (Blanchard et al., 2016; Jucker et al., 2017).

Second, it is unclear whether the CHM-based approach introduced here would work well at different CHM spatial resolutions and whether an optimal pixel size exists. Theory might suggest that this method would work best when the pixel size is roughly equal to the average tree crown area in a landscape. In this study area (La Mancomunidad), this may occur at about 5 m pixel resolution, while other

landscapes could be substantially different. Additionally, further exploration is warranted to assess the potential accuracy benefits of spreading AGWB over the tree crown. The CHM-based approach effectively distributes AGWB across the entire tree crown footprint, which, while unconventional, may be reasonable considering a large portion (up to 77%, by some accounts) of AGWB in tropical trees can be stored in the crown (Goodman et al., 2014; Jucker et al., 2017). Indeed, Mascaro et al. (2011b) found that area-based prediction accuracy increased when they distributed AGWB on a circle representing the expected crown areas of trees within a given prediction cell. Further testing of the CHM-based approach at different spatial resolutions and in other regions would help answer these questions.

Finally, recent research shows that equations combining height and crown dimensions can substantially improve biomass estimation for individual trees compared to equations using DBH alone (Jucker et al., 2017). In this study, I relied on DBH-to-AGWB equations with the added step of predicting DBH from height. Algorithms are emerging to detect individual trees with ALS data, enabling remote measurement of both height and crown area (Allouis et al., 2013; Popescu, 2007; Popescu and Wynne, 2004; Tao et al., 2014; Vége and Durrieu, 2011). An obvious next step would be to predict AGWB for individually segmented trees using height and crown dimensions extracted from ALS, avoiding DBH estimation altogether (Jucker et al., 2017). While this approach is expected to yield more accurate results than the CHM-based approach I present here, it is, however, even more

computationally demanding than the area-based approach and generalized algorithms have yet to be developed. As AGWB prediction methods based on tree segmentation continue to be developed, I recommend applying the CHM-based approach presented here in comparative studies to examine whether it could be an acceptably accurate method that could be more easily operationalized in management settings.

## **6.5 Conclusions**

I introduced a simple CHM-based approach to predict AGWB from ALS, and showed that overall prediction accuracy was comparable to area-based approaches utilizing 3D metrics from georeferenced calibration plots. The CHM-based approach better predicted AGWB in TOF (i.e., hedgerows and agroforestry), while the area-based approach tended to generalize over vegetation edges and under-predict biomass in TOF. This finding is significant due to the growing interest in monitoring TOF as a globally important reserve of AGWB. In this study, I found that 22% of AGWB was stored in TOF.

While other studies have employed area-based regression models to predict AGWB from canopy height alone (e.g., Asner et al., 2012; Asner and Mascaro, 2014; Drake et al., 2002; Price et al., 2017), I am unaware of any studies predicting AGWB directly from a CHM using tree-scale allometry, as was done in this study. The CHM-based approach does not require georeferenced plot data and the allometric

relationships on which the approach is built can be developed from input data collected at any point in time and from any applicable region. The flexibility of the CHM-based approach, combined with improvements in AGWB prediction for TOF, make it promising as a useful tool for operationalizing AGWB mapping in heterogeneous landscapes. However, more research is needed to validate the approach in other regions and at differing spatial resolutions.

# 7 Overall conclusions

## 7.1 Key research findings and contributions

### 7.1.1 *Overarching research objectives*

The research presented in this dissertation was designed to address the three overarching objectives posed in Section 1.2:

- (1) Develop, test and validate new methods to quantify multiple ES and individual ES indicators related to agricultural management at the field scale
- (2) Evaluate trade-offs and synergies among ES within the SMAS compared to other management options for smallholders
- (3) Develop methods to map ES indicators and uncertainty in heterogeneous smallholder landscapes, and apply those methods to address questions about the potential impacts of widespread SMAS adoption and the implications for policy design

The first two objectives were addressed at the field scale in Chapters 3 and 4. In Chapter 3, I built upon PCA methods used to develop indices for other applications (e.g., soil quality) and employed them to quantify multiple ES. I demonstrated how this method could be used to evaluate differences between management systems, and found that synergies among ES occur within the SMAS, while conventional management shows stronger trade-offs between ES. In Chapter 4 I demonstrated

the utility of an underutilized method for measuring hillslope erosion using pins, and validated its improved performance as an indicator of relative erosion rates.

The third objective was addressed in Chapters 5 and 6. By mapping AGWB-C at high spatial resolution using satellite imagery (Chapter 5), I showed that the SMAS can potentially store large amounts of C and that utilizing these maps to target low-C areas could substantially increase C gains per unit area converted to the SMAS. I discussed how the uncertainty associated with these maps may have important implications for how C contracts are developed, and how monitoring at the watershed or community scale can reduce uncertainty. In Chapter 6, I developed a new approach to measure AGWB in heterogeneous landscapes using airborne laser scanning data. I showed that this new approach could both improve and simplify mapping trees outside forests – an important ES indicator for smallholder landscapes.

The remainder of this section highlights specific research findings from each chapter at the field and landscape scales, while the subsequent sections (7.2 to 7.5) discuss the limitations, potential applications and future research directions of my research.

### **7.1.2 *Field-scale research findings***

Results from field-scale research conducted for this dissertation not only offer insight into the potential ES benefits of climate-smart agriculture in El Salvador, but

also contribute to a better general understanding of trade-offs and synergies between ES and provide steps toward operationalizing cost-effective ES monitoring.

In Chapter 3, I empirically demonstrated that the SMAS is an example of an adaptable agroforestry management system that can provide multiple regulating ES – approaching that provided by secondary forest-fallows – with potentially minimal impact on provisioning services. The PCA method I used to empirically weight indicators by their contribution to overall variance is, to the best of my knowledge, the first time this method has been applied to develop composite ES indices from multiple indicators. It is a relatively straightforward and statistically sound way to objectively weight indicators, and may be useful for designing ES monitoring strategies and to better understand how individual indicators contribute to overall service provision. By developing these composite ES indices, I was able to identify patterns showing that the SMAS better capitalizes on synergies between regulating and provisioning ES compared to conventional management. Specifically, I found positive relationships between soil water regulation, pest/disease control and yield, suggesting synergies with strong theoretical underpinnings.

Results from Chapter 3 also offer promising insight for how to monitor ES in a practical setting (i.e., for PES schemes). For example, I identified a subset of field proxies that correlate well with multiple ES. Measuring these simple proxies, rather than the whole suite of indicators necessary to develop ES indices, could substantially reduce monitoring costs. Additionally, I found that small trees were

correlated with different ES than large trees, suggesting that monitoring plans should be designed to measure trees of all sizes. Analyzing these field proxies can also inform management recommendations. The presence of a large number of trees appeared to have no negative impacts on yields, however there was a strong inverse relationship between canopy cover and yield, suggesting that strategic management of large trees is necessary to minimize canopy cover and avoid yield reductions.

Chapter 4 sought to improve upon existing strategies to monitor soil erosion – a notoriously challenging ES indicator to measure. I evaluated a rarely-utilized approach for analyzing data from erosion pins using the absolute value of pin height change, rather than the traditional method of using the net ‘real number’ change in pin height, which has been used with only limited success. I found that, when using erosion pins for comparative analysis between land management practices or monitoring changes in erosion over time, the absolute value of pin height change is likely a better indicator of erosion than the net real number change in pin height. The absolute value was better correlated with measured and predicted erosion rates, and was able to detect significant erosion differences between management-related soil cover classes, while the net real number value was not. Moreover, absolute value appears to better capture interactions between slope and cover management (the major factors driving erosion rates in the experimental plots), further supporting its suitability as a reliable indicator of erosion.

My field-scale research findings show that innovative analysis methods can provide practical monitoring strategies for comparing ES and ES indicators between agricultural land management alternatives. Only by analyzing multiple ES did a clear picture of the benefits of the SMAS emerge, and simple field proxies were found to correlate well with these multiple ES. While ES benefits cannot be quantified using these field proxies alone, they would indicate relative ES provision and show promise as a low-cost ES monitoring strategy for smallholder agroforestry. Similarly, using the absolute value of pin measurements alone has the ostensible drawback of being unable to quantify soil loss, however it is a better indicator of *relative* erosion between management alternatives compared to the net real number change, which seeks to calculate erosion and deposition rates. These findings support efforts to identify simple and practical field-scale methods to monitor the relative provision of multiple ES, rather than focusing on the quantification of a single ES.

### **7.1.3 Landscape-scale research findings**

While much work has been done to measure AGWB (an important ES indicator) across landscapes using remote sensing, Chapters 5 and 6 contribute to filling a research gap by investigating considerations specific to smallholder agriculture. Extreme spatiotemporal heterogeneity of C stocks exists in smallholder landscapes due to factors such as shifting cultivation, uneven canopy age-distribution in fallows, frequent but subtle forest disturbance and integrated crop-livestock systems

(Maniatis and Mollicone, 2010; Verburg et al., 2009). This results in the need for monitoring strategies different from those developed for more commonly monitored LULC transitions such as large-scale deforestation and urban expansion (Ellis, 2004).

Kearney and Smukler (2016) discussed how it may be particularly important to move toward wall-to-wall C mapping in smallholder landscapes, as opposed to relying on a 'stratify and multiply' approach where average C stock values are applied to LULC classes. The heterogeneous and highly disturbed nature of these landscapes makes it difficult to determine how to define LULC subclasses and large amounts of C are stored in trees outside of primary forests (e.g., bush-fallows, agroforests, wooded pastures, hedgerows, etc.). In this latter half of my dissertation, I built on existing remote sensing techniques to better capture heterogeneous AGWB-C stocks utilizing very high spatial resolution satellite imagery and airborne laser scanning data.

Focusing first on high-resolution satellite imagery, Chapter 5 showed that this data could be used to quantify AGWB-C at the watershed to landscape scale (100 – 10,000 ha) with uncertainties of less than 5%, even in highly heterogeneous smallholder landscapes. I suggested that a tendency in the literature to focus solely on plot-scale uncertainty of AGWB maps, without exploring aggregated uncertainty at larger scales, may be limiting the operationalization of remote-sensing-based approaches to monitor AGWB.

Utilizing the maps developed in this chapter, I demonstrated that agroforestry adoption would substantially increase C stocks in Central American hillslope agricultural landscapes. Furthermore, the potential revenue for smallholder communities from these C gains could be considerable, but is highly dependent on the price of C and the ability to quantify C storage in a cost-effective manner.

I discussed how these findings could have important implications for designing C contracts and monitoring strategies. For example, developing C contracts with entire communities at the landscape or watershed scale would enable the use of satellite-based monitoring of AGWB, thereby overcoming some of the methodological concerns hindering the inclusion of agroforestry in international and voluntary C agreements (e.g., expensive field campaigns for C monitoring on individual land holdings). The utility of spatial analysis for project planning is further underscored by the results of this study, which show that targeting areas with higher C storage potential results in 46% larger gains for the same area converted to agroforestry, compared to a random approach.

In Chapter 6, I introduced and evaluated a new approach to mapping AGWB in smallholder landscapes using airborne laser scanning. While airborne laser scanning technology has been demonstrated to produce highly accurate AGWB maps, concerns about the applicability of commonly used area-based models for heterogeneous smallholder landscapes led me to develop a method to predict AGWB directly from a canopy height model (CHM). I evaluated the overall accuracy of both

approaches using validation data and then investigated the difference between approaches when predicting AGWB in trees outside of forests using a forest fragmentation index adapted to the study area.

The CHM-based approach I developed improved overall AGWB prediction accuracy compared with the prevailing area-based approach. The CHM-based approach better modeled AGWB in small and patchy vegetation classes (e.g., agroforestry, hedgerows) compared to the area-based approach, which tended to generalize over vegetation edges – of which there are many in smallholder landscapes – resulting in under-prediction of AGWB in trees outside forests and over-prediction in bare lands.

Using the CHM-based approach, I estimated that within the study area landscape, typical of much of Central America, trees outside forests contained about 22% of all AGWB. This supports findings in other regions (e.g., Guo et al., 2014) that have indicated trees outside forests are an important and often overlooked C sink in smallholder landscapes, as well as results from Chapter 3 demonstrating the multiple ES benefits related to agroforestry, and accurately quantifying AGWB in trees outside forests is thus a key factor in monitoring ecological, economic and social functions of trees. The flexibility of the CHM-based approach, combined with improvements in AGWB prediction for trees outside forests, make it promising as a useful tool for operationalizing AGWB mapping in heterogeneous landscapes.

However, more research is needed to validate the approach in other regions and at differing spatial resolutions.

## **7.2 Limitations**

While my research made progress toward scaling up ES measurement and monitoring from the field to the landscape, I was only able to apply my methods to measure AGWB within a single landscape and under a limited number of management options. There are many similar landscapes across Central America and in other smallholder regions globally, but results and method applications from my research may not be generalizable to other landscapes, and further research is warranted. Even within the study area of northern El Salvador, there are limitations with respect to conclusions that can be drawn from my research at the field and landscape scale, each of which are discussed, in turn, below.

### ***7.2.1 Field-scale research limitations***

Several factors within the field-scale studies (Chapters 3 and 4) limit the degree to which conclusions can be drawn from this research. For example, the three-year study, while no small task, is relatively short to assess the true impacts of CSA practices such as the SMAS and organic management, and the yield performance of the conventional system may degrade over time. Many of the benefits of CSA are expected to be long-term and may take years or decades to be realized; especially those related to enhanced soil properties from tree-based systems. While my

research demonstrated some benefits of CSA within the three-year study, many soil-related benefits were not observed, although it is possible that they would occur given more time for the SMAS and organic treatments to mature. Additionally, thresholds or feedbacks may exist that would result in new long-term equilibriums, potentially quite different from the trajectories observed after just a few years.

The ES indicators and indices measured in the field trials were primarily designed to assess the ES impacts of tree-based systems (i.e., the SMAS) as compared to conventional management. Therefore, additional benefits from organic management observed elsewhere (e.g., increased mycorrhizal colonization, enhanced crop pollination) may be underestimated.

Yield results reported in Chapter 3 should also be interpreted with caution. Due to the need to place experimental plots adjacent to each other, lateral shading was substantial in SMAS treatments converted from forest-fallow and this may have impacted yields. Furthermore, the SMAS and organic treatments were new and dynamic systems in this region. Farmers were unfamiliar with management strategies and, while they did receive substantial training and oversight, the on-farm and participatory nature of this study likely resulted in a learning curve that may have impacted productivity. It is possible that, given more experience, farmers could increase the yields achieved with SMAS and organic management.

Due, in part, to the limitations mentioned above, I devoted a substantial portion of my dissertation to the methods used to measure and analyze ES in these systems. Here, some noteworthy limitations also exist. In Chapter 3, I presented a method to objectively weight ES indicators using PCA in order to develop comparable ES indices. While this method can be valuable for research, it ignores some very important concepts emerging in the ES literature related to ES demand and stakeholder perceptions. In practice, neither indicators nor indices can be weighted 'objectively', as different stakeholders have different perceptions of the relative value of services (Chan et al., 2016; Hauck et al., 2013), and demand for services varies over space and time (Chan et al., 2006). While I was able to identify promising field proxies that could be measured at low cost and still represent provision of multiple ES, my examination was limited to a simple correlation analysis and more research is needed to better understand how well these proxies truly predict ES provision, for example by evaluating whether non-linearity or thresholds exist.

In Chapter 4, I found that using the absolute value of erosion pin measurements may better represent soil loss, but this study was limited to a single year and replicated across just five sites. Given the extreme heterogeneity of this region in factors known to influence erosion (e.g., precipitation patterns, topography, management), it would be prudent to repeat this for multiple years and in different landscapes, soil types and management systems before concluding whether this method should be

widely employed. I wrote Chapter 4 as a research note in order to encourage others to do just that.

### **7.2.2 *Landscape-scale research limitations***

In Chapter 5, I discussed how, by using high spatial resolution satellite imagery, AGWB-C can be measured with low uncertainty (< 5%) in aggregation units of at least 100 ha. This conclusion has potentially important implications for how C contracts are designed and how compliance is monitored, but relies on the assumption that the model used to map AGWB is not biased. While an analysis of model residuals suggested this is true, validation in very large plots would be required to confirm with certainty that no unexpected bias exists when aggregating results to much larger areas.

Assuming that AGWB-C estimates from satellite imagery can be highly accurate only when aggregated to at least 100 ha would support a move toward community-scale contracting and monitoring, however this may introduce other administrative and legal challenges to creating such contracts. My research was only able to address one aspect of monitoring. Furthermore, the methods utilized in Chapter 5 may not be accessible for all contexts. Very high spatial resolution satellite imagery remains relatively expensive and methods to produce the spectral and textural variables used in the development of the model require some degree of GIS training, although imagery costs are coming down and open-source software is making GIS

increasingly accessible. I also did not address how map uncertainty would change as the number and distribution of field plots used for calibration changes, which would substantially impact costs.

In Chapter 6, I introduced a CHM-based approach to quantify AGWB from airborne laser scanning that could be a simple and transferrable tool; however, more research is needed to validate for other regions and contexts and develop more robust allometric equations to further reduce error. It is unclear whether the approach would work well across all vegetation structures. For example, different climates, tree species and distribution may require the use of different spatial resolutions and an optimal CHM pixel size could exist for different regions. The propagation of error through the allometric equations used to develop the model should also be quantified, and further analysis using Monte Carlo simulation and sensitivity analysis is warranted. Of specific concern are the equations used to estimate crown area. This parameter is infrequently measured, thus limiting options for utilizing existing equations or developing new ones.

## **7.3 Potential applications**

### ***7.3.1 Applications of field-scale research***

Results demonstrating the multiple ES benefits of the SMAS support the development of policies to promote its adoption for hillslope maize/bean production, and have implications for how policies are designed and SMAS

management is implemented. For example, incentives to adopt the SMAS should be coupled with training. Chapter 3 demonstrated that careful management is required to avoid light competition between crops and large trees. Yield impacts can be minimal if large trees are properly pruned, but increasing canopy cover had negative impacts on crop production. Financial support may also be necessary to overcome establishment costs and make up for potential yield reductions, especially in the early years of the system when farmers are learning how to make it work for their local conditions.

The methods I used in Chapter 3 to quantify individual ES indicators and develop composite ES indices could be incorporated into policy design and monitoring strategies. Empirical weighting of indicators by PCA could be used to compare stakeholder priorities to an objective method, and would help to identify which indicators are most important for monitoring. The field proxies identified as being highly correlated with multiple ES could be incorporated into future studies and monitoring efforts. These proxies could eventually be used to determine conditionality for meeting ES provisioning targets or even as a method to tier payments for ecosystem services (PES), although more research is needed to better understand relationships between proxies and ES.

The methods I describe in Chapter 4 to analyze data from erosion pins will hopefully inspire new studies and encourage researchers to revisit old datasets to verify my findings. If this method is indeed corroborated by other studies, it could renew

interest in using erosion pins as a simple and low-cost method to measure erosion in future research and environmental monitoring activities.

### **7.3.2 Applications of landscape-scale research**

I believe my analysis of the uncertainty of AGWB predictions from high spatial resolution satellite imagery in Chapter 5 has important implications for how C stocks are monitored using remote sensing. My results suggest that wall-to-wall AGWB maps developed using spectral imagery, and calibrated with relatively small plots, are highly accurate at predicting AGWB in areas greater than ~100 ha, even in heterogeneous smallholder landscapes. If these conclusions are indeed valid, it would suggest that an over-emphasis has been placed on plot size for model calibration and that spectral imagery and smaller plots can be used to map AGWB, provided that the unit of interest is aggregated to at least ~100 ha (e.g., watersheds or landscapes). As satellite imagery becomes more accessible, this could support the development of C contracts for agroforestry and other land management practices that increase biomass in trees outside forests.

My findings from Chapter 6 further support calls to include trees outside forests in C contracting and accounting by quantifying large amounts of AGWB in trees outside forests across a smallholder landscape. The method I introduced to map AGWB could be an appropriate tool to utilize airborne laser scanning in smallholder landscapes. The CHM-based method was not only more accurate for predicting

biomass in trees outside forests, it may prove especially useful in management settings where airborne laser scanning data was not acquired for the purpose of mapping vegetation (i.e., ground data for AGWB is not available) or resources are limited. For example, in 2014 the government of El Salvador acquired airborne laser scanning data for the entire country to improve seismic monitoring and landslide predictions, but application of this data for quantifying AGWB is limited due to a lack of ground data and the immense computer processing that would be required using traditional area-based approaches.

Finally, while measuring AGWB in smallholder landscapes and quantifying the contribution of trees outside forests are important steps toward leveraging C financing for practices such as the SMAS, results from Chapter 5 show just how important the price of C is to the viability of such endeavors. My analysis suggests that at current C prices, the incentive provided by C payments alone may not be sufficient for farmers to adopt the SMAS. This finding could further policy-makers' understanding of where C prices would need to be set in order to making financing an agroforestry project in this manner viable, and encourage bundling incentives for C storage with those for other ES expected from the SMAS, as demonstrated in Chapter 3. For example, Wendland et al. (2010) demonstrated opportunities for bundling PES for C, water and biodiversity benefits in Madagascar.

## **7.4 Future research directions**

### **7.4.1 *Field-scale research directions***

Conducting longer field trials (on the order of 5 – 10+ years) should be a priority for better understanding the ES benefits of the SMAS and other tree-based systems in smallholder agriculture. These systems are part of long-term rotations, and understanding the relative trajectories of different management options over time will require dedicated monitoring. High variability in management and environment within smallholder landscapes makes it challenging to run comparative studies on existing farms, and therefore experimentally designed and managed studies are important. By coordinating research and using common methodologies, progress toward understanding multiple ES from agriculture could be enhanced enormously.

Interesting opportunities exist to build upon the methods used in Chapter 3 to develop and evaluate ES indices using PCA-weighted indicators by comparing results to those obtained under different methods to weight indicators. For example, regional points-based indices and participatory approaches can incorporate different contexts and stakeholder values into relative ES weights (Marinidou et al., 2013; Pagiola et al., 2007; The Plan Vivo Foundation, 2013), it would be helpful to analyze how different weighting methods would change conclusions about overall ES provision and trade-offs and synergies among ES.

In order to fully examine the utility of the erosion pin analysis method described in Chapter 4, two additional types of analysis are recommended. First, research comparing the absolute value of pin height change to the net real number value should be conducted on larger datasets and across a wider variety of field types. This research could be done using many existing erosion pin datasets where additional information is available to predict erosion using the Revised Universal Soil Loss Equation (RUSLE) or collection pits were also installed. Second, I recommend new field and lab experiments be conducted to explore the potential for calibrating models to predict actual soil loss based on the absolute value of pin height change measurements. Such models would enable low-cost measurement of erosion rates, with benefits for future research comparing land management impacts on soil loss and for parameterizing landscape models predicting management-related processes such as sedimentation and eutrophication.

#### ***7.4.2 Landscape-scale research directions***

In order to validate the supposition in Chapter 5 that AGWB prediction uncertainty falls exponentially when aggregated into larger units, future studies could make efforts to obtain ground measurements of AGWB in very large plots (1 – 10+ ha). Alternatively, AGWB predicted from airborne laser scanning or ground-based LiDAR could be used as a surrogate for ground measurements in order to estimate AGWB in very large validation plots. Either way, ideally these studies would develop prediction models from relatively small plots (~0.1 ha) and validate map results

using the very large plots. By doing so, one could confirm whether an unbiased model with high uncertainty at the plot scale can predict AGWB at larger scales with low uncertainty.

Predicting AGWB in individual trees using airborne laser scanning data may prove to be the most accurate method for biomass mapping, and great strides have been made recently to develop algorithms that detect individual trees and delineate their crowns (Allouis et al., 2013; Popescu, 2007; Popescu and Wynne, 2004; Tao et al., 2014; Vége and Durrieu, 2011). Recent research shows that equations combining height and crown dimensions can substantially improve biomass estimation for individual trees compared to equations using DBH alone (Jucker et al., 2017).

Therefore, studies applying equations developed by Jucker et al. (2017) and others to trees delineated from airborne laser scanning are encouraged. These studies could compare the performance of global, regional and local equations to evaluate the appropriate scale(s) at which equations can accurately be applied.

While such an approach is expected to produce more accurate results than the CHM-based method introduced in Chapter 6, it would be computationally demanding and generalized tree-detection algorithms have yet to be developed for monitoring outside of research applications. By comparison, the CHM-based method may prove to be a simple and useful management tool. As segmentation algorithms continue to be developed and used to map AGWB, they could be compared to the CHM-based method to examine whether it is an acceptably accurate tool. Additionally, the CHM-

based method should be further tested in other regions using varying spatial resolutions and allometric models to determine its sensitivity to each of these factors. Finally, in order to advance the development of segmentation and CHM-based methods to predict AGWB, crown area should be included in forest inventories and other studies that measure trees.

## **7.5 Final reflections**

This dissertation underscores the continued need to develop accurate methods for measuring ES at multiple scales and evaluate trade-offs and synergies between them. My research addressed these issues by quantifying and comparing multiple ES from CSA alternatives in smallholder agriculture, and advancing methods to accurately measure ES in individual fields and across heterogeneous landscapes. My research also highlights the importance of adapting ES measurement methods into tools that support decision makers and enable cost-effective monitoring for policies such as PES. One way to enable such applications is to find simple but effective monitoring methods, for example by using field proxies (e.g., Chapter 3), finding novel ways to interpret basic field measurements (e.g., Chapter 4) or developing generalized and accessible remote sensing applications (e.g., Chapter 6). Regardless of the complexity of monitoring tools proposed to policy makers, communicating the uncertainty associated with these tools (e.g., Chapter 5) is critical to support informed decision-making.

Designing innovative policy mechanisms to address agriculture's mounting pressure on regulating ES will require greater understanding of the impacts of land management on ES and effective methods to monitor changes over time, both of which are emphasized by my research. However, in order to develop these policies in a timely manner to reverse global climate change and address acute issues of poverty, it should be recognized that there will always be uncertainty and limitations in our ability to quantify ES. While we should invest in research to reduce uncertainty and overcome limitations, we must weigh the trade-offs between increasing certainty and inaction, and consider designing policies in such a way to incorporate what we do know about ES provisioning, acknowledge what we do not know, and maintain the flexibility to incorporate new knowledge as becomes available.

## References

- Abawi, G.S., Corrales, M.A.P., 1990. Root rots of beans in Latin America and Africa: Diagnosis, research methodologies, and management strategies. Centro Internacional de Agricultura Tropical (CIAT), Cali, Columbia.
- Achard, F., Eva, H.D., Stibig, H.-J., Mayaux, P., Gallego, J., Richards, T., Malingreau, J.-P., 2002. Determination of Deforestation Rates of the World's Humid Tropical Forests. *Science* 297, 999–1003. doi:10.1126/science.1070656
- Adesina, A.A., Coulibaly, O., Manyong, V.M., Sanginga, P.C., Mbila, D., Chianu, J., Kamleu, D.G., 1999. Policy shifts and adoption of alley farming in West and central Africa. IITA, Nigeria.
- Allen, R.G., Pereira, L.S., Raes, D., Smith, M., 1998. FAO Irrigation and Drainage Paper (No. 56). Rome.
- Allouis, T., Durrieu, S., Vega, C., Couteron, P., 2013. Stem volume and above-ground biomass estimation of individual pine trees from LiDAR data: Contribution of full-waveform signals. *IEEE J. Sel. Top. Appl. Earth Obs. Remote Sens.* 6, 924–934. doi:10.1109/JSTARS.2012.2211863
- Anderson, J.M., Ingram, J.S.I., 1993. Tropical soil biology and fertility: a handbook of methods, 2nd ed. CAB International, Wallingford, Oxon, UK.
- Asner, G.P., Mascaro, J., 2014. Mapping tropical forest carbon: Calibrating plot estimates to a simple LiDAR metric. *Remote Sens. Environ.* 140, 614–624. doi:10.1016/j.rse.2013.09.023
- Asner, G.P., Mascaro, J., Anderson, C., Knapp, D.E., Martin, R.E., Kennedy-Bowdoin, T., van Breugel, M., Davies, S., Hall, J.S., Muller-Landau, H.C., Potvin, C., Sousa, W., Wright, J., Bermingham, E., 2013. High-fidelity national carbon mapping for resource management and REDD+. *Carbon Balance Manag.* 8, 7. doi:10.1186/1750-0680-8-7
- Asner, G.P., Mascaro, J., Muller-Landau, H.C., Vieilledent, G., Vaudry, R., Rasamoelina, M., Hall, J.S., van Breugel, M., 2012. A universal airborne LiDAR approach for tropical forest carbon mapping. *Oecologia* 168, 1147–60. doi:10.1007/s00442-011-2165-z
- Asner, G.P., Powell, G.V.N., Mascaro, J., Knapp, D.E., Clark, J.K., Jacobson, J., Kennedy-Bowdoin, T., Balaji, A., Paez-Acosta, G., Victoria, E., Secada, L., Valqui, M., Hughes, R.F., 2010. High-resolution forest carbon stocks and emissions in the Amazon. *Proc. Natl. Acad. Sci. U. S. A.* 107, 16738–42. doi:10.1073/pnas.1004875107
- Ayanu, Y.Z., Conrad, C., Nauss, T., Wegmann, M., Koellner, T., 2012. Quantifying and mapping ecosystem services supplies and demands: a review of remote sensing applications.

- Ayarza, M.A., Welchez, L.A., 2004. Drivers effecting the development and sustainability of the Quesungual Slash and Mulch Agroforestry System (QSMAS) on hillsides of Honduras.
- Ayarza, M., Huber-Sannwald, E., Herrick, J.E., Reynolds, J.F., García-Barrios, L., Welchez, L. a., Lentes, P., Pavón, J., Morales, J., Alvarado, A., Pinedo, M., Baquera, N., Zelaya, S., Pineda, R., Amézquita, E., Trejo, M., 2010. Changing human–ecological relationships and drivers using the Quesungual agroforestry system in western Honduras. *Renew. Agric. Food Syst.* 25, 219–227. doi:10.1017/S1742170510000074
- Bagstad, K.J., Semmens, D.J., Waage, S., Winthrop, R., 2013. A comparative assessment of decision-support tools for ecosystem services quantification and valuation. *Ecosyst. Serv.* 5, 27–39. doi:10.1016/j.ecoser.2013.07.004
- Balvanera, P., Uriarte, M., Almeida-Leñero, L., Altesor, A., DeClerck, F., Gardner, T., Hall, J., Lara, A., Litter, P., Peña-Claros, M., Silva Matos, D.M., Vogl, A.L., Romero-Duque, L.P., Arreola, L.F., Caro-Borrero, Á.P., Gallego, F., Jain, M., Little, C., de Oliveira Xavier, R., Paruelo, J.M., Peinado, J.E., Poorter, L., Ascarrunz, N., Correa, F., Cunha-Santino, M.B., Hernández-Sánchez, A.P., Vallejos, M., 2012. Ecosystem services research in Latin America: The state of the art. *Ecosyst. Serv.* 2, 56–70. doi:10.1016/j.ecoser.2012.09.006
- Barnosky, A.D., Brown, J.H., Daily, G.C., Dirzo, R., Ehrlich, A.H., Ehrlich, P.R., Eronen, J.T., Fortelius, M., Hadly, E. a., Leopold, E.B., Mooney, H. a., Myers, J.P., Naylor, R.L., Palumbi, S., Stenseth, N.C., Wake, M.H., 2014. Introducing the Scientific Consensus on Maintaining Humanity’s Life Support Systems in the 21st Century: Information for Policy Makers, *The Anthropocene Review*. doi:10.1177/2053019613516290
- Beer, J., Muschler, R., Kass, D., Somarriba, E., Kass, D., Somarriba, E., 1998. Shade management in coffee and cacao plantations. *Agrofor. Syst.* 38, 139–164. doi:10.1023/A:1005956528316
- Benito, G., Gutiérrez, M., Sancho, C., 1992. Erosion rates in badland areas of the central Ebro Basin (NE-Spain). *CATENA* 19, 269–286. doi:http://dx.doi.org/10.1016/0341-8162(92)90002-S
- Bianchi, F.J.J. a, Booij, C.J.H., Tscharrntke, T., 2006. Sustainable pest regulation in agricultural landscapes: a review on landscape composition, biodiversity and natural pest control. *Proc. Biol. Sci.* 273, 1715–27. doi:10.1098/rspb.2006.3530
- Blanchard, E., Birnbaum, P., Ibanez, T., Boutreux, T., Antin, C., Ploton, P., Vincent, G., Pouteau, R., Vandrot, H., Hequet, V., Barbier, N., Droissart, V., Sonké, B., Texier, N., Kamdem, N.G., Zebaze, D., Libalah, M., Couteron, P., 2016. Contrasted allometries between stem diameter, crown area, and tree height in five tropical biogeographic areas. *Trees - Struct. Funct.* 30, 1953–1968. doi:10.1007/s00468-016-1424-3

- Brandeis, T., Delaney, M., Royer, L., Parresol, B., 2006. Allometric Equations for Predicting Puerto Rican Dry Forest Biomass and Volume 197–202.
- Breiman, L., 2001. Random Forests. *Mach. Learn.* 45, 5–32. doi:10.1023/A:1010933404324
- Brown, L.C., Foster, G.R., 1987. Storm erosivity using idealized intensity distributions. *Trans. ASAE* 30, 379. doi:10.13031/2013.31957
- Brown, S., 2002. Measuring carbon in forests: current status and future challenges. *Environ. Pollut.* 116, 363–72.
- Brown, S., 1997. Estimating biomass and biomass change of tropical forests: a primer, FAO forest. ed. Food and Agriculture Organization of the United Nations, Rome.
- Brown, S., Gillespie, A., Lugo, A., 1989. Biomass estimation methods for tropical forests with applications to forest inventory data. *For. Sci.* 35, 881–902.
- Bruijnzeel, L.A., 2004. Hydrological functions of tropical forests: Not seeing the soil for the trees?, *Agriculture, Ecosystems and Environment*. doi:10.1016/j.agee.2004.01.015
- Brussaard, L., Pulleman, M.M., Ouédraogo, É., Mando, A., Six, J., 2007. Soil fauna and soil function in the fabric of the food web. *Pedobiologia (Jena)*. 50, 447–462. doi:10.1016/j.pedobi.2006.10.007
- Cacho, O.J., Lipper, L., Moss, J., 2013. Transaction costs of carbon offset projects: A comparative study. *Ecol. Econ.* 88, 232–243. doi:10.1016/j.ecolecon.2012.12.008
- Castillo-Santiago, M.A., Ricker, M., de Jong, B.H.J., 2010. Estimation of tropical forest structure from SPOT-5 satellite images. *Int. J. Remote Sens.* 31, 2767–2782. doi:10.1080/01431160903095460
- Castro, A., Menjívar, J.C., Barrios, E., Asakawa, N., Borrero, G., García, E., Rao, I., 2010. Dinámica del nitrógeno y el fósforo del suelo bajo tres sistemas de uso de la tierra en laderas de Honduras. *Acta Agronómica* 59, 410–419.
- Castro, A., Rivera, M., Ferreira, O., Pavon, J., Garcia, E., Amezquita, E., Ayarza, M., Barrios, E., Rondon, M., Pauli, N., Baltodano, M.E., Mendoza, B., Welchez, L.A., Rao, I.M., 2009. Quesungual slash and mulch agroforestry system (QSMAS): Improving crop water productivity, food security and resource quality in the sub-humid tropics. Cali, Colombia.
- Chan, K.M.A., Balvanera, P., Benessaiah, K., Chapman, M., Díaz, S., Gómez-Baggethun, E., Gould, R., Hannahs, N., Jax, K., Klain, S., Luck, G.W., Martín-López, B., Muraca, B., Norton, B., Ott, K., Pascual, U., Satterfield, T., Tadaki, M., Taggart, J., Turner, N., 2016. Opinion: Why protect nature? Rethinking values and the environment. *Proc. Natl. Acad. Sci.* 113, 1462–1465. doi:10.1073/pnas.1525002113

- Chan, K.M. a, Shaw, M.R., Cameron, D.R., Underwood, E.C., Daily, G.C., 2006. Conservation planning for ecosystem services. *PLoS Biol.* 4, 2138–2152. doi:10.1371/journal.pbio.0040379
- Chave, J., Andalo, C., Brown, S., Cairns, M. a, Chambers, J.Q., Eamus, D., Fölster, H., Fromard, F., Higuchi, N., Kira, T., Lescure, J.-P., Nelson, B.W., Ogawa, H., Puig, H., Riéra, B., Yamakura, T., 2005. Tree allometry and improved estimation of carbon stocks and balance in tropical forests. *Oecologia* 145, 87–99. doi:10.1007/s00442-005-0100-x
- Chave, J., Réjou-Méchain, M., Búrquez, A., Chidumayo, E., Colgan, M.S., Delitti, W.B.C., Duque, A., Eid, T., Fearnside, P.M., Goodman, R.C., Henry, M., Martínez-Yrizar, A., Mugasha, W.A., Muller-Landau, H.C., Mencuccini, M., Nelson, B.W., Ngomanda, A., Nogueira, E.M., Ortiz-Malavassi, E., Péliissier, R., Ploton, P., Ryan, C.M., Saldarriaga, J.G., Vieilledent, G., 2014. Improved allometric models to estimate the aboveground biomass of tropical trees. *Glob. Chang. Biol.* 20, 3177–3190. doi:10.1111/gcb.12629
- Chave, J., Riéra, B., Dubois, M., 2001. Estimation of biomass in a neotropical forest of French Guiana: spatial and temporal variability. *J. Trop. Ecol.* 17, 79–96.
- Chhatre, A., Agrawal, A., 2009. Trade-offs and synergies between carbon storage and livelihood benefits from forest commons. *Proc. Natl. Acad. Sci.* 106, 17667–17670. doi:10.1073/pnas.0905308106
- Costanza, R., d’Arge, R., De Groot, R., Farber, S., Grasso, M., Hannon, B., Limburg, K., Naeem, S., O’neill, R. V., Paruelo, J., 1998. The value of the world’s ecosystem services and natural capital. *Ecol. Econ.* 25, 3–16.
- Couper, P., 2003. Effects of silt-clay content on the susceptibility of river banks to subaerial erosion. *Geomorphology* 56, 95–108. doi:10.1016/S0169-555X(03)00048-5
- Couper, P., Stott, T., Maddock, I., 2002. Insights into river bank erosion processes derived from analysis of negative erosion-pin recordings: Observations from three recent UK studies. *Earth Surf. Process. Landforms* 27, 59–79. doi:10.1002/esp.285
- Craswell, E., Lefroy, R., 2001. The role and function of organic matter in tropical soils. *Nutr. Cycl. Agroecosystems* 61, 7–18. doi:10.1023/A
- Current, D., Lutz, E., Scherr, S.J., 1995a. Costs, benefits, and farmer adoption of agroforestry: project experience in Central America and the Caribbean (No. 14), World Bank Environment Paper. The World Bank, Washington, DC.
- Current, D., Lutz, E., Scherr, S.J., 1995b. The Costs and Benefits of Agroforestry To Farmers. *World Bank Res. Obs.* 10, 151–180. doi:10.1093/wbro/10.2.151
- Czerepowicz, L., Case, B., Doscher, C., 2012. Using satellite image data to estimate aboveground shelterbelt carbon stocks across an agricultural landscape. *Agric. Ecosyst. Environ.* 156, 142–150.

- Dagang, A.B.K., Nair, P., 2003. Silvopastoral research and adoption in Central America: recent findings and recommendations for future directions. *Agrofor. Syst.* 59, 149–155. doi:10.1007/BF00115736
- Daily, G., 1997. Introduction: What are ecosystem services?, in: Daily, G. (Ed.), *Nature's Services: Societal Dependence on Natural Ecosystems*. Island Press, Washington, DC, pp. 1–10.
- Davis, A.S., Hill, J.D., Chase, C.A., Johanns, A.M., Liebman, M., 2012. Increasing Cropping System Diversity Balances Productivity, Profitability and Environmental Health. *PLoS One* 7, 1–8. doi:10.1371/journal.pone.0047149
- Daw, T., Brown, K., Rosendo, S., Pomeroy, R., 2011. Applying the ecosystem services concept to poverty alleviation: the need to disaggregate human well-being. *Environ. Conserv.* 38, 370–379. doi:10.1017/S0376892911000506
- de Foresta, H., Somarriba, E., Temu, A., Boulanger, D., Feuilly, H., Gauthier, M., 2013. Towards the Assessment of Trees Outside Forests. Resource Assessment Working Paper 183. (No. 183), Forest Resources Assessment Working Paper. Rome.
- de Groot, R.S., Alkemade, R., Braat, L., Hein, L., Willemen, L., 2010. Challenges in integrating the concept of ecosystem services and values in landscape planning, management and decision making. *Ecol. Complex.* 7, 260–272. doi:10.1016/j.ecocom.2009.10.006
- de Sousa, K.F.D., Detlefsen, G., de Melo Virginio Filho, E., Tobar, D., Casanoves, F., 2016. Timber yield from smallholder agroforestry systems in Nicaragua and Honduras. *Agrofor. Syst.* 90, 207–218. doi:10.1007/s10457-015-9846-2
- De Sy, V., Herold, M., Achard, F., Asner, G.P., Held, A., Kellndorfer, J., Verbesselt, J., 2012. Synergies of multiple remote sensing data sources for REDD+ monitoring. *Curr. Opin. Environ. Sustain.* 4, 696–706. doi:10.1016/j.cosust.2012.09.013
- Delgado, M.E.M., Canters, F., 2012. Modeling the impacts of agroforestry systems on the spatial patterns of soil erosion risk in three catchments of Claveria, the Philippines. *Agrofor. Syst.* 85, 411–423. doi:10.1007/s10457-011-9442-z
- Diaz-Fierros, V., Benito Rueda, R., Pérez Moreira, R., 1987. Evaluation of the U.S.L.E. for the prediction of erosion in burn forest areas in Galicia (N.W. SPAIN). *Catena* 14, 189–199.
- Dixon, J., Gulliver, A., Gibbon, D., 2001. *Farming systems and poverty. Improving farmers' livelihoods in a changing world*. Food and Agriculture Organization of the United Nations, Rome, Italy.
- Drake, J.B., Dubayah, R.O., Clark, D.B., Knox, R.G., Blair, J.B., Hofton, M.A., Chazdon, R.L., Weishampel, J.F., Prince, S., 2002. Estimation of tropical forest structural characteristics, using large-footprint lidar. *Remote Sens. Environ.* 79, 305–319. doi:10.1016/S0034-4257(01)00281-4

- Eckert, S., 2012. Improved Forest Biomass and Carbon Estimations Using Texture Measures from WorldView-2 Satellite Data. *Remote Sens.* 4, 810–829. doi:10.3390/rs4040810
- Edenhofer, O., Pichs-Madruga, R., Sokona, Y., Kadner, S., Minx, J., Brunner, S., Agrawala, S., Baiocchi, G., Bashmakov, I.A., Blanco, G., Broome, J., Bruckner, T., Bustamante, M., Clarke, L., Conte Grand, M., Creutzig, F., Cruz-Núñez, X., Dhakal, S., Dubash, N.K., Eickemeier, P., Farahani, E., Fischedick, M., Fleurbaey, M., Gerlagh, R., Gómez-Echeverri, L., Gupta, S., Harnisch, J., Jiang, K., Jotzo, F., Kartha, S., Klasen, S., Kolstad, C., Krey, V., Kunreuther, H., Lucon, O., Masera, O., Mulugetta, Y., Norgaard, R.B., Patt, A., Ravindranath, N.H., Riahi, L., Roy, J., Sagar, A., Schaeffer, R., Schlömer, S., Seto, K.C., Seyboth, K., Sims, R., Smith, P., Somanathan, E., Stavins, R., von Stechow, C., Sterner, T., Sugiyama, T., Suh, S., Ürge-Vorsatz, D., Urama, K., Venables, A., Victor, D.G., Weber, E., Zhou, D., Zou, J., Zwickel, T., 2014. Technical Summary, Technical Summary. In: *Climate Change 2014: Mitigation of climate change. Contribution of Working Group III to the Fifth Assessment Report of the Intergovernmental Panel on Climate Change.* Cambridge University Press, Cambridge, United Kingdom and New York, NY, USA. doi:10.1103/PhysRevD.70.106002
- Edeso, J.M., Merino, A., González, M.J., Marauri, P., 1999. Soil erosion under different harvesting managements in steep forestlands from northern Spain. *L. Degrad. Dev.* 10, 79–88.
- Ellis, E.C., 2004. Long-Term Ecological Changes in the Densely Populated Rural Landscapes of China, in: DeFries, R.S., Asner, G.P., Houghton, R.A. (Eds.), *Ecosystems and Land Use Change.* American Geophysical Union, Washington, DC, pp. 303–320. doi:10.1029/153GM23
- Elwell, H.A., Stocking, M.A., 1976. Vegetal cover to estimate soil erosion hazard in Rhodesia. *Geoderma* 15, 61–70. doi:10.1016/0016-7061(76)90071-9
- Engel, S., Muller, A., 2016. Payments for environmental services to promote “climate-smart agriculture”? Potential and challenges. *Agric. Econ.* 47, 173–184. doi:10.1111/agec.12307
- ESRI, 2011. ArcGIS Desktop: Release 10.1.
- Exelis Visual Information Solutions, 2010. ENVI 5.0.
- Fang, Z., Bailey, R.L., 1998. Height–diameter models for tropical forests on Hainan Island in southern China. *For. Ecol. Manage.* 110, 315–327. doi:10.1016/S0378-1127(98)00297-7
- FAO, 2016. *The State of Food and Agriculture 2016 [In Brief].* Rome, Italy. doi:ISBN: 978-92-5-107671-2 I
- FAO, 2013a. *FAO Statistical Yearbook 2013, The effects of brief mindfulness intervention on acute pain experience: An examination of individual difference.* Food and Agriculture

Organization of the United Nations, Rome, Italy.

- FAO, 2013b. *Climate-Smart Agriculture Sourcebook, Sourcebook on Climate-Smart Agriculture, Forestry and Fisheries*.
- FAO, 2005. *El Sistema Agroforestal Quesungual*. Litografía López, Rome, Italy.
- Fazakas, Z., Nilsson, M., Olsson, H., 1999. Regional forest biomass and wood volume estimation using satellite data and ancillary data. *Agric. For. Meteorol.* 98–99, 417–425. doi:10.1016/S0168-1923(99)00112-4
- Feng, X., Fu, B., Yang, X., Lü, Y., 2010. Remote sensing of ecosystem services: An opportunity for spatially explicit assessment. *Chinese Geogr. Sci.* 20, 522–535. doi:10.1007/s11769-010-0428-y
- Ferguson, B.G., Vandermeer, J., Morales, H., Griffith, D.M., 2003. Post-agricultural succession in El Petén, Guatemala. *Conserv. Biol.* 17, 818–828. doi:10.1046/j.1523-1739.2003.01265.x
- Finegan, B., Delgado, D., 2000. Structural and floristic heterogeneity in a 30-year-old Costa Rican rain forest restored on pasture through natural secondary succession. *Restor. Ecol.* 8, 380–393. doi:10.1046/j.1526-100x.2000.80053.x
- Foley, J.A., Defries, R., Asner, G.P., Barford, C., Bonan, G., Carpenter, S.R., Chapin, F.S., Coe, M.T., Daily, G.C., Gibbs, H.K., Helkowski, J.H., Holloway, T., Howard, E.A., Kucharik, C.J., Monfreda, C., Patz, J.A., Prentice, I.C., Ramankutty, N., Snyder, P.K., 2005. Global Consequences of Land Use. *Science* 309, 570–574. doi:10.1126/science.1111772
- Fonte, S.J., Barrios, E., Six, J., 2010. Earthworms, soil fertility and aggregate-associated soil organic matter dynamics in the Quesungual agroforestry system. *Geoderma* 155, 320–328. doi:10.1016/j.geoderma.2009.12.016
- Fonte, S.J., Six, J., 2010. Earthworms and litter management contributions to ecosystem services in a tropical agroforestry system. *Ecol. Appl.* 20, 1061–1073. doi:10.1890/09-0795.1
- Franzluebbers, A.J., 2002. Water infiltration and soil structure related to organic matter and its stratification with depth. *Soil Tillage Res.* 66, 197–205. doi:10.1016/S0167-1987(02)00027-2
- Fuchs, H., Magdon, P., Kleinn, C., Flessa, H., 2009. Estimating aboveground carbon in a catchment of the Siberian forest tundra: Combining satellite imagery and field inventory. *Remote Sens. Environ.* 113, 518–531. doi:10.1016/j.rse.2008.07.017
- García, E.D., 2011. Evaluación del impacto del uso ganadero sobre suelo y vegetación en el Sistema Agroforestal Quesungual (SAQ) en el sur de Lempira, Honduras. CATIE.

- García, M., Riaño, D., Chuvieco, E., Danson, F.M., 2010. Estimating biomass carbon stocks for a Mediterranean forest in central Spain using LiDAR height and intensity data. *Remote Sens. Environ.* 114, 816–830. doi:10.1016/j.rse.2009.11.021
- Gibbs, H.K., Brown, S., Niles, J.O., Foley, J. a, 2007. Monitoring and estimating tropical forest carbon stocks: making REDD a reality. *Environ. Res. Lett.* 2, 45023. doi:10.1088/1748-9326/2/4/045023
- Goetz, S., Baccini, A., Laporte, N., Johns, T., Walker, W., Kellndorfer, J., Houghton, R., Sun, M., 2009. Mapping and monitoring carbon stocks with satellite observations: a comparison of methods. *Carbon Balance Manag.* 4, 1–7. doi:10.1186/1750-0680-4-2
- Goetz, S., Dubayah, R., 2011. Advances in remote sensing technology and implications for measuring and monitoring forest carbon stocks and change. *Carbon Manag.* 2, 231–244. doi:10.4155/cmt.11.18
- GOFC-GOLD, 2013. A sourcebook of methods and procedures for monitoring and reporting anthropogenic greenhouse gas emissions and removals associated with deforestation, gains and losses of carbon stocks in forests remaining forests, and forestation, GOFC-GOLD Report version COP19-1.
- Gómez-Castro, H., Pinto-Ruiz, R., Guevara-Hernández, F., Gonzalez-Reyna, A., 2010. Estimaciones de biomasa aérea y carbono almacenado en *Gliricidia sepium* (lam.) y *Leucaena leucocephala* (jacq.) y su aplicación en sistemas silvopastoriles. *Inf. Técnica Económica Agrar.* 106, 256–270.
- Goodman, R.C., Phillips, O.L., Baker, T.R., 2014. The importance of crown dimensions to improve tropical tree biomass estimates. *Ecol. Appl.* 24, 680–698. doi:10.1890/13-0070.1
- Gosling, P., Hodge, A., Goodlass, G., Bending, G.D., 2006. Arbuscular mycorrhizal fungi and organic farming. *Agric. Ecosyst. Environ.* 113, 17–35. doi:10.1016/j.agee.2005.09.009
- Gotelli, N.J., Colwell, R.K., 2001. Quantifying Biodiversity: Procedures and Pitfalls in the Measurement and Comparison of Species Richness. *Ecol. Lett.* 4, 379–391. doi:10.1046/j.1461-0248.2001.00230.x
- Graeb, B.E., Chappell, M.J., Wittman, H., Ledermann, S., Kerr, R.B., Gemmill-Herren, B., 2016. The State of Family Farms in the World. *World Dev.* 87, 1–15. doi:10.1016/j.worlddev.2015.05.012
- Green, R.E., 2005. Farming and the Fate of Wild Nature. *Science* 307, 550–555. doi:10.1126/science.1106049
- Gregr, E.J., Chan, K.M. a, 2014. Leaps of Faith: How Implicit Assumptions Compromise the Utility of Ecosystem Models for Decision-making. *Bioscience* 65, 43–54. doi:10.1093/biosci/biu185

- Grêt-Regamey, A., Brunner, S.H., Altwegg, J., Bebi, P., 2013. Facing uncertainty in ecosystem services-based resource management. *J. Environ. Manage.* 127, S145–S154. doi:10.1016/j.jenvman.2012.07.028
- Groom, B., Palmer, C., 2012. REDD+ and rural livelihoods. (Special Issue: REDD+ and conservation.). *Biol. Conserv.* 154, 42–52. doi:10.1016/j.biocon.2012.03.002
- Guo, Z.D., Hu, H.F., Pan, Y.D., Birdsey, R.A., Fang, J.Y., 2014. Increasing biomass carbon stocks in trees outside forests in China over the last three decades. *Biogeosciences* 11, 4115–4122. doi:10.5194/bg-11-4115-2014
- Haigh, M., 1977. The use of erosion pins in the study of slope evolution, Shorter Technical Methods (II). Technical Bulletin No. 18. Norwich, UK.
- Haines-Young, R., Potschin, M., 2013. Common International Classification of Ecosystem Services (CICES): Consultation on Version 4, August-December 2012.
- Hancock, G.R., Lowry, J.B.C., 2015. Hillslope erosion measurement—a simple approach to a complex process. *Hydrol. Process.* 29, 4809–4816. doi:10.1002/hyp.10608
- Hancock, G.R., Murphy, D., Evans, K.G., 2010. Hillslope and catchment scale soil organic carbon concentration: An assessment of the role of geomorphology and soil erosion in an undisturbed environment. *Geoderma* 155, 36–45. doi:10.1016/j.geoderma.2009.11.021
- Harley, R., Riddell, M., Ndobe, S.N., 2012. REDD+ Beyond Carbon: Insights from a Community Payments for Ecosystem Services Project in Cameroon, Bioclimate Research and Development. Edinburgh, Scotland, UK.
- Harris, N.L., Brown, S., Hagen, S.C., Saatchi, S.S., Petrova, S., Salas, W., Hansen, M.C., Potapov, P. V., Lotsch, A., 2012. Baseline Map of Carbon Emissions from Deforestation in Tropical Regions. *Science* 336, 1573–1576. doi:10.1126/science.1217962
- Harvey, C. a., Chacón, M., Donatti, C.I., Garen, E., Hannah, L., Andrade, A., Bede, L., Brown, D., Calle, A., Chará, J., Clement, C., Gray, E., Hoang, M.H., Minang, P., Rodríguez, A.M., Seeberg-Elverfeldt, C., Semroc, B., Shames, S., Smukler, S., Somarriba, E., Torquebiau, E., van Etten, J., Wollenberg, E., 2013. Climate-smart landscapes: opportunities and challenges for integrating adaptation and mitigation in tropical agriculture. *Conserv. Lett.* 0, 1–14. doi:10.1111/conl.12066
- Hauck, J., Görg, C., Varjopuro, R., Ratamáki, O., Jax, K., 2013. Benefits and limitations of the ecosystem services concept in environmental policy and decision making: Some stakeholder perspectives. *Environ. Sci. Policy* 25, 13–21. doi:10.1016/j.envsci.2012.08.001
- Hegde, R., Bull, G.Q., 2011. Performance of an agro-forestry based Payments-for-Environmental-Services project in Mozambique: A household level analysis. *Ecol. Econ.*

71, 122–130. doi:10.1016/j.ecolecon.2011.08.014

- Hellin, J., Welchez, L.A., Cherrett, I., 1999. The Quezungual System: An indigenous agroforestry system from western Honduras. *Agrofor. Syst.* 46, 229–237. doi:10.1023/A:1006217201200
- Henry, M., Tittonell, P., Manlay, R.J., Bernoux, M., Albrecht, A., Vanlauwe, B., 2009. Biodiversity, carbon stocks and sequestration potential in aboveground biomass in smallholder farming systems of western Kenya. *Agric. Ecosyst. Environ.* 129, 238–252. doi:10.1016/j.agee.2008.09.006
- Holmes, K., Kyriakidis, P., Chadwick, O., 2005. Multi-Scale Variability in Tropical Soil Nutrients following Land-Cover Change. *Biogeochemistry* 74, 173–203.
- Horton, R.E., 1933. The role of infiltration in the hydrologic cycle. *Eos, Trans. Am. Geophys. Union* 14, 446–460.
- Hughes, R., Kauffman, J., Jaramillo, V., 1999a. Biomass, carbon and nutrient dynamics of secondary forests in a humid tropical region of Mexico. *Ecology* 80, 1892–1907. doi:10.1890/0012-9658(1999)080[1892:BCANDO]2.0.CO;2
- Hughes, R., Kauffman, J., Jaramillo, V., 1999b. BIOMASS, CARBON, AND NUTRIENT DYNAMICS OF SECONDARY FORESTS IN A HUMID TROPICAL REGION OF MEXICO. *Ecology* 80, 1892–1907.
- Hunter, M.C., Smith, R.G., Schipanski, M.E., Atwood, L.W., Mortensen, D.A., 2017. Agriculture in 2050: Recalibrating Targets for Sustainable Intensification. *Bioscience* XX, 1–6. doi:10.1093/biosci/bix010
- IICA, 2009. Mapeo del Mercado de Semillas de Maíz y Frijol en Centroamérica, Proyecto Red SICTA. Managua, Nicaragua.
- Isenburg, M., 2016. LAStools, “Efficient LiDAR Processing Software.”
- Jack, B.K., Kousky, C., Sims, K.R.E., 2008. Designing payments for ecosystem services: Lessons from previous experience with incentive-based mechanisms. *Proc. Natl. Acad. Sci. U. S. A.* 105, 9465–70. doi:10.1073/pnas.0705503104
- Jackson, B., Pagella, T., Sinclair, F., Orellana, B., Henshaw, A., Reynolds, B., McIntyre, N., Wheeler, H., Eycott, A., 2013. Polyscape: A GIS mapping framework providing efficient and spatially explicit landscape-scale valuation of multiple ecosystem services. *Landsc. Urban Plan.* 112, 74–88. doi:10.1016/j.landurbplan.2012.12.014
- Jensen, J.R., 2005. *Introductory digital image processing: a remote sensing perspective.* Prentice Hall Inc., Upper Saddle River, N.J.
- Jucker, T., Caspersen, J., Chave, J., Antin, C., Barbier, N., Bongers, F., Dalponte, M., van Ewijk,

- K.Y., Forrester, D.I., Haeni, M., Higgins, S.I., Holdaway, R.J., Iida, Y., Lorimer, C., Marshall, P.L., Momo, S., Moncrieff, G.R., Ploton, P., Poorter, L., Rahman, K.A., Schlund, M., Sonké, B., Sterck, F.J., Trugman, A.T., Usoltsev, V.A., Vanderwel, M.C., Waldner, P., Wedeux, B.M.M., Wirth, C., Wöll, H., Woods, M., Xiang, W., Zimmermann, N.E., Coomes, D.A., 2017. Allometric equations for integrating remote sensing imagery into forest monitoring programmes. *Glob. Chang. Biol.* 23, 177–190. doi:10.1111/gcb.13388
- Kareiva, P., Watts, S., McDonald, R., Boucher, T., 2007. Domesticated nature: shaping landscapes and ecosystems for human welfare. *Science* 316, 1866–1869. doi:10.1126/science.1140170
- Karp, D.S., Mendenhall, C.D., Sandí, R.F., Chaumont, N., Ehrlich, P.R., Hadly, E.A., Daily, G.C., 2013. Forest bolsters bird abundance, pest control and coffee yield. *Ecol. Lett.* 16, 1339–1347. doi:10.1111/ele.12173
- Kayitakire, F., Hamel, C., Defourny, P., 2006. Retrieving forest structure variables based on image texture analysis and IKONOS-2 imagery. *Remote Sens. Environ.* 102, 390–401. doi:10.1016/j.rse.2006.02.022
- Kearney, S.P., Smukler, S.M., 2016. Determining Greenhouse Gas Emissions and Removals Associated with Land-Use and Land-Cover Change, in: Rosenstock, T.S., Rufino, M.C., Butterbach-Bahl, K., Wollenberg, E., Richards, M. (Eds.), *Methods for Measuring Greenhouse Gas Balances and Evaluating Migration Options in Smallholder Agriculture*. Springer. doi:10.1007/978-3-319-29794-1\_3
- Kennedy, C.M., Lonsdorf, E., Neel, M.C., Williams, N.M., Ricketts, T.H., Winfree, R., Bommarco, R., Brittain, C., Burley, A.L., Cariveau, D., 2013. A global quantitative synthesis of local and landscape effects on wild bee pollinators in agroecosystems. *Ecol. Lett.* 16, 584–599.
- Kirby, K.R., Potvin, C., 2007. Variation in carbon storage among tree species: Implications for the management of a small-scale carbon sink project. *For. Ecol. Manage.* 246, 208–221. doi:10.1016/j.foreco.2007.03.072
- Kosoy, N., Corbera, E., 2010. Payments for ecosystem services as commodity fetishism. *Ecol. Econ.* 69, 1228–1236. doi:10.1016/j.ecolecon.2009.11.002
- Kosoy, N., Corbera, E., Brown, K., 2008. Participation in payments for ecosystem services: Case studies from the Lacandon rainforest, Mexico. *Geoforum* 39, 2073–2083. doi:10.1016/j.geoforum.2008.08.007
- Kosoy, N., Martinez-Tuna, M., Muradian, R., Martinez-Alier, J., 2007. Payments for environmental services in watersheds: Insights from a comparative study of three cases in Central America. *Ecol. Econ.* 61, 446–455. doi:10.1016/j.ecolecon.2006.03.016
- Kremen, C., Miles, A., 2012. Ecosystem services in biologically diversified versus conventional farming systems: Benefits, externalities, and trade-offs. *Ecol. Soc.* 17.

doi:10.5751/ES-05035-170440

- Kremen, C., Ostfeld, R., 2005. A Call to Ecologists: Measuring, Analyzing and Managing Ecosystem Services. *Front. Ecol. Environ.* 3, 540–548.
- Kremen, C., Williams, N.M., Thorp, R.W., 2002. Crop pollination from native bees at risk from agricultural intensification. *Proc. Natl. Acad. Sci. U. S. A.* 99, 16812–16816. doi:10.1073/pnas.262413599
- Kuyah, S., Dietz, J., Muthuri, C., Jamnadass, R., Mwangi, P., Coe, R., Neufeldt, H., 2012. Allometric equations for estimating biomass in agricultural landscapes: II. Belowground biomass. *Agric. Ecosyst. Environ.* 158, 225–234. doi:10.1016/j.agee.2012.05.010
- La Via Campesina, 2014. UN-masking Climate Smart Agriculture [WWW Document]. Press Release. URL <https://viacampesina.org/en/index.php/main-issues-mainmenu-27/sustainable-peasants-agriculture-mainmenu-42/1670-un-masking-climate-smart-agriculture> (accessed 3.22.17).
- Lang, T., Barling, D., 2012. Food security and food sustainability: Reformulating the debate. *Geogr. J.* 178, 313–326. doi:10.1111/j.1475-4959.2012.00480.x
- Lefsky, M.A., W.B., C., Parker, G.G., Harding, D.J., 2002. Lidar remote sensing for ecosystem studies. *Bioscience* 52, 19–30.
- Leh, M.D.K., Matlock, M.D., Cummings, E.C., Nalley, L.L., 2013. Quantifying and mapping multiple ecosystem services change in West Africa. *Agric. Ecosyst. Environ.* 165, 6–18. doi:10.1016/j.agee.2012.12.001
- Levick, S.R., Hessenmöller, D., Schulze, E.D., 2016. Scaling wood volume estimates from inventory plots to landscapes with airborne LiDAR in temperate deciduous forest. *Carbon Balance Manag.* 11, 14. doi:10.1186/s13021-016-0048-7
- Lim, K., Park, Y., Engel, B., Kim, N., 2011. SATEEC GIS system for spatiotemporal analysis of soil erosion and sediment yield, in: Godone, D. (Ed.), *Soil Erosion Studies*. InTech, pp. 253–280. doi:10.5772/25111
- Lim, K., Treitz, P., Wulder, M., Benoît, S., Flood, M., 2003. LiDAR remote sensing of forest structure. *Prog. Phys. Geogr.* 27, 88–106. doi:10.1191/0309133303pp360ra
- Lin, C., Thomson, G., Popescu, S., 2016. An IPCC-Compliant Technique for Forest Carbon Stock Assessment Using Airborne LiDAR-Derived Tree Metrics and Competition Index. *Remote Sens.* 8, 528. doi:10.3390/rs8060528
- Lorenz, K., Lal, R., 2014. Soil organic carbon sequestration in agroforestry systems. A review. *Agron. Sustain. Dev.* 34, 443–454. doi:10.1007/s13593-014-0212-y

- Lu, D., 2006. The potential and challenge of remote sensing-based biomass estimation. *Int. J. Remote Sens.* 27, 1297–1328. doi:10.1080/01431160500486732
- Lu, D., Chen, Q., Wang, G., Moran, E., Batistella, M., Zhang, M., Vaglio Laurin, G., Saah, D., 2012. Aboveground Forest Biomass Estimation with Landsat and LiDAR Data and Uncertainty Analysis of the Estimates. *Int. J. For. Res.* 2012, 1–16. doi:10.1155/2012/436537
- Luck, G.W., Chan, K.M. a., Fay, J.P., 2009. Protecting ecosystem services and biodiversity in the world's watersheds. *Conserv. Lett.* 2, 179–188. doi:10.1111/j.1755-263X.2009.00064.x
- Luedeling, E., Sileshi, G., Beedy, T., Dietz, J., 2011. Carbon Sequestration Potential of Agroforestry Systems. *Adv. Agrofor., Advances in Agroforestry* 8, 61–83. doi:10.1007/978-94-007-1630-8
- Luffman, I.E., Nandi, A., Spiegel, T., 2015. Gully morphology, hillslope erosion, and precipitation characteristics in the Appalachian Valley and Ridge province, southeastern USA. *Catena* 133, 221–232. doi:10.1016/j.catena.2015.05.015
- Lumley, T., 2009. leaps: Regression subset selection.
- Lusiana, B., van Noordwijk, M., Johana, F., Galudra, G., Suyanto, S., Cadisch, G., 2014. Implications of uncertainty and scale in carbon emission estimates on locally appropriate designs to reduce emissions from deforestation and degradation (REDD+). *Mitig. Adapt. Strateg. Glob. Chang.* 19, 757–772. doi:10.1007/s11027-013-9501-z
- Lutz, D. a., Washington-Allen, R. a., Shugart, H.H., 2008. Remote sensing of boreal forest biophysical and inventory parameters: A review. *Can. J. Remote Sens.* 34. doi:10.5589/m08-057
- MAG, 2016. Retrospectiva de precios de granos básicos 2001 - 2016 [WWW Document]. *Retrospect. Mens. precios Prod. Agropecu.* URL <http://www.mag.gob.sv/retrospectiva-mensual-de-precios-de-productos-agropecuarios/> (accessed 4.8.16).
- Magurran, A.E., 1988. *Ecological Diversity and Its Measurement*, First. ed, Statewide Agricultural Land Use Baseline 2015. Springer Netherlands. doi:10.1007/978-94-015-7358-0\_1
- Maindonald, J.H., Braun, W.J., 2014. DAAG: Data Analysis And Graphics data and functions.
- Maniatis, D., Mollicone, D., 2010. Options for sampling and stratification for national forest inventories to implement REDD+ under the UNFCCC. *Carbon Balance Manag.* 5, 1–14. doi:10.1186/1750-0680-5-9
- Marinidou, E., Finegan, B., Jiménez-Ferrer, G., Delgado, D., Casanoves, F., 2013. Concepts and a methodology for evaluating environmental services from trees of small farms in

- Chiapas, México. *J. Environ. Manage.* 114, 115–124.  
doi:10.1016/j.jenvman.2012.10.046
- MARN, 2013. Datos históricos de precipitación: estaciones G-12 de Concepción Quezaltepeque y G-7 de Arcatao (1971 - 2012). *Pers. Commun.*
- Mascaro, J., Asner, G.P., Muller-Landau, H.C., Van Breugel, M., Hall, J., Dahlin, K., 2011a. Controls over aboveground forest carbon density on Barro Colorado Island, Panama. *Biogeosciences* 8, 1615–1629. doi:10.5194/bg-8-1615-2011
- Mascaro, J., Detto, M., Asner, G.P., Muller-Landau, H.C., 2011b. Evaluating uncertainty in mapping forest carbon with airborne LiDAR. *Remote Sens. Environ.* 115, 3770–3774. doi:10.1016/j.rse.2011.07.019
- Mbow, C., Van Noordwijk, M., Luedeling, E., Neufeldt, H., Minang, P.A., Kowero, G., 2014. Agroforestry solutions to address food security and climate change challenges in Africa. *Curr. Opin. Environ. Sustain.* 6, 61–67. doi:10.1016/j.cosust.2013.10.014
- McCool, D.K., Brown, L.C., Foster, G.R., Mutchler, C.K., Meyer, L.D., 1987. Revised slope steepness factor for the universal soil loss equation. doi:10.13031/2013.30576
- McDonald, M.A., Healey, J.R., Stevens, P.A., 2002. The effects of the secondary clearance forest and subsequent land-use on erosion losses and soil properties in the Blue Mountains of Jamaica. *Agric. Ecosyst. Environ.* 92, 1–19.
- McGaughey, R.J., 2014. FUSION/LDV: Software for LIDAR Data Analysis and Visualization.
- Mehlich, A., 1984. Mehlich 3 soil test extractant: A modification of Mehlich 2 extractant. *Commun. Soil Sci. Plant Anal.* 15, 1409–1416.
- Millennium Ecosystem Assessment, 2005. *Ecosystems and Human Well-Being, Ecosystems.* Island Press, Washington, DC. doi:10.1196/annals.1439.003
- Mitchell, M.G.E., Bennett, E.M., Gonzalez, A., 2014. Forest fragments modulate the provision of multiple ecosystem services. *J. Appl. Ecol.* 51, 909–918. doi:10.1111/1365-2664.12241
- Morris, K.S., Mendez, V.E., Lovell, S.T., Olson, M., 2013. Conventional food plot management in an organic coffee cooperative: Explaining the paradox. *Agroecol. Sustain. Food Syst.* 37, 762–787. doi:10.1080/21683565.2013.774303
- Mukherjee, A., Lal, R., 2014. Comparison of Soil Quality Index Using Three Methods. *PLoS One* 9, 1–15. doi:10.1371/journal.pone.0105981
- Muller-Landau, H.C., Condit, R.S., Chave, J., Thomas, S.C., Bohlman, S.A., Bunyavejchewin, S., Davies, S., Foster, R., Gunatilleke, S., Gunatilleke, N., Harms, K.E., Hart, T., Hubbell, S.P., Itoh, A., Kassim, A.R., LaFrankie, J. V., Lee, H.S., Losos, E., Makana, J.R., Ohkubo, T.,

- Sukumar, R., Sun, I.F., Nur Supardi, M.N., Tan, S., Thompson, J., Valencia, R., Muñoz, G.V., Wills, C., Yamakura, T., Chuyong, G., Dattaraja, H.S., Esufali, S., Hall, P., Hernandez, C., Kenfack, D., Kiratiprayoon, S., Suresh, H.S., Thomas, D., Vallejo, M.I., Ashton, P., 2006. Testing metabolic ecology theory for allometric scaling of tree size, growth and mortality in tropical forests. *Ecol. Lett.* 9, 575–588. doi:10.1111/j.1461-0248.2006.00904.x
- Naeem, B.S., Ingram, J.C., Varga, A., Agardy, T., Barten, P., Bennett, G., Bloomgarden, E., Bremer, L.L., Burkill, P., Cattau, M., Ching, C., Colby, M., Cook, D.C., Costanza, R., Declerck, F., Freund, C., Gartner, T., Gunderson, J., Jarrett, D., Kinzig, A.P., Kiss, A., Koontz, A., Kumar, P., Lasky, J.R., Masozera, M., Meyers, D., Milano, F., Nichols, E., Olander, L., Olmsted, P., Perge, E., Perrings, C., Polasky, S., Potent, J., Prager, C., Quétier, F., Redford, K., Saterson, K., Thoumi, G., Vargas, M.T., Vickerman, S., Weisser, W., Wilkie, D., Wunder, S., 2015. Get the science right when paying for nature's services. *Science* 347, 1206–1207. doi:10.1126/science.aaa1403
- Nagothu, U.S., 2016. *Climate Change and Agricultural Development: Improving Resilience Through Climate Smart Agriculture, Agroecology and Conservation*. Routledge.
- Návar, J., 2009. Allometric equations for tree species and carbon stocks for forests of northwestern Mexico. *For. Ecol. Manage.* 257, 427–434. doi:10.1016/j.foreco.2008.09.028
- Nelson, E., Mendoza, G., Regetz, J., Polasky, S., Tallis, H., Cameron, D.R., Chan, K.M.A., Daily, G.C., Goldstein, J., Kareiva, P.M., Lonsdorf, E., Naidoo, R., Ricketts, T.H., Shaw, M.R., 2009. Modeling multiple ecosystem services, biodiversity conservation, commodity production, and tradeoffs at landscape scales. *Front. Ecol. Environ.* 7, 4–11. doi:10.1890/080023
- Nichol, J.E., Sarker, M.L.R., 2011. Improved Biomass Estimation Using the Texture Parameters of Two High-Resolution Optical Sensors. *IEEE Trans. Geosci. Remote Sens.* 49, 930–948. doi:10.1109/TGRS.2010.2068574
- Nutto, L., Spathelf, P., Rogers, R., 2005. Managing diameter growth and natural pruning of Parana pine, *Araucaria angustifolia* (Bert.) O Ktze., to produce high value timber. *Ann. For. Sci.* 62, 163–173.
- Nziguheba, G., Merckx, R., Palm, C. a., 2005. Carbon and nitrogen dynamics in a phosphorus-deficient soil amended with organic residues and fertilizers in western Kenya. *Biol. Fertil. Soils* 41, 240–248. doi:10.1007/s00374-005-0832-0
- Okubo, S., Parikesit, D.M., Harashina, K., Takeuchi, K., Umezaki, M., 2010. Land use/cover classification of a complex agricultural landscape using single-dated very high spatial resolution satellite-sensed imagery. *Can. J. Remote Sens.* 36, 722–736. doi:10.5589/m11-010
- Ordóñez Barragan, J., 2004. Main factors influencing maize production in the Quesungual

agroforestry system in Southern Honduras: An exploratory study. Wageningen University. doi:10.1017/CBO9781107415324.004

- Pagiola, S., Ramírez, E., Gobbi, J., de Haan, C., Ibrahim, M., Murgueitio, E., Ruíz, J.P., 2007. Paying for the environmental services of silvopastoral practices in Nicaragua. *Ecol. Econ.* 64, 374–385. doi:10.1016/j.ecolecon.2007.04.014
- Paine, C.E.T., Marthens, T.R., Vogt, D.R., Purves, D., Rees, M., Hector, A., Turnbull, L.A., 2012. How to fit nonlinear plant growth models and calculate growth rates: An update for ecologists. *Methods Ecol. Evol.* 3, 245–256. doi:10.1111/j.2041-210X.2011.00155.x
- Palm, C.A., van Noordwijk, M., Woomer, P., Alegre, J.C., Arévalo, L., Castilla, C.E., Cordeiro, D.G., Hairiah, K., Kotto-Same, J., Moukam, A., Parton, W.J., Ricse, A., Rodrigues, V., Sitompul, S.M., 2005. Carbon losses and sequestration after land use change in the humid tropics, in: Palm, C.A., Vosti, S.A., Sanchez, P.A., Ericksen, P.J. (Eds.), *Slash-and-Burn Agriculture: The Search for Alternatives*. Columbia University Press, New York New York USA, pp. 41–63.
- Palmer, M., 2003. Propagation of Uncertainty through Mathematical Operations [WWW Document]. MIT Sch. Modul. Progr. Fluid Mech. URL [http://web.mit.edu/fluids-modules/www/exper\\_techniques/2.Propagation\\_of\\_Uncertaint.pdf](http://web.mit.edu/fluids-modules/www/exper_techniques/2.Propagation_of_Uncertaint.pdf) (accessed 6.16.15).
- Palomo, I., Felipe-Lucia, M.R., Bennett, E.M., Martín-López, B., Pascual, U., 2016. Disentangling the Pathways and Effects of Ecosystem Service Co-Production, in: *Advances in Ecological Research*. Elsevier Ltd., pp. 245–283. doi:10.1016/bs.aecr.2015.09.003
- Pan, Y., Birdsey, R.A., Fang, J., Houghton, R., Kauppi, P.E., Kurz, W.A., Phillips, O.L., Shvidenko, A., Lewis, S.L., Canadell, J.G., Ciais, P., Jackson, R.B., Pacala, S.W., McGuire, A.D., Piao, S., Rautiainen, A., Sitch, S., Hayes, D., 2011. A large and persistent carbon sink in the world's forests. *Science* 333, 988–993. doi:10.1126/science.1201609
- Pattanayak, S.K., Mercer, D.E., Sills, E., Yang, J.C., 2003. Taking stock of agroforestry adoption studies. *Agrofor. Syst.* 57, 173–186. doi:10.1023/A:1024809108210
- Pauli, N., Barrios, E., Conacher, A.J., Oberthür, T., 2011. Soil macrofauna in agricultural landscapes dominated by the Quesungual Slash-and-Mulch Agroforestry System, western Honduras. *Appl. Soil Ecol.* 47, 119–132. doi:10.1016/j.apsoil.2010.11.005
- Pebesma, E.J., 2004. Multivariable geostatistics in S: the gstat package. *Comput. Geosci.* 30, 683–691.
- Pelletier, J., Kirby, K.R., Potvin, C., 2012. Significance of carbon stock uncertainties on emission reductions from deforestation and forest degradation in developing countries. *For. Policy Econ.* 24, 3–11. doi:10.1016/j.forpol.2010.05.005
- Penman, J., Gytarsky, M., Hiraishi, T., Krug, T., Kruger, D., Pipatti, R., Buendia, L., Miwa, K.,

- Ngara, T., 2003. Good Practice Guidance for Land Use , Land-Use Change and Forestry. IPCC National Greenhouse Gas Inventories Programme, Kanagawa, Japan.
- Pilgrim, E.S., Macleod, C.J.A., Blackwell, M.S.A., Bol, R., Hogan, D. V., Chadwick, D.R., Cardenas, L., Misselbrook, T.H., Haygarth, P.M., Brazier, R.E., Hobbs, P., Hodgson, C., Jarvis, S., Dungait, J., Murray, P.J., Firbank, L.G., 2010. Interactions among agricultural production and other ecosystem services delivered from european temperate grassland systems, *Advances in Agronomy*. Elsevier Ltd. doi:10.1016/B978-0-12-385040-9.00004-9
- Pinheiro, J., Bates, D., DebRoy, S., Sarkar, D., R Development Core Team, 2013. *nlme: Linear and Nonlinear Mixed Effects Models*.
- Pinheiro, J.C., Bates, D.M., 2000. *Mixed-Effects Models in S and S-Plus*. Springer-Verlag, New York.
- Pollini, J., 2009. Agroforestry and the search for alternatives to slash-and-burn cultivation: From technological optimism to a political economy of deforestation. *Agric. Ecosyst. Environ.* 133, 48–60. doi:10.1016/j.agee.2009.05.002
- Popescu, S.C., 2007. Estimating biomass of individual pine trees using airborne lidar. *Biomass and Bioenergy* 31, 646–655. doi:10.1016/j.biombioe.2007.06.022
- Popescu, S.C., Wynne, R.H., 2004. Seeing the trees in the forest: using lidar and multispectral data fusion with local filtering and variable window size for estimating tree height. *Photogramm. Eng. Remote* 70, 589–604.
- Power, A.G., 2010. Ecosystem services and agriculture: tradeoffs and synergies. *Philos. Trans. R. Soc. Lond. B. Biol. Sci.* 365, 2959–2971. doi:10.1098/rstb.2010.0143
- Pribyl, D.W., 2010. A critical review of the conventional SOC to SOM conversion factor. *Geoderma* 156, 75–83. doi:10.1016/j.geoderma.2010.02.003
- Price, B., Gomez, A., Mathys, L., Gardi, O., Schellenberger, A., Ginzler, C., Thürig, E., 2017. Tree biomass in the Swiss landscape: nationwide modelling for improved accounting for forest and non-forest trees. *Environ. Monit. Assess.* 189, 106. doi:10.1007/s10661-017-5816-7
- R Core Team, 2013. *R: A Language and Environment for Statistical Computing*.
- Ramankutty, N., Evan, A.T., Monfreda, C., Foley, J.A., 2008. Farming the planet: 1. Geographic distribution of global agricultural lands in the year 2000. *Global Biogeochem. Cycles* 22, 1–19. doi:10.1029/2007GB002952
- Rana, P., Tokola, T., Korhonen, L., Xu, Q., Kumpula, T., Vihervaara, P., Mononen, L., 2013. Training Area Concept in a Two-Phase Biomass Inventory Using Airborne Laser Scanning and RapidEye Satellite Data. *Remote Sens.* 6, 285–309. doi:10.3390/rs6010285

- Raudsepp-hearne, C., Peterson, G.D., Bennett, E.M., 2010. Ecosystem service bundles for analyzing tradeoffs in diverse landscapes. *Proc. Natl. Acad. Sci.* 107, 5242–5247. doi:10.1073/pnas.0907284107
- Ravindranath, N., Ostwald, M., 2008. *Carbon Inventory Methods: Handbook for Greenhouse Gas Inventory, Carbon Mitigation and Roundwood Production Projects*, 29th ed. Springer Netherlands.
- Renard, K., Foster, G., Weesies, G.A., McCool, D.K., Yoder, D.C., 1997. Predicting soil erosion by water: a guide to conservation planning with the revised universal soil loss equation (RUSLE), *Agricultural Handbook 703, Agriculture Handbook Number 703*. USDA Agricultural Research Service, Beltsville, MD.
- Richards, M.B., Méndez, V.E., 2014. Interactions between carbon sequestration and shade tree diversity in a smallholder coffee cooperative in El Salvador. *Conserv. Biol.* 28, 489–497. doi:10.1111/cobi.12181
- Riitters, K., Wickham, J., Neill, R.O., Jones, B., Smith, E.R., 2000. Global-Scale Patterns of Forest Fragmentation. *Conserv. Ecol.* 4, 1–20.
- Riitters, K.H., Wickham, J.D., O’Neill, R. V, Jones, K.B., Smith, E.R., Coulston, J.W., Wade, T.G., Smith, J.H., 2002. Fragmentation of Continental United States Forests. *Ecosystems* 5, 815–822. doi:10.1007/s10021002-0209-2
- Rioux, J., Juan, M.G.S., Neely, C., Seeberg-Elverfeldt, C., Karttunen, K., Rosenstock, T., Kirui, J., Massoro, E., Mpanda, M., Kimaro, A., Masoud, T., Mutoko, M., Mutabazi, K., Kuehne, G., Poultouchidou, A., Avagyan, A., Tapio-Bistrom, M.-L., Bernoux, M., 2016. *Planning, implementing and evaluating Climate-Smart Agriculture in Smallholder Farming Systems (No. 11), Mitigation of Climate Change in Agriculture Series*. Rome.
- Robertson, G.P., Gross, K.L., Hamilton, S.K., Landis, D.A., Schmidt, T.M., Snapp, S.S., Swinton, S.M., 2014. Farming for ecosystem services: An ecological approach to production agriculture. *Bioscience* 64, 404–415. doi:10.1093/biosci/biu037
- Rosenstock, T.S., Rufiano, M.C., Butterbach-Bahl, K., Wollenberg, E., Richards, M., 2016. *Methods for Measuring Greenhouse Gas Balances and Evaluating Mitigation Options in Smallholder Agriculture*, 1st ed. Springer International Publishing.
- Rousseau, L., Fonte, S.J., Téllez, O., Van Der Hoek, R., Lavelle, P., 2013. Soil macrofauna as indicators of soil quality and land use impacts in smallholder agroecosystems of western Nicaragua. *Ecol. Indic.* 27, 71–82. doi:10.1016/j.ecolind.2012.11.020
- Saatchi, S.S., Harris, N.L., Brown, S., Lefsky, M., Mitchard, E.T.A., Salas, W., Zutta, B.R., Buermann, W., Lewis, S.L., Hoga, S., White, L., Silman, M., Morel, A., 2011. Benchmark map of forest carbon stocks in tropical regions across three continents. *Proc. Natl. Acad. Sci. U. S. A.* 108, 9899–9904. doi:10.1073/pnas.1019576108

- Sarker, L.R., Nichol, J.E., 2011. Improved forest biomass estimates using ALOS AVNIR-2 texture indices. *Remote Sens. Environ.* 115, 968–977. doi:10.1016/j.rse.2010.11.010
- Satterfield, T., Gregory, R., Klain, S., Roberts, M., Chan, K.M., 2013. Culture, Intangibles and metrics in environmental management. *J. Environ. Manage.* 117, 103–114. doi:10.1016/j.jenvman.2012.11.033
- Saxton, K., Rawls, W., 2006. Soil Water Characteristic Estimates by Texture and Organic Matter for Hydrologic Solutions. *Soil Sci. Soc. Am. J.* 70, 1569–1578. doi:10.2136/sssaj2005.0117
- Scherr, S.J., Shames, S., Friedman, R., 2012. From climate-smart agriculture to climate-smart landscapes. *Agric. Food Secur.* 1, 12. doi:10.1186/2048-7010-1-12
- Schipanski, M.E., Barbercheck, M., Douglas, M.R., Finney, D.M., Haider, K., Kaye, J.P., Kemanian, A.R., Mortensen, D.A., Ryan, M.R., Tooker, J., White, C., 2014. A framework for evaluating ecosystem services provided by cover crops in agroecosystems. *Agric. Syst.* 125, 12–22. doi:10.1016/j.agsy.2013.11.004
- Schmitt-Harsh, M., Evans, T.P., Castellanos, E., Randolph, J.C., 2012. Carbon stocks in coffee agroforests and mixed dry tropical forests in the western highlands of Guatemala. *Agrofor. Syst.* 86, 141–157. doi:10.1007/s10457-012-9549-x
- Schnell, S., Altrell, D., Ståhl, G., Kleinn, C., 2015. The contribution of trees outside forests to national tree biomass and carbon stocks--a comparative study across three continents. *Environ. Monit. Assess.* 187, 4197. doi:10.1007/s10661-014-4197-4
- Schoon, M.L., Robards, M.D., Brown, K., Engle, N., Meek, C.L., Biggs, R., 2015. Politics and the resilience of ecosystem services, in: *Principles for Building Resilience: Sustaining Ecosystem Services in Social-Ecological Systems*. pp. 32–49. doi:10.1017/CBO9781316014240.003
- Segura, M., Kanninen, M., Suárez, D., 2006. Allometric models for estimating aboveground biomass of shade trees and coffee bushes grown together. *Agrofor. Syst.* 68, 143–150. doi:10.1007/s10457-006-9005-x
- Sexton, J.O., Noojipady, P., Anand, A., Song, X., McMahan, S., Huang, C., Feng, M., Channan, S., Townshend, J.R., 2015. A model for the propagation of uncertainty from continuous estimates of tree cover to categorical forest cover and change. *Remote Sens. Environ.* 156, 418–425. doi:10.1016/j.rse.2014.08.038
- Shannon, C.E., 1948. The Shannon information entropy of protein sequences. *Bell Syst. Tech. J.* 27, 379–423, NaN-656. doi:10.1016/S0006-3495(96)79210-X
- Shepherd, K.D., Shepherd, G., Walsh, M.G., 2015. Land health surveillance and response: A framework for evidence-informed land management. *Agric. Syst.* 132, 93–106. doi:10.1016/j.agsy.2014.09.002

- Shi, Z., Wen, A., Zhang, X., Yan, D., 2011. Comparison of the soil losses from 7Be measurements and the monitoring data by erosion pins and runoff plots in the Three Gorges Reservoir region, China. *Appl. Radiat. Isot.* 69, 1343–1348. doi:10.1016/j.apradiso.2011.05.031
- Sileshi, G.W., 2014. A critical review of forest biomass estimation models, common mistakes and corrective measures. *For. Ecol. Manage.* 329, 237–254. doi:10.1016/j.foreco.2014.06.026
- Sirvent, J., Desir, G., Gutierrez, M., Sancho, C., Benito, G., 1997. Erosion rates in badland areas recorded by collectors, erosion pins and profilometer techniques (Ebro Basin, NE-Spain). *Geomorphology* 18, 61–75. doi:10.1016/S0169-555X(96)00023-2
- Smukler, S.M., Sánchez-Moreno, S., Fonte, S.J., Ferris, H., Klonsky, K., O’Geen, a. T., Scow, K.M., Steenwerth, K.L., Jackson, L.E., 2010. Biodiversity and multiple ecosystem functions in an organic farmscape. *Agric. Ecosyst. Environ.* 139, 80–97. doi:10.1016/j.agee.2010.07.004
- SNET, 2005. Balance hídrico integrado y dinámico en El Salvador: componente evaluación de recursos hídricos.
- Sprugel, D.G., 1983. Correcting for bias in log-transformed allometric equations. *Ecology* 64, 209–210. doi:10.2307/1937343
- Steenwerth, K.L., Hodson, A.K., Bloom, A.J., Carter, M.R., Cattaneo, A., Chartres, C.J., Hatfield, J.L., Henry, K., Hopmans, J.W., Horwath, W.R., Jenkins, B.M., Kebreab, E., Leemans, R., Lipper, L., Lubell, M.N., Msangi, S., Prabhu, R., Reynolds, M.P., Sandoval Solis, S., Sischo, W.M., Springborn, M., Tittonell, P., Wheeler, S.M., Vermeulen, S.J., Wollenberg, E.K., Jarvis, L.S., Jackson, L.E., 2014. Climate-smart agriculture global research agenda: scientific basis for action. *Agric. Food Secur.* 3, 11. doi:10.1186/2048-7010-3-11
- Stephenson, N.L., Das, A.J., Condit, R., Russo, S.E., Baker, P.J., Beckman, N.G., Coomes, D. a, Lines, E.R., Morris, W.K., Rüger, N., Alvarez, E., Blundo, C., Bunyavejchewin, S., Chuyong, G., Davies, S.J., Duque, A., Ewango, C.N., Flores, O., Franklin, J.F., Grau, H.R., Hao, Z., Harmon, M.E., Hubbell, S.P., Kenfack, D., Lin, Y., Makana, J.-R., Malizia, A., Malizia, L.R., Pabst, R.J., Pongpattananurak, N., Su, S.-H., Sun, I.-F., Tan, S., Thomas, D., van Mantgem, P.J., Wang, X., Wiser, S.K., Zavala, M.A., 2014. Rate of tree carbon accumulation increases continuously with tree size. *Nature* 507, 90–3. doi:10.1038/nature12914
- Stringer, L.C., Dougill, A.J., Thomas, A.D., Spracklen, D. V., Chesterman, S., Speranza, C.I., Rueff, H., Riddell, M., Williams, M., Beedy, T., Abson, D.J., Klintonberg, P., Syampungani, S., Powell, P., Palmer, A.R., Seely, M.K., Mkwambisi, D.D., Falcao, M., Siteo, A., Ross, S., Kopolu, G., 2012. Challenges and opportunities in linking carbon sequestration, livelihoods and ecosystem service provision in drylands. *Environ. Sci. Policy* 19–20, 121–135. doi:10.1016/j.envsci.2012.02.004
- Strobl, C., Boulesteix, A.-L., Kneib, T., Augustin, T., Zeileis, A., 2008. Conditional variable

importance for random forests. *BMC Bioinformatics* 9, 307. doi:10.1186/1471-2105-9-307

Suárez, D., 2002. Cuantificación y valoración económica del servicio ambiental almacenamiento de carbono en sistemas agroforestales de café en la Comarca Yassica Sur, Matagalpa, Nicaragua. CATIE.

Svetnik, V., Liaw, A., Tong, C., Christopher Culberson, J., Sheridan, R.P., Feuston, B.P., 2003. Random Forest: A Classification and Regression Tool for Compound Classification and QSAR Modeling. *J. Chem. Inf. Comput. Sci.* 43, 1947–1958. doi:10.1021/ci034160g

Tao, S., Guo, Q., Li, L., Xue, B., Kelly, M., Li, W., Xu, G., Su, Y., 2014. Airborne Lidar-derived volume metrics for aboveground biomass estimation: A comparative assessment for conifer stands. *Agric. For. Meteorol.* 198–199, 24–32. doi:10.1016/j.agrformet.2014.07.008

The Plan Vivo Foundation, 2013. The Plan Vivo Standard 2013, The Plan Vivo Standard for Community Payments for Ecosystem Services Programmes. doi:10.1017/CBO9781107415324.004

The World Bank, 2016. Population density (people per sq. km of land area) [WWW Document]. Food Agric. Organ. World Bank Popul. Estim. URL <http://data.worldbank.org/indicator/EN.POP.DNST> (accessed 3.30.17).

The World Bank, 2008. Sustainable Land Management Sourcebook, Agriculture and Rural Development. The World Bank, Washington, DC. doi:10.1596/978-0-8213-7432-0

Thomazini, A., Mendonça, E.S., Cardoso, I.M., Garbin, M.L., 2015. SOC dynamics and soil quality index of agroforestry systems in the Atlantic rainforest of Brazil. *Geoderma Reg.* 5, 15–24. doi:10.1016/j.geodrs.2015.02.003

Tittonell, P., Giller, K.E., 2013. When yield gaps are poverty traps: The paradigm of ecological intensification in African smallholder agriculture. *F. Crop. Res.* 143, 76–90. doi:10.1016/j.fcr.2012.10.007

Tsui, O.W., Coops, N.C., Wulder, M. a., Marshall, P.L., 2013. Integrating airborne LiDAR and space-borne radar via multivariate kriging to estimate above-ground biomass. *Remote Sens. Environ.* 139, 340–352. doi:10.1016/j.rse.2013.08.012

Tubiello, F.N., Salvatore, M., Ferrara, A.F., House, J., Federici, S., Rossi, S., Biancalani, R., Condor Golec, R.D., Jacobs, H., Flammini, A., Prospero, P., Cardenas-Galindo, P., Schmidhuber, J., Sanz Sanchez, M.J., Srivastava, N., Smith, P., 2015. The Contribution of Agriculture, Forestry and other Land Use activities to Global Warming, 1990-2012. *Glob. Chang. Biol.* 21, 2655–2660. doi:10.1111/gcb.12865

Tully, K.L., Lawrence, D., Scanlon, T.M., 2012. More trees less loss: Nitrogen leaching losses decrease with increasing biomass in coffee agroforests. *Agric. Ecosyst. Environ.* 161,

137–144. doi:10.1016/j.agee.2012.08.002

- US Interagency Working Group on the Social Cost of Carbon, 2015. Technical Support Document: - Technical Update of the Social Cost of Carbon for Regulatory Impact Analysis- Under Executive Order 12866 -- July 2015 Revision.
- Vågen, T.-G., Shepherd, K.D., Walsh, M.G., Winowiecki, L., Desta, L.T., Tondoh, J.E., 2010. AfSIS Technical Specifications, Soil Health Surveillance.
- Vågen, T.-G., Winowiecki, L. a, 2013. Mapping of soil organic carbon stocks for spatially explicit assessments of climate change mitigation potential. *Environ. Res. Lett.* 8, 15011. doi:10.1088/1748-9326/8/1/015011
- Vaglio Laurin, G., Chen, Q., Lindsell, J. a., Coomes, D. a., Frate, F. Del, Guerriero, L., Pirotti, F., Valentini, R., 2014. Above ground biomass estimation in an African tropical forest with lidar and hyperspectral data. *ISPRS J. Photogramm. Remote Sens.* 89, 49–58. doi:10.1016/j.isprsjprs.2014.01.001
- van Breugel, M., Ransijn, J., Craven, D., Bongers, F., Hall, J.S., 2011. Estimating carbon stock in secondary forests: Decisions and uncertainties associated with allometric biomass models. *For. Ecol. Manage.* 262, 1648–1657. doi:10.1016/j.foreco.2011.07.018
- Véga, C., Durrieu, S., 2011. Multi-level filtering segmentation to measure individual tree parameters based on Lidar data: Application to a mountainous forest with heterogeneous stands. *Int. J. Appl. Earth Obs. Geoinf.* 13, 646–656. doi:10.1016/j.jag.2011.04.002
- Velasquez, E., Lavelle, P., Andrade, M., 2007. GISQ , a multifunctional indicator of soil quality. *Soil Biol. Biochem.* 39, 3066–3080. doi:10.1016/j.soilbio.2007.06.013
- Verburg, P.H., van de Steeg, J., Veldkamp, A., Willemen, L., 2009. From land cover change to land function dynamics: A major challenge to improve land characterization. *J. Environ. Manage.* 90, 1327–1335. doi:10.1016/j.jenvman.2008.08.005
- Verchot, L. V., Noordwijk, M., Kandji, S., Tomich, T., Ong, C., Albrecht, A., Mackensen, J., Bantilan, C., Anupama, K. V., Palm, C., 2007. Climate change: linking adaptation and mitigation through agroforestry. *Mitig. Adapt. Strateg. Glob. Chang.* 12, 901–918. doi:10.1007/s11027-007-9105-6
- Walkley, A., Black, I.A., 1934. An examination of the Degtjareff method for determining soil organic matter, and a proposed modification of the chromic acid titration method. *Soil Sci.* 37, 29–38.
- Welches, L.A., Cherrett, I., 2002. The Quesungual system in Honduras - An alternative to slash-and-burn. *LEISA Mag.* 10–11.
- Wendland, K.J., Honzák, M., Portela, R., Vitale, B., Rubinoff, S., Randrianarisoa, J., 2010.

Targeting and implementing payments for ecosystem services: Opportunities for bundling biodiversity conservation with carbon and water services in Madagascar. *Ecol. Econ.* 69, 2093–2107. doi:10.1016/j.ecolecon.2009.01.002

White, J.C., Wulder, M.A., Varhola, A., Vastaranta, M., Coops, N.C., Cook, B.D., Pitt, D., Woods, M., 2013. A best practices guide for generating forest inventory attributes from airborne laser scanning data using an area-based approach, Information Report FI-X-010. Victoria, British Columbia.

Wilson, J.P., Gallant, J.C., 2000. Digital Terrain Analysis, in: *Terrain Analysis: Principles and Applications*. Wiley, pp. 1–27. doi:10.5194/hess-4-225-2000

Wittman, H., Powell, L.J., Corbera, E., 2015. Financing the agrarian transition? The Clean Development Mechanism and agricultural change in Latin America. *Environ. Plan. A* 47, 2031–2046. doi:10.1068/a130218p

Wunder, S., 2008. Payments for environmental services and the poor: concepts and preliminary evidence. *Environ. Dev. Econ.* 13, 279–297. doi:10.1017/S1355770X08004282

Yarbrough, L.D., Easson, G., 2005. Quickbird 2 tasseled cap transform coefficients: a comparison of derivation methods, in: Pecora 16 Symposium “Global Priorities in Land Remote Sensing.” Sioux Falls, South Dakota, USA.

Zeide, B., 1993. Analysis of Growth Equations. *For. Sci.* 39, 594–616. doi:10.1111/j.1461-0248.2006.00883.x

Zhang, X., Ni-meister, W., 2014. Remote Sensing of Forest Biomass, in: Hanes, J.M. (Ed.), *Biophysical Applications of Satellite Remote Sensing*. Springer Berlin Heidelberg, pp. 63–98. doi:10.1007/978-3-642-25047-7

Zolkos, S.G., Goetz, S.J., Dubayah, R., 2013. A meta-analysis of terrestrial aboveground biomass estimation using lidar remote sensing. *Remote Sens. Environ.* 128, 289–298. doi:10.1016/j.rse.2012.10.017

Zörb, C., Senbayram, M., Peiter, E., 2014. Potassium in agriculture--status and perspectives. *J. Plant Physiol.* 171, 656–69. doi:10.1016/j.jplph.2013.08.008

# Appendices

## Appendix A

### *Description of indicator development methods for the water regulation index used in*

#### *Chapter 2*

I used a crop water balance model developed by the FAO (1998) to estimate deep percolation of precipitation and crop water stress during the 2015 growing season. The model was parameterized using precipitation data and infiltration rates (described in Section 2.5.2) and calibrated with biweekly soil moisture measurements taken to 7.9" (20 cm) depth using a FieldScout TDR 100 soil moisture meter from Spectrum Technologies, Inc. (Aurora, IL, USA). Crop water stress and deep percolation were calculated as follows.

The FAO model is based on soil water availability and the daily water balance, expressed in terms of depletion at the end of the day, according to the equation:

$$D_{r,i} = D_{r,i-1} - (P_i - RO_i) + K_{s,i}ET_{c,i} + DP_i \quad \text{[Equation A.1]}$$

where:

$D_{r,i}$  = root zone depletion at the end of day  $i$  (mm),

$P_i$  = precipitation on day  $i$  (mm),

$RO_i$  = runoff on day  $i$  (mm),

$K_{s,i}$  = water stress coefficient

$ET_{c,i}$  = crop evapotranspiration on day  $i$  (mm),

$DP_i$  = deep percolation beyond the root zone on day  $i$  (mm)

$D_{r,0}$  was set as the first day for which VWC was measured (April 30, 2015) and the model run to through the last day of VWC measurement (December 18, 2015). For every day that soil VWC was measured in the field,  $D_r$  was derived from the measured soil moisture content as:

$$D_r = 1000(q_{FC} - q_i)Z_r \quad \text{[Equation A.2]}$$

where  $q_{FC}$  is the soil field capacity,  $q_i$  is the measured soil volumetric water content (VWC) and  $Z_r$  is the rooting depth (limited to 20 cm as this was the depth of the soil moisture probe). For all other days without field measurements, daily depletion was estimated using Equation S1 above. Precipitation ( $P$ ) and runoff ( $RO$ ) were estimated as described in Section 2.5.2. Crop evapotranspiration ( $ET_c$ ) was estimated using monthly crop coefficients for maize, beans and secondary forests identified by El Salvador's National Hydrologic Service (SNET, 2005).

When daily water depletion exceeded readily available water held in the soil, plants were expected to experience water stress and a water stress coefficient ( $K_s$ , ranging from 0 – 1) was calculated following methods outlined by the FAO (1998). Readily

available water was calculated as the difference between field capacity and permanent wilting point. Field capacity was estimated based on the highest VWC value measured in the field and permanent wilting point calculated from soil properties (SOM, clay and sand content) using the equation developed by Saxton and Rawls (2006) for VWC at 1500 kPa.

A  $K_s$  coefficient of 1 indicates no water stress and full evapotranspiration rates, while a coefficient of less than one indicates limited evapotranspiration due to water stress. I then calculated the number of days for which the coefficient was less than one and divided by the total number of days during the growing season to estimate the proportion of days in which crops experienced water stress for each plot, the *Drought stress* ES indicator in Table 3.

Any water remaining after subtracting  $RO$  and  $ET_c$  from  $P$  was assumed to have percolated below 20 cm and thus attributed to deep percolation ( $DP$ ), used as the *Deep percolation* ES indicator in Table 3.

## Supplementary Tables for Chapter 2

**Table A - 1. Descriptive statistics by treatment for field proxies measured in individual plots**

CONV = conventional management; ORG = organic (conventional management without chemical inputs); SMAS-1 = the slash-and-mulch agroforestry system, converted from CONV; SMAS-2 = the same as SMAS-1, but converted from FOR and; FOR = forest-fallow. n = 5 for each treatment.

Field Metric [units]	CONV	ORG	SMAS-1	SMAS-2	FOR
<i>Stem Count (All) [trees ha-1]</i>					
Mean	517	2433	867	2217	3883
Min	0	1792	250	1708	3125
Max	1042	3625	1542	2750	5500
CV (%)	76.2	34.3	53.9	23.5	25.8
<i>Stem Count (DBH &lt; 10 cm) [trees ha-1]</i>					
Mean	433	2000	768	2033	3233
Min	0	1333	208	1500	2417
Max	833	3292	1417	2625	5167
CV (%)	73.7	39.5	58.0	25.0	35.3
<i>Stem Count (DBH 10+ cm) [trees ha-1]</i>					
Mean	83	433	98	183	650
Min	0	167	0	83	333
Max	208	833	200	250	833
CV (%)	93.5	58.3	79.8	41.3	34.4
<i>Canopy Cover [%]</i>					
Mean	25	69	36	42	96
Min	7	53	8	22	85
Max	43	93	65	73	100
CV (%)	65.1	24.1	74.3	57.2	6.9
<i>Soil Cover (Visible) [%]</i>					
Mean	30	48	36	37	70
Min	3	15	12	3	32
Max	45	77	65	62	93
CV (%)	56.8	48.5	57.2	67.7	33.7
<i>Soil Cover (Biomass) [kg ha-1]</i>					
Mean	4422	6685	4033	6225	7635
Min	3352	4718	3504	5168	6730
Max	4778	8143	4653	7195	9825
CV (%)	13.7	19.6	11.6	12.5	16.4
<i>Infiltration [mm ha-1]</i>					
Mean	5.52	16.02	11.31	8.99	18.98
Min	1.92	4.72	0.89	0.83	1.02
Max	10.86	40.83	44.67	29.75	62.34
CV (%)	60.1	99.9	166.1	133.0	132.1
<i>Soil Organic Matter [%]</i>					
Mean	4.29	4.54	4.10	4.35	4.76
Min	2.86	3.42	3.35	2.86	3.11
Max	5.28	6.66	5.28	6.07	5.97
CV (%)	21.8	27.6	20.0	29.4	24.4
<i>Bulk Density [g cm-3]</i>					
Mean	0.94	0.99	0.93	0.89	0.89
Min	0.82	0.83	0.72	0.77	0.72
Max	1.07	1.14	1.16	1.11	1.17
CV (%)	10.4	11.9	18.8	15.2	18.7

**Table A - 2. Select results from principal component analysis of ecosystem service indices**

Relative contributions (a.k.a. loadings or rotations) of each ecosystem service composite index to the first two principle components (PC)

Composite Index	PC1	PC2
Production Value	-0.4522	0.1557
Pest & Disease Control	-0.2276	0.4954
Erosion Control	0.5391	0.3454
Water Regulation	-0.3137	0.3640
Soil Composition	-0.1305	0.4096
Carbon (C) Storage	0.1659	0.3320
Aboveground Biodiversity (AGBD)	0.5401	0.2889
Belowground Biodiversity (BGBD)	-0.1359	0.3423

**Table A - 3. Expected benefits, costs and net profit of each maize-bean production system**

Based on measured yields, inputs, labor requirements and regional prices in the third year of production. CONV = conventional management; ORG = organic (conventional management without chemical inputs); SMAS-1 = the slash-and-mulch agroforestry system, converted from CONV; SMAS-2 = the same as SMAS-1, but converted from FOR and; FOR = forest-fallow.

	CONV	ORG	SMAS-1	SMAS-2
	----- USD (\$) -----			
<i>Benefits</i>				
Maize	1,403	744	1,385	507
Beans	1,565	1,724	1,266	974
Fuelwood	22	22	33	66
Fruit (Jocote)	-	-	57	-
Total Income	2,990	2,491	2,741	1,548
<i>Costs</i>				
Labor	947	1,307	987	830
Services	114	311	109	34
Inputs <sup>†</sup>	1,164	4,568	1,110	1,108
Total Costs	2,225	6,186	2,206	1,973
<i>Net Profit</i>	765	(3,696)	535	(425)

<sup>†</sup> A major contributor to the cost of inputs was composted chicken manure (known locally as *boccachi*), for which I used the market price. I should be noted that *boccachi* could be produced on-farm, provided the farmer has access to the necessary materials, or replaced with alternatives on-farm, in which case this cost could be reduced substantially.

**Supplementary Figures for Chapter 2**

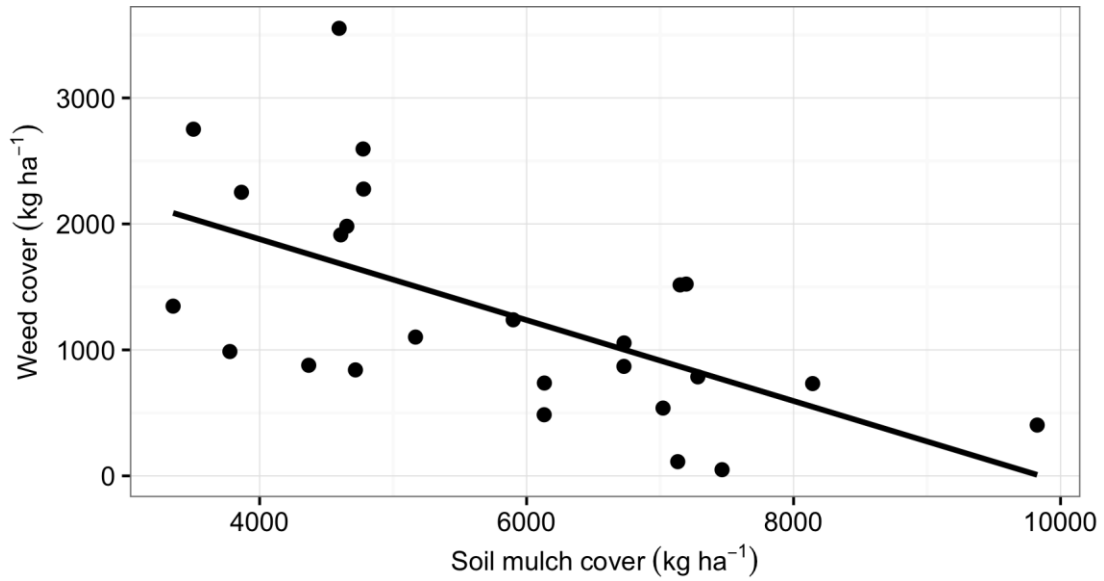


**Figure A - 1. Correlation between weed biomass and soil mulch cover**

Pearson's correlation ( $r = -0.603$ ,  $p = 0.001$ ) in all treatment plots ( $n = 25$ ). Greater soil mulch cover was highly correlated with less weed presence.

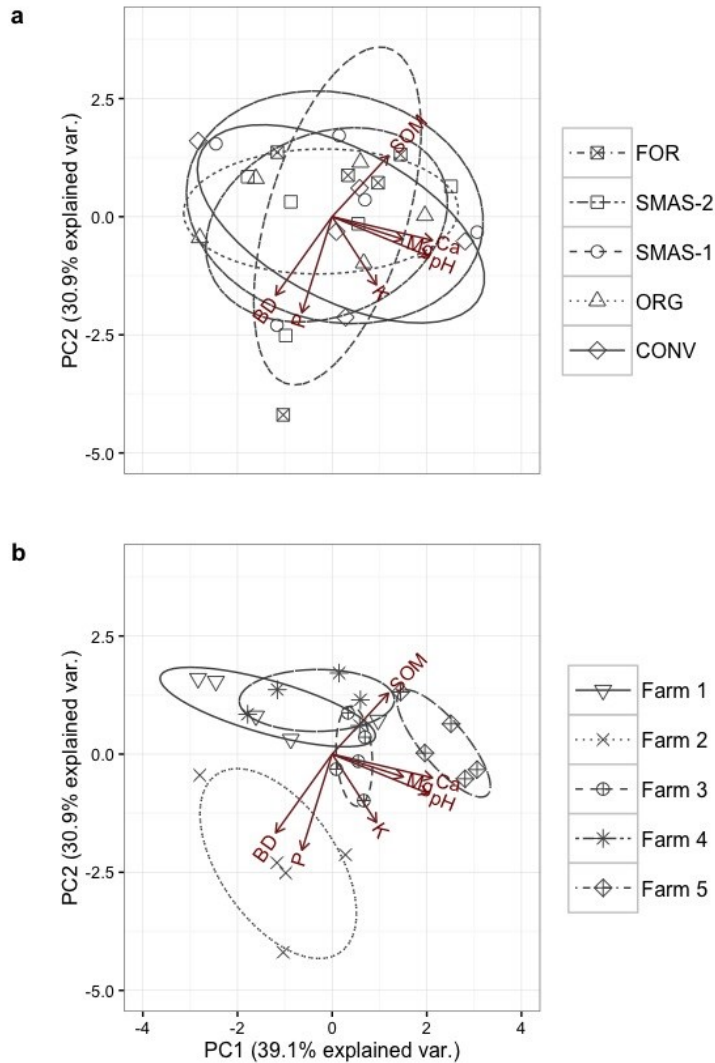


**Figure A - 2. Co-variation of soil properties by treatment and farm location**

Distance biplot of the (scaled) first two principal components of soil properties by (a) treatment and (b) farm location. Little variability in soil properties by treatments is demonstrated by the overlapping ellipses in (a), while soil properties did vary by site, shown by greater ellipse separation in (b). For treatments, CONV = conventional management; ORG = organic (conventional management without chemical inputs); SMAS-1 = the slash-and-mulch agroforestry system, converted from CONV; SMAS-2 = the same as SMAS-1, but converted from FOR and; FOR = forest-fallow. For soil properties, BD = bulk density; Ca = calcium; K = potassium; Mg = magnesium; P = phosphorus; pH = acidity and; SOM = soil organic matter

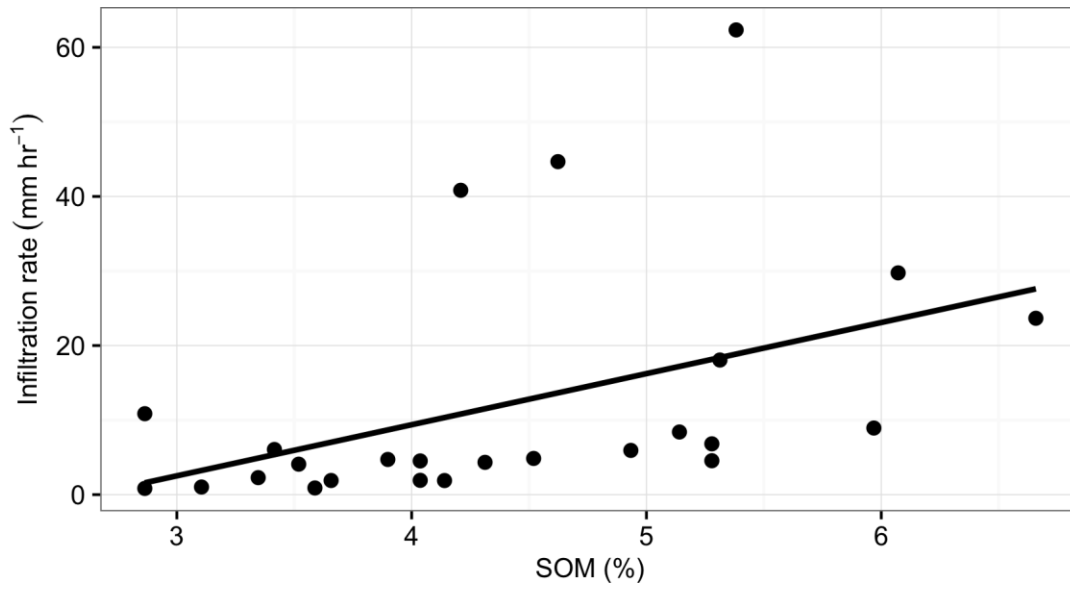


**Figure A - 3. Correlation between SOM and infiltration rates**

Pearson's correlation ( $r = 0.443$ ,  $p = 0.027$ ) for all treatment plots ( $n = 25$ ). Greater soil organic matter (SOM) was associated with increased rates of infiltration, as measured using mini-disk infiltrometer.

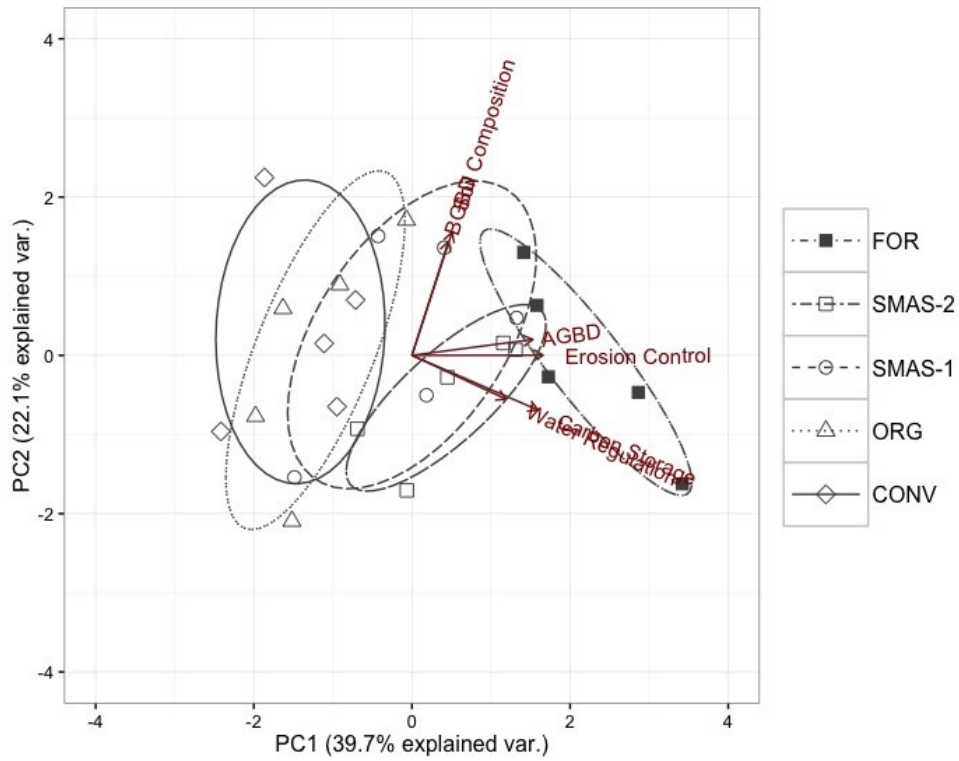


**Figure A - 4. Co-variation of non-production ES indices by treatment**

Distance biplot of the (scaled) first two principal components of non-production ecosystem service (ES) composite indices for all treatments: CONV = conventional management; ORG = organic (conventional management without chemical inputs); SMAS-1 = the slash-and-mulch agroforestry system, converted from CONV; SMAS-2 = the same as SMAS-1, but converted from forest-fallow and; FOR = forest-fallow. AGBD and BGBD are aboveground and belowground biodiversity, respectively. C Storage and Water Regulation are overlaid along to PC1 axis and BGBD and Soil Composition are overlaid along the PC2 axis, making them difficult to read.

## Appendix B

### *Allometric equations used to derive aboveground woody biomass*

#### *Species-specific equations*

The most commonly encountered tree species across all land uses, in terms of total basal area, were *Pinus oocarpa Schiede ex Schltdl.* (14.78%), *Curatella americana L.* (11.24%), *Cordia alliodora (Ruiz & Pav.) Oken* (8.20%), *Cochlospermum vitifolium (Willd.) Spreng.* (7.20%), *Lysiloma divaricatum (Jacq.) J.F. Macbr.* (6.83%) and *Gliricidia sepium (Jacq.) Kunth ex Walp.* (5.69%).

Species-specific allometric equations (SS1 – SS15) were used to estimate aboveground woody biomass (AGWB) for all species listed in Table B - 1. A total of 15 species-specific equations were found in the literature from various studies and deemed appropriate for application to this study. Equations were considered appropriate if developed from destructive sampling of trees in the same genus and/or species from locations with a similar climate. All 15 equations came from studies done in Central America, Mexico or the Caribbean.

The 15 equations were applied to 23 individual species from this study, as sometimes the equation was developed using multiple species within a single genus. Species-specific equations were only applied to individual trees from this study when the measured DBH did not exceed the maximum DBH of the sampled trees used to develop the equation. When trees measured in this study had a DBH outside

the species-specific equation's range, or when a species-specific equation was not found, one of three appropriate mixed-species equations for trees (M1 – M3) was used.

*Mixed-species equations (DBH  $\geq$  10 cm)*

The equation from van Breugal et al. (2011), referred to as Equation M1 in Table B - 1, was chosen as the primary equation to be used for trees with a DBH  $\geq$  10 cm when species-specific equations were not available. Equation M1 was chosen because: a) it was developed in a similar climate (MAP of 2300mm with dry period from December to April); b) it was developed for secondary forests (0 – 25 years after abandonment); c) 7 of the 23 species used to derive the equation were also found in this study; d) it included a large number of destructively sampled trees (244) and; e) it provided a conservative equation compared to other identified mixed-species equations. Equation M1 was therefore used for all remaining species with DBH  $\geq$  10 cm but  $\leq$  29 cm, as 29 cm was the maximum DBH of trees used in the van Breugal et al. 2011 study.

For remaining trees with DBH  $>$  29 cm, Equation M2 (Chave et al., 2005) was used. Equation M2 was derived from a compilation of 27 published and unpublished datasets resulting in a total of 2,410 individual trees. This equation was developed primarily from undisturbed forests and was therefore not considered appropriate for use as the primary equation for all trees in this study as most sample locations

showed evidence of disturbance. However, it is likely appropriate for the large trees in this study, and this is how it was applied. In total, Equation M2 was used to estimate the biomass of about 18.5% of the trees in this study.

*Mixed-species equations (DBH < 10 cm)*

For trees with DBH < 10 cm, Equation M3 (Hughes et al., 1999b) was used. I chose this model, in part, because it was: a) developed specifically for trees with DBH < 10cm; b) developed for secondary forests/fallows in agricultural landscapes; c) was developed for a similar climate in Mexico (although somewhat wetter with a MAP of ~ 4000 cm) and; d) relatively conservative compared to other models. It also included four of the same genus and/or species found in this study.

*Coppiced trees and diameter-height equations*

Any tree in the sampling plots that had been cut through the bole above a height of 1.3 m was noted as “coppiced.” In order to estimate the biomass of coppiced trees, a discount factor was applied to the expected biomass of the tree had the tree not been coppiced. The discount factor was calculated based on the expected height of the coppiced tree based on its DBH and the actual measured height. In order to do this, mixed-species diameter-height equations were developed using all tree species in this study for which coppiced individuals were observed and for which height and diameter measurements were obtained.

Separate diameter-height equations were derived for trees with DBH  $\geq 10$  cm and those with DBH  $< 10$  cm. Fifteen different regression models were tested using measured diameters and heights of trees to identify which best fit the data.

Fourteen models were chosen from a study by Fang and Bailey (1998) that compared 33 different diameter-height models for tropical forests in China (Model No. 1 – 22 in Table B - 2 and Table B - 3) along with a standard linear regression model (Model No. 0). The models chosen from Fang and Bailey (1998) were so chosen based on their performance in the study and their use in other studies (Brown et al., 1989; Zeide, 1993). Best fit was determined by comparing the R-square, root square error (RSE) and Akaike information criterion (AIC) of results.

The final models chosen were:

$$\text{DBH} \geq 10 \text{ cm (Model No. 2):} \quad H = -4.493 + 4.909 \times \ln(D)$$

$$\text{DBH} < 10 \text{ cm (Model No. 3):} \quad \ln(H) = 0.59904 + 0.50059 \times \ln(D)$$

where,  $H$  = expected height and  $D$  = diameter at breast height (DBH). When more than one DBH was recorded for an individual tree (e.g., when branching occurred below 1.3 m), the maximum recorded DBH was used to develop the height-diameter equation. The diameter-height equations were then used to predict the expected height ( $H$ ) for each coppiced tree based on the measured DBH. The measured height of the coppiced tree was then divided by the expected height to develop a “discount” factor (e.g., if the observed height was 10m and the predicted height was 12m, the

discount factor would be  $10/12 = 0.833$ ). This discount factor was then multiplied by the expected biomass of a full tree with the measured DBH to estimate the actual biomass of the coppiced tree.

#### *Wood-specific gravity*

Wood specific gravity (WSG) was required for Equation M2 (Chave et al., 2005). WSG was found in the literature for 72 of the 143 trees in the BLA study identified to the genus and/or species level. For any individual for which no WSG data could be found I applied a simple arithmetic average of the 72 species. This average ended up being 0.55, which seems reasonable compared to the averages found for two well-known studies looking at WSG (among other things) of trees in tropical climates: 0.54 found by Chave et al. (2005) and 0.6 found by Brown (1997).

## Supplementary Tables for Chapter 5

**Table B - 1. Allometric equations used to derive aboveground woody biomass**

Equation No.	Source	Family	Scientific name(s)	Common name(s)	Max DBH	Complete equation	Correction factor	Notes
M1	(van Breugel et al., 2011)	Mixed - trees	Mixed - trees		29.0	$\ln Y = -1.863 + 2.208 \times \ln(D)$	1.100	Developed in Panama (MAP of 2300 mm); see Table 2 in article
M2	(Chave et al., 2005)	Mixed - trees	Mixed - trees		138.0	$Y = p(\exp(-1.499 + 2.148 \ln(D) + 0.207(\ln(D))^2 - 0.0281(\ln(D))^3))$	N/A	For moist forest with wood specific gravity (p) and without height
M3	(Hughes et al., 1999b)	Mixed - trees	Mixed - trees		9.9	$Y = (\exp(4.9375 + 1.0583 \ln(D^2)))1.14/10^6$	1.140	Developed in Mexico (MAP > 4000 mm); original equation in Mg so final value divided by $10^6$ to convert to kg
SS1	(Segura et al., 2006)	Boraginaceae	<i>Cordia alliodora</i> ; <i>Cordia</i> spp.	laurel	44.0	$\log_{10} Y = -0.755 + 2.072 * \log_{10}(D)$	N/A	Developed in Nicaragua (MAP 600 - 2000 mm); equation for <i>Cordia alliodora</i>
SS2	(Segura et al., 2006)	Mimosaceae	<i>Inga</i> spp. 1; <i>Inga</i> spp. 2; <i>Inga vera</i> ; <i>Inga paterno</i> Harms	pepeto; pepeto gigante; pepeto de río; paterna	30.0	$\log_{10} Y = -0.889 + 2.317 * \log_{10}(D)$	N/A	Developed in Nicaragua (MAP 600 - 2000 mm); mixed equation for two <i>Inga</i> species ( <i>I. punctata</i> and <i>I. tonduzzi</i> ); max DBH was estimated from 2 in article
SS3	(van Breugel et al., 2011)	Malpighiaceae	<i>Byrsonima crassifolia</i> (L.) Kunth	mano de leon	23.0	$\ln(Y) = -1.696 + 2.226 * \ln(D)$	1.030	Developed in Panama (MAP of 2300 mm); see Table 1 in article
SS4	(van Breugel et al., 2011)	Bixaceae	<i>Cochlospermum vitifolium</i>	tecomasuche	20.2	$\ln(Y) = -2.23 + 2.034 * \ln(D)$	1.010	Developed in Panama (MAP of 2300 mm); see Table 1 in article
SS5	(van Breugel et al., 2011)	Melastomataceae	<i>Conostegia xalapensis</i> (Bonpl.) D. Don ex DC.	unknown	7.2	$\ln(Y) = -1.354 + 1.952 * \ln(D)$	1.053	Developed in Panama (MAP of 2300 mm); see Table 1 in article
SS6	(van Breugel et al., 2011)	Melastomataceae	<i>Miconia argentea</i> (Sw.) DC.; <i>Miconia albicans</i> (Sw.) Steud.	sirin; sirin de montaña	22.0	$\ln(Y) = -2.054 + 2.389 * \ln(D)$	1.023	Developed in Panama (MAP of 2300 mm); see Table 1 in article; equation is for <i>Miconia argentea</i>
SS7	(van Breugel et al., 2011)	Malvaceae	<i>Apeiba tibourbou</i> Aubl.	peine de mico	24.3	$\ln(Y) = -2.788 + 2.27 * \ln(D)$	1.018	Developed in Panama (MAP of 2300 mm); see Table 1 in article
SS8	(van Breugel et al., 2011)	Annonaceae	<i>Annona holosericea</i> Saff.; <i>Annona</i> spp.	anonita o sincuyita; anona	26.5	$\ln(Y) = -2.772 + 2.562 * \ln(D)$	1.038	Developed in Panama (MAP of 2300 mm); see Table 1 in article; equation is for <i>Annona spraguei</i>

Equation No.	Source	Family	Scientific name(s)	Common name(s)	Max DBH	Complete equation	Correction factor	Notes
SS9	(van Breugel et al., 2011)	Ulmaceae	Trema micrantha (L.) Blume	capulin macho	18.6	$\ln(Y) = -2.305 + 2.351 * \ln(D)$	1.033	Developed in Panama (MAP of 2300 mm); see Table 1 in article
SS10	(van Breugel et al., 2011)	Flacourtiaceae	Casearia sylvestris Sw.	falso almendro	15.1	$\ln(Y) = -1.939 + 2.437 * \ln(D)$	1.013	Developed in Panama (MAP of 2300 mm); see Table 1 in article
SS11	(Návar, 2009)	Mimosaceae	Lysiloma divaricatum (Jacq.) J.F. Macbr; Lysiloma acapulsenae	sicahuite o sincahuite; quebracho	32.6	$Y = 0.37 * D^{1.96}$	N/A	Developed in Mexico (MAP 900 mm); mixed equation for tropical dry forest developed using 6 species, of which 26% were L. divaricatum
SS12	(Návar, 2009)	Pinaceae	Pinus oocarpa	pino	49.8	$Y = 0.1354 * D^{2.3033}$	N/A	Developed in Mexico (MAP 900 mm); mixed equation for "other pine species" which includes P. oocarpa
SS13	(Návar, 2009)	Fagaceae	Quercus insignis M. Martens & Galeotti; Quercus spp.	roble	62.5	$Y = 0.0890 * D^{2.5226}$	N/A	Developed in Mexico (MAP 900 mm); mixed equation for Quercus spp., primarily Gambel oak (Q. gambelii) and net-leaf oak (Q. rugosa)
SS14	(Brandeis et al., 2006)	Burseraceae	Bursera simaruba	jiote	45.0	$\ln(Y) = \ln[0.307631 * D^{1.540044} + 0.072847 * (D^2 * H)^{0.899279}]$	N/A	Developed in Puerto Rico (MAP of 650 mm); half of the trees used to develop this equation were B. simaruba; Max DBH was estimated from Figure 1 in article
SS15	Castellanos et al. 2010 (cited in Schmitt-Harsh et al., 2012)	Rubiaceae	Coffea arabica L.	café	9.0	$Y = 0.1955 * D^{1.648}$	N/A	Developed in Guatemala (MAP of 2504 mm); equation found in Schmitt-Harsh et al. 2012

Where Y = total AGWB in kg; D = bole diameter at 1.3m in cm (DBH); H = height in cm; p = wood specific gravity (WSG);

**Table B - 2. Result of analysis of potential diameter-height regression models for large trees (DBH ≥ 10 cm)**

Model No. †	Model form ††	a	b	c	R-square	RSE	AIC
0	$y = a + b \cdot D$	6.0147***	0.1874***		0.253	3.83	4620
1	$y^{-1} = a + b \cdot D^{-1}$	0.06352***	1.02063***		0.136	0.0562	-2438
2	$y = a + b \cdot \text{LOG}(D)$	-4.493***	4.909***		0.243	3.85	4631
3	$\text{LOG}(y) = a + b \cdot \text{LOG}(D)$	0.8785***	0.4506***		0.203	0.396	829
4	$\text{LOG}(y) = a + b \cdot D^{-1}$	2.708***	-8.751***		0.185	0.401	848
5	$y = a + bD + cD^2$	15.236***	-91.836***		0.205	3.95	4673
6	$y = a + bD^{-1} + cD^2$	12.6***	-58.3***	0.00126***	0.247	3.84	4628
7	$y = a \cdot (D^b)$	2.4891***	0.4635***			3.82	4619
8	$y = \exp(a + b/(D + 1))$	2.872***	-11.125***			3.9	4651
9	$y = a \cdot \exp(b/D)$	17.207***	-9.976***			3.91	4655
10	$y = a \cdot (1 - \exp(-b \cdot D))$	16.1768***	0.05***			3.9	4652
11	$y = a \cdot D/(b+D)$	21.56***	22.35***			3.86	4636
12	$y = (D^2)/(a + b \cdot D)^2$	1.61929***	0.23030***			3.89	4646
18	$y = a + b \cdot (1 - \exp(-c \cdot D - D_{\min}))$	7.63077***	28.39618(NS)	0.00807(NS)		3.82	4619
20	$y = a + b/(D+c)$	58.7(NS)	-11322.2(NS)	211.5(NS)		3.82	4619

† Model number refers to Table 4 in Fang and Bailey 1998, except model number 0 which is a standard linear regression

†† y = tree height; D = diameter at 1.3m (DBH)

\* = significant at  $p < 0.05$ ; \*\* = significant at  $p < 0.01$ ; \*\*\* = significant at  $p < 0.001$ ; (NS) = not significant ( $p \geq 0.05$ )

**Table B - 3. Result of analysis of potential diameter-height regression models for small trees (DBH 1 < 10 cm)**

Model No. <sup>†</sup>	Model form <sup>††</sup>	a	b	c	R-square	RSE	AIC
0	$y = a + b \cdot D$	1.57877***	0.53308***		0.4686	1.348	2188.511
1	$y^{-1} = a + b \cdot D^{-1}$	0.217679***	0.315553***		0.3348	0.1194	-894.5634
2	$y = a + b \cdot \text{LOG}(D)$	1.37666***	1.94613***		0.4419	1.381	2219.758
3	$\text{LOG}(y) = a + b \cdot \text{LOG}(D)$	0.59904***	0.50059***		0.4634	0.3402	437.5712
4	$\text{LOG}(y) = a + b \cdot D^{-1}$	1.57144***	-1.01157***		0.3417	0.3768	567.5305
5	$y = a + bD + cD^2$	5.0746***	-3.7130***		0.2903	1.558	2372.589
6	$y = a + bD^{-1} + cD^2$	3.387764***	-1.483419***	0.040115***	0.4578	1.361	2202.324
7	$y = a \cdot (D^b)$	1.76563***	0.56682***			1.347	2187.671
8	$y = \exp(a + b/(D + 1))$	2.09863***	-3.46825***			1.369	2208.646
9	$y = a \cdot \exp(b/D)$	6.7934***	-1.9181***			1.41	2245.67
10	$y = a \cdot (1 - \exp(-b \cdot D))$	6.7726***	0.22665***			1.37	2209.412
11	$y = a \cdot D/(b+D)$	9.6069***	5.5846***			1.362	2201.903
12	$y = (D^2)/(a + b \cdot D)^2$	0.539333***	0.358106***			1.381	2219.827
18	$y = a + b \cdot (1 - \exp(-c \cdot D - D_{\min}))$	1.57630***	12.29907*	0.05531(NS)		1.347	2188.348
20	$y = a + b/(D+c)$	22.54*	-630.48(NS)	29.65(NS)		1.346	2188.227

<sup>†</sup> Model number refers to Table 4 in Fang and Bailey 1998, except model number 0 which is a standard linear regression

<sup>††</sup> y = tree height; D = diameter at 1.3m (DBH)

\* = significant at p < 0.05; \*\* = significant at p < 0.01; \*\*\* = significant at p < 0.001; (NS) = not significant (p ≥ 0.05)

**Table B - 4. Results for validation and grid simulation analysis of AGWB-C map uncertainty**

Aggregation Unit	Area (ha)	Measured AGWB-C ----- <i>Mg ha<sup>-1</sup></i> -----	Mapped AGWB-C	Observed Error	Map Uncertainty
Farm Plot (01-02)	0.44	0.2	3.6	1874.0%	70.3%
Farm Plot (01-14)	0.36	2.9	4.7	61.6%	66.2%
Farm Plot (04-10)	0.33	8.1	3.2	60.2%	53.5%
Farm Plot (05-03)	0.62	9.4	3.2	66.3%	47.1%
Farm Plot (06-10)	0.33	1.7	2.9	75.5%	53.6%
Farm Plot (08-07)	0.89	12.7	13.4	5.9%	35.7%
Farm Plot (10-07)	0.46	3.3	5.7	74.6%	47.6%
Farm Plot (14-05)	0.19	1.3	3.7	187.1%	68.4%
Farm Plot (14-05)	0.35	1.8	7.1	297.9%	50.5%
Farm Plot (14-06)	0.54	32.6	15.5	52.4%	39.3%
Forest Plot (N50)	0.96	97.3	101.3	4.1%	38.5%
<hr/>					
Grid Simulation	0.1				98.2%
Grid Simulation	1				33.8%
Grid Simulation	10				11.6%
Grid Simulation	100				4.0%
Grid Simulation	1,000				1.3%
Grid Simulation	10,000				0.5%

**Supplementary Figures for Chapter 5**

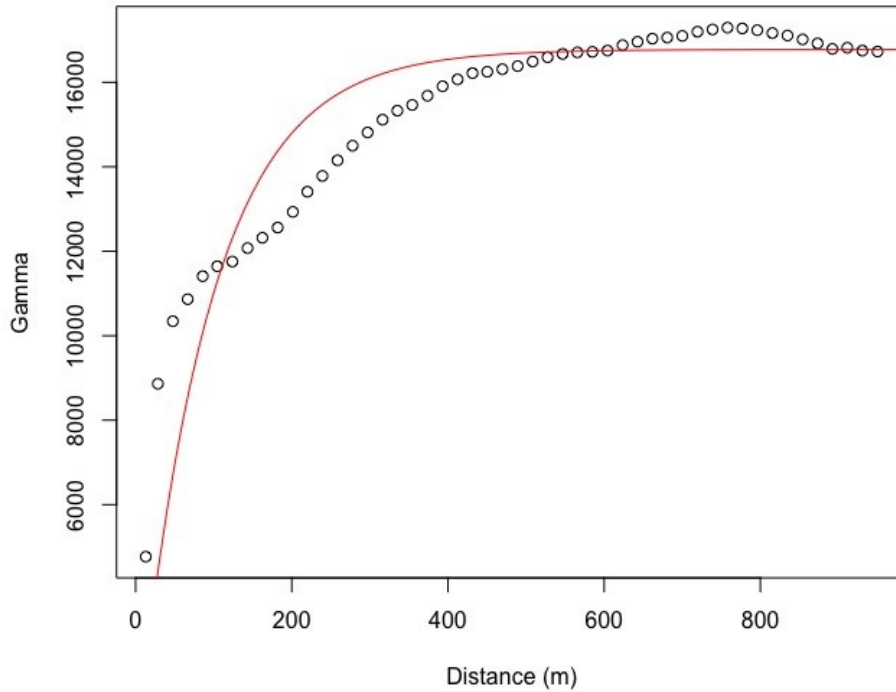


**Figure B - 1. Spatial autocorrelation of AGWB-C prediction uncertainty**

The mean of 1000 variograms run on 1-km x 1-km subsets of the study area for the aboveground woody biomass carbon (AGWB-C) prediction uncertainty map. Line shows the fit of an exponential model to the final mean variogram, with a nugget of 0 and an effective range (95% of the sill) of 281 m.

## 7.6 Appendix C

### *Supplementary Table for Chapter 6*

**Table C - 1. Plot metrics used in random forest modeling to predict AGWB with the area-based approach**

Metrics extracted from calibration plot polygons using the *CloudMetrics* tool in FUSION/LDV. See McGaughy (2014) for details.

No.	Elevation metric	No. (cont.)	Elevation metric (cont.)
1	<b>Total return count above 1.3 m *</b>	25	Elev L1
2	Return 1 count above 1.3 m	26	Elev L2
3	<b>Return 2 count above 1.3 m *</b>	27	<b>Elev L3 *</b>
4	<b>Return 3 count above 1.3 m *</b>	28	<b>Elev L4 *</b>
5	Return 4 count above 1.3 m	29	Elev L CV
6	Return 5 count above 1.3 m	30	Elev L skewness
7	Return 6 count above 1.3 m	31	<b>Elev L kurtosis *</b>
8	Return 7 count above 1.3 m	32	Elev P01
9	Return 8 count above 1.3 m	33	Elev P05
10	Return 9 count above 1.3 m	34	<b>Elev P10 *</b>
11	Other return count above 1.3 m	35	<b>Elev P20 *</b>
12	Elev minimum	36	Elev P25
13	Elev maximum	37	Elev P30
14	Elev mean	38	Elev P40
15	<b>Elev mode *</b>	39	Elev P50
16	Elev stddev	40	Elev P60
17	Elev variance	41	Elev P70
18	Elev CV	42	Elev P75
19	Elev IQ	43	Elev P80
20	<b>Elev skewness *</b>	44	Elev P90
21	<b>Elev kurtosis *</b>	45	Elev P95
22	Elev AAD	46	Elev P99
23	MAD median	47	Canopy relief ratio
24	MAD mode	48	<b>Elev quadratic mean *</b>
		49	Elev cubic mean

\* Metrics chosen for the reduced random forest model using conditional variable importance ranking